

LUCI

User Manual



THE LARGE BINOCULAR TELESCOPE OBSERVATORY

SCIENCE OPERATIONS

LUCI

User Manual

Document Name:	LUCI_UserMan.pdf
CAN ID Number:	604s1nn
Issue Number:	1.98 (<i>DRAFT</i>)
Issue Date:	September 7, 2016
Prepared by:	J.Heidt & D.Thompson

Distribution List		
Recipient	Institute / Company	No. of Copies
C. Veillet	LBTO	1 (file)
A. Conrad	LBTO	1 (file)
M. Wagner	LBTO	1 (file)
D. Thompson	LBTO	1 (file)
W. Seifert	LSW	1 (file)
R. Gredel	MPIA	1 (file)
H. Mandel	LSW	1 (file)

Document Change Record		
Issue	Date	Reasons / Remarks
1.30	03.05.2010	Final/original LUCI1 User Manual
1.90	17.02.2016	New document
1.95	19.08.2016	Internal release for comments
1.98	09.09.2016	First public release for comments

<i>CONTENTS</i>	3
-----------------	---

Contents

List of Figures	6
------------------------	----------

List of Tables	8
-----------------------	----------

1 Introduction	9
-----------------------	----------

1.1 Citing and Acknowledging LUCI	11
---	----

1.2 Online Materials	12
--------------------------------	----

1.3 Acronyms and Abbreviations	13
--	----

2 The Instruments	14
--------------------------	-----------

2.1 Cameras	14
-----------------------	----

2.2 Gratings	15
------------------------	----

2.3 Filters	17
-----------------------	----

2.4 Masks	18
---------------------	----

2.5 Detectors	18
-------------------------	----

2.6 Calibration Units	20
---------------------------------	----

3 The LUCI User Interface	22
----------------------------------	-----------

3.1 Observation Execution Panel	22
---	----

3.1.1 The status panels	24
-----------------------------------	----

3.1.2 The messaging panel	24
-------------------------------------	----

3.2 Real-Time Display	25
---------------------------------	----

3.2.1 The Real-Time Display Control GUI	25
---	----

3.2.2 Image display and image analysis	26
--	----

3.2.3 Long Slit alignment	26
-------------------------------------	----

3.2.4 MOS alignment	27
-------------------------------	----

3.3 Instrument Control Manager GUI	27
--	----

3.4 Readout Manager GUI	28
-----------------------------------	----

3.5 Telescope Service GUI	29
-------------------------------------	----

3.6 GEIRS	29
---------------------	----

3.7 LUCI Software Start-Up	29
--------------------------------------	----

4 Observation Preparation Tools	30
--	-----------

4.1	Telescope Mode	30
4.2	Exposure Time Calculator	31
4.3	LUCI Mask Simulator	32
4.4	Scriptor — Observing Tool	32
4.5	Finding Charts	33
4.6	The README File	34
4.7	Working with a Binocular Telescope	34
5	Sensitivity	36
5.1	Photometric Zero Points and Sky Backgrounds	36
5.2	Limiting Magnitudes	37
6	Calibration	38
6.1	Darks	38
6.2	Flatfields	39
6.2.1	Twilight (Imaging) Flats	40
6.3	Photometric (Imaging) Standards	40
6.4	Spectroscopic Standards	40
6.5	Wavelength Calibration	41
6.6	Correcting for	41
6.6.1	Non-linearity	41
6.6.2	Persistence	42
6.6.3	Crosstalk	43
6.6.4	Photometric Gradients	43
6.6.5	Image quality and distortions	44
6.7	Ghost Images	44
6.8	Internal Flexure	45
7	Overheads	46
7.1	Telescope overheads	46
7.2	Instrument overheads	47
7.3	Detector overheads	47
7.4	The Human Element	48

<i>CONTENTS</i>	5
8 Observational Considerations	49
8.1 The Atmosphere	49
8.1.1 Absorption: Spatial and Spectral	49
8.1.2 Background: Thermal and OH Emission, Moonlight	50
8.1.3 Variability: Turbulence and Weather	50
8.2 The Telescope	51
8.2.1 Guiding	51
8.2.2 Collimation	53
8.2.3 Thermal Background	53
8.2.4 Dither, Dither, Dither	53
8.2.5 Adaptive Optics Observations	54
9 Archive	55
A Filter and Grating Bandpasses	56
B Arc-line identification and night-sky emission line plots	60

List of Figures

1	Both LUCIs on the LBT	9
2	LUCI optics diagram	14
3	Readout modes	19
4	The LUCI observation execution panel	22
5	The LUCI Real-Time Display	26
6	The Instrument Manager GUI	27
7	The Readout Manager GUI	28
8	The Telescope Service GUI	29
9	The GEIRS Display GUI	29
10	Example Finding Chart	33
11	SYNC and ASYNC Motions	35
12	imaging flatfield from LUCI2	39
13	Persistence of the LUCI2 detector	42
14	Pixel and channel crosstalk.	43
15	Relative atmospheric absorption in the near infrared	49
16	Background emission in the near infrared	50
17	The guide probe is seen by LUCI when on axis!	51
18	The patrol field for the LUCI AGw unit	52
19	Internal pupil cold stop in the K band	53
20	LBT Archive login	55
21	LBT Archive Database search page	55
22	Wavelength dependencies of the efficiencies for the gratings.	56
23	Transmission of the broad-band filters in the LUCI instruments	57
24	Transmission of the narrow-band filters in the LUCI instruments	58
25	Transmission of the narrow-band and order sorting filters in the LUCI instruments	59
26	Argon arc-lines for G150	61
27	Xenon arc-lines for G150	62
28	Neon arc-lines for G150	63
29	Argon arc-lines for G200 in H and K	64
30	Xenon arc-lines for G200 in H and K	65

LIST OF FIGURES

7

31	Neon arc-lines for G200 in H and K	66
32	Argon arc-lines for G210 in z-band	67
33	Xenon arc-lines for G210 in z-band	68
34	Neon arc-lines for G210 in z-band	69
35	Argon arc-lines for G210 in J-band	70
36	Xenon arc-lines for G210 in J-band	71
37	Neon arc-lines for G210 in J-band	72
38	Argon arc-lines for G210 in H-band	73
39	Xenon arc-lines for G210 in H-band	74
40	Neon arc-lines for G210 in H-band	75
41	Argon arc-lines for G210 in K-band	76
42	Xenon arc-lines for G210 in K-band	77
43	Neon arc-lines for G210 in K-band	78
44	Nightsky emission line in z- and J-bands.	79
45	Nightsky emission line in H- and K-bands.	80

List of Tables

1	Pixel scales and fields of view	14
2	Grating Characteristics for SL observations	15
3	Grating Characteristics for AO observations	16
4	Wavelengths that can be set at the center of the detector.	16
5	Characteristics of the available filters	17
6	High Extinction Filter Combinations.	17
7	Permanent masks in the LUCI instruments	18
8	LUCI H2RG detector performance.	18
9	Imaging ZPs and sky background count rates.	36
10	Imaging limiting magnitudes	37
11	Spectroscopic limiting magnitudes	37
12	Intensities of the flatfields per second for the filters and the N3.75 camera.	39
13	Recommended spectroscopic flat integration times for the N1.8 camera and 0''5 longslit.	40
14	Recommended integration times for spectroscopic arcs with the N1.8 camera and 0''5 longslit.	41
15	LUCI H2RG Linearization	42
16	Radial Distortion Coefficients	44
17	Telescope overheads	46
18	Instrument overheads	47
19	Readout overheads	47
20	Human overheads	48

1 Introduction

The two LBT Utility Camera in the Infrared (LUCI) instruments are an independent pair of basically identical cryogenic multi-mode NIR instruments that are capable of imaging, longslit and MOS spectroscopy in seeing-limited mode over a 4-arcminute field of view, as well as adaptive-optics imaging and longslit spectroscopy over a 30-arcsecond field of view using a natural AO reference star. The instruments work over a wavelength range from the dichroic dewar entrance window cut-on at $0.95\ \mu\text{m}$ through the red end of the K filter at $2.4\ \mu\text{m}$. LUCI1 is located at the left (SX) *front bent Gregorian* f/15 focus, and LUCI2 is located on the right (DX) side, see Figure 1.

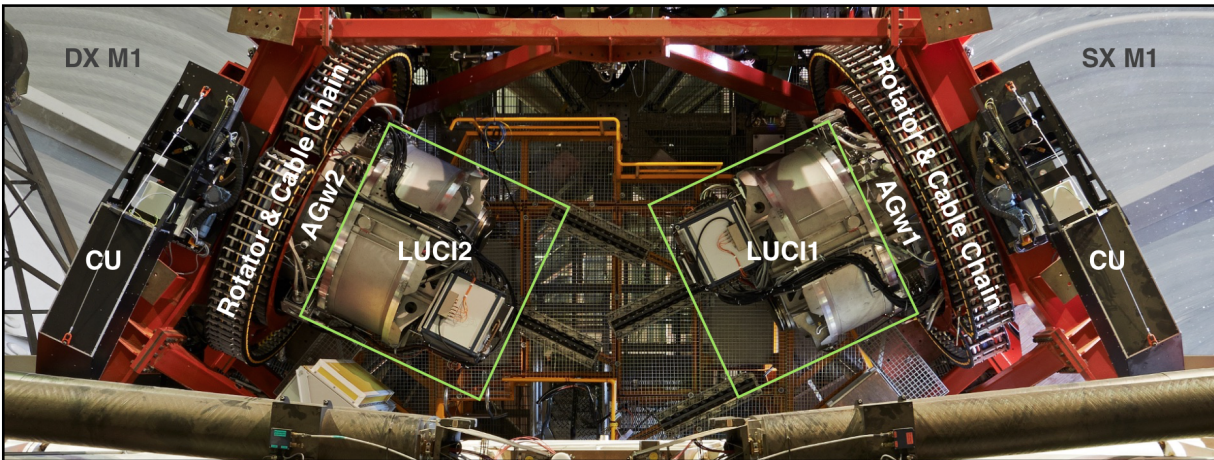


Figure 1: Both LUCIs mounted on the LBT as seen from above, so left and right are reversed. The calibration units (CU), AGws, and the rotator & cable chain mechanisms are also identified.

The instruments feature cryogenic MOS units housing a set of ten “permanent” facility longslit and calibration masks, as well as another 23 exchangeable user-designed MOS slit masks. There are also focal plane units (FPUs) which secure the masks in the LUCI focal plane, and a MOS “robot” that is used to move the masks between storage and the FPU. Custom masks are exchanged a few times per semester to accommodate different partner science programs. One empty auxiliary cryostat is coupled to a vacuum gate on the instruments to extract the current set of masks, and then a second pre-loaded and pre-cooled auxiliary cryostat is used to insert the new masks. The cabinet exchange is done on the telescope itself and takes less than a day, maximizing the availability of the LUCI instruments for science observations.

Both instruments are near their final configurations, now equipped with Hawaii 2-RG detectors as well as their N30 cameras for AO work. In addition a ground-layer AO system (ARGOS), using multiple green lasers for each telescope system, is being commissioned.

One or the other LUCI has been available to the LBT partnership since December 2009 for monocular seeing-limited science observations. As of this writing (July 2016) both LUCIs are nearing completion of commissioning all modes. As the new modes (AO imaging and spectroscopy, ARGOS, homogeneous and mixed binocular modes) are commissioned, they will be released to our science community.

This document is the primary reference for potential users of the near-infrared LUCI instruments at the LBT (the *User Manual*). In this *LUCI User Manual* we cover all of the material needed to have a basic understanding of the instruments and their use. It includes information needed to prepare observations of your science target, such as the sensitivity of the instrument, suggestions for calibration, dithering strategies, etc. More detailed information is often available elsewhere, such as for the MOS mask preparation that is

covered in the LMS manual, and not repeated here. Links to all of the associated information are listed in Section 1.2.

These associated documents and webpages include additional details about the instruments (the *Instrument Manual*) and a quick reference webpage for observers sitting at the telescope (the *cookbook*). Preparing multi-slit masks is covered in the *LMS User Manual*. A web-based *Exposure Time Calculator (ETC)* is provided to help to determine the exposure times needed for your science while a *Scripting tool (Scriptor)* allows to prepare scripts for the execution of scientific observations and calibrations. As we transition to using the observation planning tools being developed for *Q* and binocular observations, the *observation planning tool (OPT)* will take over the functions of Scriptor. Some material that changes often, such as the list of installed slit-masks or any recent news or status changes are collected on the *Instrument Webpage*. Together these are intended to be the complete reference for the LUCI instruments.

In Section 2 we describe the physical instrument parameters, such as the cameras, gratings, and detectors. The software User Interface is described in Section 3, while the details of actually using it to take observations are given on the cookbook. In Section 4 the observation preparation tools are covered, with additional details on preparing a complete observation plan. In Section 5 we discuss the sensitivity, throughputs, and limiting magnitudes one might expect from observations. That information is programmed into the Exposure Time Calculator (ETC). Section 6 covers the details of proper calibration of imaging and spectroscopic data taken with LUCI. Overheads, particularly important to correctly handle for efficient binocular observing, are discussed in Section 7. A general discussion about observational considerations for when working in the near infrared is covered in Section 8. Retrieving data from the LBT archive [ref] is covered in Section 9. Finally, appendixes are included for the individual filter and grating bandpass plots, arc lamp and night sky plots to aid in identification.

As both LUCI instruments are still in the AO commissioning phase and some of the properties of LUCI1 with the new detector are not determined yet, some of the tables in this document contain place-holders. They will be filled as time and the commissioning progresses. Many of the figures in this *User's Manual* are shown fairly small, but in most cases you can zoom in on the PDF file to get the full detail. Comments or suggestions for improvement are highly appreciated. Please send any inquiries to the [LBT science operations group](#).

Blue text within this document designates internal navigation cross-references and can be used to jump to that referenced location (see the Table of Contents, for example). Magenta text designates links to outside documents, websites, or other resources, such as the [mailto](#) link at the end of the previous paragraph.

1.1 Citing and Acknowledging LUCI

Technical Description:

Seifert, W., Appenzeller, I., Baumeister, H., Bizenberger, P., Bomans, D., Dettmar R.-J., Grimm, B., Herbst, T., Hofmann, R., Jütte, M., Laun, W., Lehmitz, M., Lemke, R., Lenzen, R., Mandel, H., Polsterer, K., Rohloff, R.-R., Schütze, A., Seltmann, A., Thatte, N., Weiser, P., and Xu, W.,
The NIR Spectrograph LUCIFER for the LBT,
Proc. SPIE, 4841, 962 (2003).

2008 Status:

Mandel, H. G., Seifert, W., Heidt, J., Quirrenbach, A., Germeroth, A., Felz C., Müller, P., Lenzen, R., Lehmitz, M., Laun, W., Mall, U., Naranjo, V., Weiser, P., Jütte, M., Knierim, V., Polsterer, K., Dettmar, R., Hofmann, R., Buschkamp, P., and Weisz, H.,
LUCIFER status report summer 2008,
Proc. SPIE, 7014, 124 (2008).

MOS Unit details:

Hofmann, R., Gemperlein, H., Grimm, B., Jütte, M., Mandel, H., Polsterer, K., and Weisz, H.,
The cryogenic MOSunit for LUCIFER,
Proc. SPIE, 5492, 1243 (2004).

Buschkamp, P., Gemperlein, H., Hofmann, R., Polsterer, K., Ageorges, N., Eisenhauer, F., Lederer, R., Honsberg, M., Huag, M., Eibl, J., Seifert, W., and Genzel, R.,
The LUCIFER MOS: a full cryogenic mask handling unit for the nearinfrared multiobject spectrograph,
Proc. SPIE, 7735, 268, 2010.

Commissioning:

Ageorges, N., Seifert, W., Jütte, M., Knierim, V., Lehmitz M., Buschkamp, P., Polsterer, K.,
LUCIFER1 commissioning at the LBT,
Proc. SPIE, 7735, 56, (2010).

Seifert, W., Ageorges, N., Lehmitz, M., Buschkamp, P., Knierim, V., Polsterer, K., and Germeroth, A.,
Results of LUCIFER1 commissioning,
Proc. SPIE, 7735, 292, (2010).

Other:

Storz, C., ; Naranjo, V., Mall, U., Ramos, J., Bizenberger, P., Panduro, J., *Standard modes of MPIA's current H2/H2RG-readout systems*, Proc. SPIE, 8453, 14, (2012).

1.2 Online Materials

Here we collect a number of useful links to additional information covering LUCI and the LBT Observatory, as well as some outside information or data that is beyond the scope of this document. Everything in magenta below is a clickable link to outside information.

LBT Observatory

[Main LBTO website](#)

LUCI

[Instrument Webpage \[TBD\]](#)

[User Manual \[this document\]](#)

[LMS Manual & Software](#)

[ETC webpage](#)

[Scriptor webpage](#)

[Observing Cookbook](#)

External Links

[NIR photometric standard stars](#)

[GEMINI Telluric compilation](#)

[RSA finder chart tool \(for 2MASS/SDSS\)](#)

[Gran Telescope CANARIAS blank fields](#)

Old LUCI Material

[Old SciOps Website](#)

[Old LUCI1 Webpage](#)

[Old LUCI1 User Manual](#)

Other Reference Materials

[Aladin user manual](#)

1.3 Acronyms and Abbreviations

ADC	Atmospheric Dispersion Corrector
ADU	Analog to Digital Unit, also called <i>counts</i> or <i>DN</i>
ADI	Angular Differential Imaging
AGw	Acquisition, Guiding & Wavefront sensing system
AO	Adaptive Optics
CWL	Central Wavelength
DIT	Detector Integration Time
DN	Data Number, also called <i>counts</i> or <i>ADU</i>
ETC	Exposure Time Calculator
FC	Flexure Compensation
FIMS	FORS Instrument Mask Simulator
FOV	Field of View
FPU	Focal Plane Unit
FWHM	Full-Width at Half-Maximum
GUI	Graphical User Interface
IMGUI	Instrument Manager GUI
LBT	Large Binocular Telescope
LMS	LUCI Mask preparation Software
LUCI	LBT Utility Camera in the Infrared
LUCI	Landessternwarte's Über Contraption in the Infrared
NDIT	Number of Detector Integration Time
obsN	Observer workstation #N [N=1,2,3,4,5 or 6] at the LBT
OPT	Observation Planning Tool
PSF	Point Spread Function
QE	Quantum Efficiency
RON	Readout Noise
RMGUI	Readout Manager GUI
SNR	Signal-to-Noise Ratio
TMGUI	Telescope Manager GUI
TCS	Telescope Control Software
UI	User Interface
wfs	Wavefront sensor

2 The Instruments

The LUCI instruments share a common optical design, differing only slightly in their “as built” configurations. The instruments work over a wavelength range from the dichroic dewar entrance window cut-on at $0.89\ \mu\text{m}$ (LUCI1) or $0.95\ \mu\text{m}$ (LUCI2) through the red end of the K filter at $2.4\ \mu\text{m}$. LUCI1 is located at the left (SX) *front bent Gregorian* $f/15$ focus of the LBT, and LUCI2 is located on the right (DX). The instruments have up to 33 masks that can be placed in the telescope focal plane, allowing both longslit and multi-object spectroscopy to be done. The instruments are kept on the telescope under vacuum and cooled by two closed-cycle He coolers that are synchronized to minimize vibrations transmitted to the telescope.

The refractive collimators take the $f/15$ input from the telescopes and form $\sim 104\ \text{mm}$ diameter images of the secondary mirrors on $\sim 102\ \text{mm}$ diameter internal cold pupil stops. Three interchangeable cameras (N1.8, N3.75, and N30) in each instrument produce different pixel scales on the Hawaii 2RG detectors primarily for spectroscopy, imaging, and adaptive optics, respectively. Three gratings are available, working in different resolution regimes spanning from low ($R \sim$ a few hundred) to medium ($R < 30000$) resolution. Thus the LUCI instruments can do seeing-limited imaging, multi-object and longslit spectroscopy over a $4' \times 4'$ field of view, as well as diffraction-limited imaging and longslit spectroscopy over a $30'' \times 30''$ field of view. The details about all of these modes and other functional components in the instruments are given in this section.

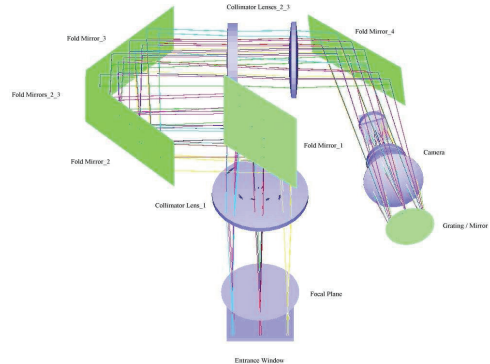


Figure 2: Diagram of the LUCI optics showing the positions of the major components and fold mirrors, resulting in an overall compact design.

The four fold mirrors overall keep the instrument compact. Two of them, FM1 and FM4, are motorized, allowing for fine-tuning the alignment of the optics after the instrument has cooled down and reached its stable operating temperature. These are also used to make small adjustments with changes in cameras and gratings to keep the pupil aligned and the field stop centered on the detector. The last fold mirror (FM4) is also used to close either a passive (from a lookup table) or active (from fiducial marks on the masks) flexure compensation loop to correct internal flexure within the instruments that occurs with changes in elevation or rotation.

2.1 Cameras

There are three interchangeable cameras (N1.8, N3.75, and N30) in each LUCI instrument. While any camera can be used in any mode, they each have a preferred usage for which they were designed. The scales, fields of view, and primary use are listed in Table 1, with additional details discussed below.

Table 1: The pixel scales (uncertainties in the last 2 digits), fields of view and primary usage for the three cameras in each of the LUCIs.

Camera	LUCI1 [''/pix]	LUCI2 [''/pix]	Recommended Usable Field	Primary Use
N1.8	0.2500 (40)	0.2500 (40)	$4' \times 2.8'$	Spectroscopy
N3.75	0.1190 (30)	0.1178 (30)	$4' \times 4'$	Imaging
N30	0.0150 (05)	0.0150 (05)	$30'' \times 30''$	AO

The all-refractive N3.75 camera is the standard imaging camera for seeing-limited observations, including the acquisition imaging needed for longslit or MOS mask alignment. At $0.12''/\text{pixel}$ it is well-sampled for almost all conditions at the LBT, and covers a $4' \times 4'$ field of view (FoV). It has

relatively low distortion and is well corrected for color across all NIR bands. Even in the available narrow-band filters it reaches the background limit on sky in short exposure times. This camera is also used for working with ARGOS, as well as *Enhanced Seeing Mode* (ESM). It can also be used for spectroscopy, the trade off as compared to the N1.8 camera is between resolution and free spectral range.

The all-refractive N1.8 camera is the standard spectroscopic camera for seeing-limited observations. You see the same vertical 4' FoV as with the N3.75 camera, but the coarser sampling puts that image across only the central ~ 970 pixels. The horizontal restriction in the FoV to 2.8' is because the slit masks are held in a cylindrical shape to follow the curved telescope focal surface along the Y direction. As you move off the center of the field in X, the slitlets on a MOS mask become increasingly out of focus with respect to both the telescope (giving higher slit losses) and the instrument (decreasing the effective resolution). This camera *can* be used for imaging, but the distortions and color correction are not as good as in the N3.75 camera.

The catadioptric N30 camera is the standard camera for adaptive optics imaging and spectroscopy. The 15 mas/pixel scale gives Nyquist sampled diffraction-limited images at one micron. The N30 cameras in LUCI1 and LUCI2 are slightly different. In LUCI2 (the first to be installed) the camera is made with metal mirrors. Concern over the delivered image quality prompted construction of a camera using glass mirrors for LUCI1. After application of non-common-path aberrations, though, both cameras produce diffraction-limited images with high Strehl ratios.

2.2 Gratings

The grating unit holds a mirror for imaging as well as three gratings (G210 and G200 in both LUCIs, G150 in LUCI1 and G040 in LUCI2) for spectroscopy. These grating complements are the primary difference between LUCI1 and LUCI2. The gratings are named for their groove density, for example the G210 grating has 210 grooves per millimeter.

Grating	Band	Order	λ_{cen} [μm]	50% Cut on/off [μm]	Resolution [$\lambda_{\text{cen}}/\delta\lambda$]	Free Spectral Range [μm]	Dispersion [$\mu\text{m}/\text{pix}$]
G210	K	2	2.20	2.02 – 3.18	5000	0.328	0.mm
G210	H	3	1.65	1.41 – 1.90	5900	0.202	0.mm
G210	J	4	1.25	1.09 – 1.41	5800	0.150	0.mm
G210	z	5	0.97	0.89 – 1.11	5400	0.124	0.mm
G200	HK	1	1.93	1.32 – 2.40	1900/2600	0.880	0.mm
G200	zJ	2	1.17	0.90 – 1.25	2100/2400	0.440	0.mm
G150	Ks	2	2.15	1.81 – 2.40	4150	0.533	0.mm
G040	K	2	2.20	2.02 – 3.18	5000	0.nnn	0.mm
G040	H	3	1.65	1.41 – 1.90	5900	0.nnn	0.mm
G040	J	4	1.25	1.09 – 1.41	5800	0.nnn	0.mm
G040	z	5	0.97	0.89 – 1.11	5400	0.nnn	0.mm

Table 2: General characteristics of the gratings for seeing-limited observations. The resolution is given in all cases for the N1.80 camera using a 2-pixel ($0'' 5$) wide slit at the central wavelength for all gratings. See text for scaling to the N3.75 camera).

While any combination of grating and camera can be used, we list in Table 2 the basic characteristics for seeing-limited observations assuming the N1.8 camera is used with a 2-pixel ($0'' 5$) wide slit. On the left side of the table are listed the orders, central wavelengths, and grating efficiency ranges (wavelengths where the grating is above 50% of its peak efficiency in that order, see Figure 22 for the plots) for each viable grating and

broadband filter combination. On the right side are listed the effective resolution at the central wavelength, the free spectral range (width of the wavelength range on the detector for that central wavelength), and dispersion for these default configurations. The quoted spectral resolution includes the contribution from the instrumental resolution.

For any spectrograph, the resolution is to first order inversely proportional to the slit width. If you double the slit width the resolution will be about half, though this ignores any contribution from the instrumental PSF. The free spectral range in the N3.75 camera will be about $0.47\times$ that in the N1.8 camera while the dispersion will go up by a factor of $2.1\times$ ($= 1.0/0.47$). These are both just driven by the ratio of the camera scales. The spatial scale for the gratings (i.e. along the slit) is also only dependent on the camera used, and is as given in Table 1. The resolution in LUCIn will be slightly worse, about N%, than the values in Table 2 because of a somewhat lower image quality in its N1.8 camera as compared to LUCIm.

Grating & Band	Resolution [$\lambda_{\text{cen}}/\Delta\lambda$]	Free Spectral Range [μm]	Dispersion [$\mu\text{m}/\text{pix}$]
G040 K	8000	0.nnn	0.mm
G040 H	8000	0.nnn	0.mm
G040 J	8000	0.nnn	0.mm
G040 z	8000	0.nnn	0.mm
G210 K	40000	0.nnn	0.mm
G210 H	40000	0.nnn	0.mm
G210 J	40000	0.nnn	0.mm
G210 z	40000	0.nnn	0.mm

Table 3: General characteristics of the gratings available for diffraction-limited observations. The resolution is given for the N30 camera using the $0''.13$ (about 9 pixels) wide slit at the central wavelength for these bands. The quoted spectral resolution includes the contribution from the instrumental resolution.

The dispersion listed were derived from arc lamp or night sky OH emission lines. The quoted spectral resolution includes the contribution from the instrumental resolution.

It is important to keep in mind that the AO slit is matched to the size of the first zeroes of the Airy disk in the K band, the reddest band in which the LUCIs can work. Any narrower than this and the source would begin to diffract through the slit, spreading the light out in the dispersion direction! At shorter wavelengths the Airy disk is smaller, so the slit will be somewhat oversized. Thus for point source spectroscopy the actual resolution should be driven by the size of the Airy disk instead of the slit width.

All of the gratings can be tilted in order to center a selected wavelength at the center of the detector. Table 4 shows the range of central wavelengths it is possible to reach by tilting the gratings. These ranges given represent the physical limits of what can be achieved with the grating tilt and do not take into account the limits of the filters used for order separation, or the grating efficiency. In practice, it is possible to center on the detector nearly any wavelength that is passed by the standard order-sorting filters.

For AO spectroscopy even the gratings must be diffraction-limited. Although both G210 gratings were made with the same master, only the one in LUCI2 is truly diffraction-limited. The G040 grating, also in LUCI2, is the only other DL grating available as of this writing (July 2016). As we gain experience with AO spectroscopy, the plan is to obtain at least one diffraction-grating for LUCI1. The consequence of using one of the non-DL gratings for DL spectroscopy is that the PSF at the detector will be distorted by the aberrations in the grating...this is not recommended.

The main characteristics of these two gratings, when used for AO observations with the N30 camera and the $0''.13$ wide longslit, are listed in Table 3. The grating efficiency ranges and central wavelengths are identical to those listed in Table 2 and thus not repeated here. The effective resolution at the central wavelength, the free spectral range, and the disper-

Table 4: Wavelengths that can be set at the center of the detector.

Grating	Band	λ_{range} [μm]
G210	K	2.06 ... 2.40
G210	H	1.50 ... 1.75
G210	J	1.15 ... 1.35
G210	z	0.85 ... 1.02
G200	HK	0.90 ... 1.20
G200	zJ	1.50 ... 2.40
G150	Ks	1.95 ... 2.40
G040	K	2.06 ... 2.40
G040	H	1.50 ... 1.75
G040	J	1.15 ... 1.35
G040	z	0.85 ... 1.02

2.3 Filters

Each instrument has two 15-position filter wheels. The two LUCIs are currently equipped with a nearly identical set of 19 science filters, including broad- and narrow-band filters and a couple order-sorting filters for the low-resolution grating. The central wavelength, FWHM, peak and mean transmissions are listed for both instruments in Tab. 5. Plots of their transmission curves are shown in Appendix A.

Table 5: Characteristics of the available filters

Filter Name	Filter wheel	LUCI1				LUCI2			
		λ_C [μm]	FWHM [μm]	τ_{peak} %	τ_{avg} %	λ_C [μm]	FWHM [μm]	τ_{peak} %	τ_{avg} %
z	2	0.957	0.195	98.4	94.3	0.965	0.196	93.8	89.9
J	2	1.247	0.305	91.2	83.2	1.250	0.301	90.9	87.1
H	2	1.653	0.301	95.0	90.5	1.651	0.291	92.1	85.4
K	2	2.194	0.408	90.1	85.7	2.199	0.408	92.1	84.5
K _s	2	2.163	0.270	90.7	86.8	2.161	0.270	91.7	85.9
zJspec	2	1.175	0.405	93.1	90.4	1.175	0.405	93.1	90.4
HKspec	2	1.950	0.981	95.0	86.3	1.953	0.998	95.7	88.3
Y1	1	1.007	0.069	67.3	65.2	1.007	0.069	67.3	65.2
Y2	1	1.074	0.065	94.2	92.8	1.074	0.065	94.2	92.8
OH_1060	1	1.065	0.010	68.6	65.2	1.065	0.010	68.6	65.2
OH_1190	1	1.194	0.010	80.4	78.6	1.194	0.010	80.4	78.6
HeI	1	1.088	0.015	65.2	64.6	1.088	0.015	65.2	64.6
P_gam	1	1.097	0.010	81.1	80.0	1.096	0.010	70.4	68.9
P_beta	1	1.283	0.012	86.1	85.5	1.284	0.013	85.8	85.2
J_low	1	1.199	0.112	95.4	93.5	1.199	0.112	95.4	93.5
J_high	1	1.303	0.108	95.3	93.2	1.303	0.108	95.3	93.2
FeII	1	1.646	0.018	91.2	89.5	1.645	0.018	91.1	88.0
H2	1	2.124	0.023	87.9	84.9	2.127	0.023	83.9	82.0
Br_gam	1	2.170	0.024	79.4	76.5	2.171	0.023	83.1	82.0

One position in each wheel is dedicated to a *clear* filter and another holds a *blind* filter. The clear filters are to maintain approximately the same focus on the detector through all filter combinations. When you request an observation with a specific filter, whether broad- or narrow-band, you will automatically get a clear filter in the other filter wheel. The blind filters are aluminum plugs that help block stray light from getting to the detector, such as when taking dark frames. Both instruments also include a *PV_lens* (pupil viewer) that is used to view the telescope pupil and internal cold stop, for alignment.

It is sometimes helpful to cross two filters not normally used together. The obvious combinations, crossing a narrow-band filter with its corresponding broad-band filter (e.g. Br_gam and K), only lead to a couple tenths of a magnitude extinction. There are a few combinations that take advantage of overlapping wings of lower transmission to produce higher extinctions. These are useful for acquiring bright targets like telluric standards for spectroscopic calibration. Crossing filters for telluric acquisitions is done automatically by Scriptor. The useful combinations are listed in Table 6.

Table 6: High Extinction Filter Combinations.

Filter Wheel 1	Filter Wheel 2	Extinction [mag]
P_gam	J	0.8
HeI	J	2.35
OH_1060	z	3.9
HeI	z	7

2.4 Masks

The LUCIs include space for up to 33 focal plane masks. Ten “permanent” masks include a range of longslit widths, a field stop and longslit for adaptive optics observations, and a few technical masks needed to keep the instrument calibrated. These are listed in Table 7. The 1''00 or narrower longslits for seeing-limited observing are all 230 arcseconds long. The combined 2''0 and 1''5 slits are each 100'' long. The offsets from the mask center to the slit center is $\pm 56''7$, with the 1''5 slit below center and the 2''0 slit above center.

There is space for another 23 masks in an exchangeable cabinet in each LUCI. This cabinet exchange is done through vacuum gates on the instruments with the help of two pre-cooled auxiliary cryostats, one to pull the old masks out and another to insert the new masks.

Custom multi-object masks can be designed using the LMS software (see link in Section 1.2). A full description of how to use the LMS software to design MOS masks is

included in the LMS User Manual, so we do not repeat it here. LMS produces as output a *Gerber file* as well as a *.lms* file. The Gerber file is uploaded to our laser milling machine to cut the masks. The masks are cut out of 150 μm thick rolled stainless steel sheet that has been painted flat black on the side facing into LUCI to reduce reflections. The *.lms* file is used by the LUCI observing software to know where the slits and alignment stars should be for mask alignment on sky.

2.5 Detectors

Both LUCIs are now equipped with Teledyne HAWAII-2RG (H2RG) Mercury Cadmium Telluride (HgCdTe) detectors. These detectors have 2048×2048 pixels² with an 18 μm pixel pitch, though the “R” in H2RG means that there is a border of 4 pixels around the edge that are used as *reference pixels* and are not illuminated. The QE of both detectors is quite similar and relatively constant, about 83% from the dewar’s dichroic window cut-on to the red end of the K filter. This is a significant increase in QE ($\sim 60\%$) over the original first-generation Hawaii-2 detectors. The dark current and read noise are low, allowing for background-limited observations in most imaging and spectroscopic configurations.

There is significant persistence and nonlinearity with these detectors, discussed in more detail below. On sky, the detectors are oriented in standard astronomical fashion, with north up and east to the left when the position angle is zero. Table 8 summarizes the basic properties of both detectors, with additional details given in the following text where needed.

Table 7: Permanent mask names and descriptions for both LUCIs.

Mask name	Description
blind	Mask for taking dark current images
SpectroSieve	Pinhole array for spectroscopic calibrations
OpticSieve	Pinhole array for imaging calibrations
LS_2.0_1.5arcsec	Longslit with 2.0 and 1.5 arcsec wide segments
LS_1.00arcsec	Longslit 1.00 arcsec wide
LS_0.75arcsec	Longslit 0.75 arcsec wide
LS_0.50arcsec	Longslit 0.50 arcsec wide
LS_0.25arcsec	Longslit 0.25 arcsec wide
N30LS_0.13arcsec	Longslit 0.13 arcsec wide
N30_FieldStop	Field stop for the N30 camera

Table 8: LUCI H2RG detector performance.

Parameter	LUCI1	LUCI2
Gain (e-/ADU)	TBD	2.0
Dark Current (e-/sec/pix)	TBD	0.006
Read Noise (e-)		
LIR	TBD	10.0
MER	TBD	4.8
Full Well Capacity (10^3 e-)	TBD	122
Linearity (% at 80% full well)	TBD	16%
Crosstalk @Saturation	TBD	$\leq 0.2\%$
Persistence (% after 5 min)	TBD	0.03%
Minimum DIT (sec)		
LIR	2.503	2.503
MER	6.256	6.256

The detectors are read out by 32 amplifiers in parallel to keep the minimum DIT relatively low, although it still takes a little more than 2.5 seconds to read out the full detector in LIR mode reading 100 kilo-pixels per second per amplifier. Each amplifier channel is 64 pixels high (one *line*) and 2048 pixels long. On the Aladin display GUI the amplifier channels are horizontal, read out from left to right. Images of the spectroscopic slits are vertical on the detector, thus for spectroscopy the dispersion direction is horizontal. Wavelengths increase to the right.

Saturation is around 55k ADU in both LUCIs. We recommend you stay below \sim half-well ($<27k$ ADU) for peak counts on your science targets to be safe. If you linearize (Section 6.6.1) your data, and you should, it is possible to work nearly up to saturation. However you are then sensitive to small changes in seeing that could push you up over the limit.

The LUCI instruments support three different detector readout modes appropriate for various observing applications/modes of the LUCI instruments. These are: line-interlaced read (LIR), multiple endpoint read (MER), and sample-up-the-ramp (SUR). There are different regimes in observing where one of these modes is preferred over the other, so they are discussed in a bit more detail below. The complete details on these different modes can be found in Storz et al (Proc SPIE, Vol. 8453, p. 14+ 2012), we just include here enough to understand the basic differences and trade-offs with these three modes.

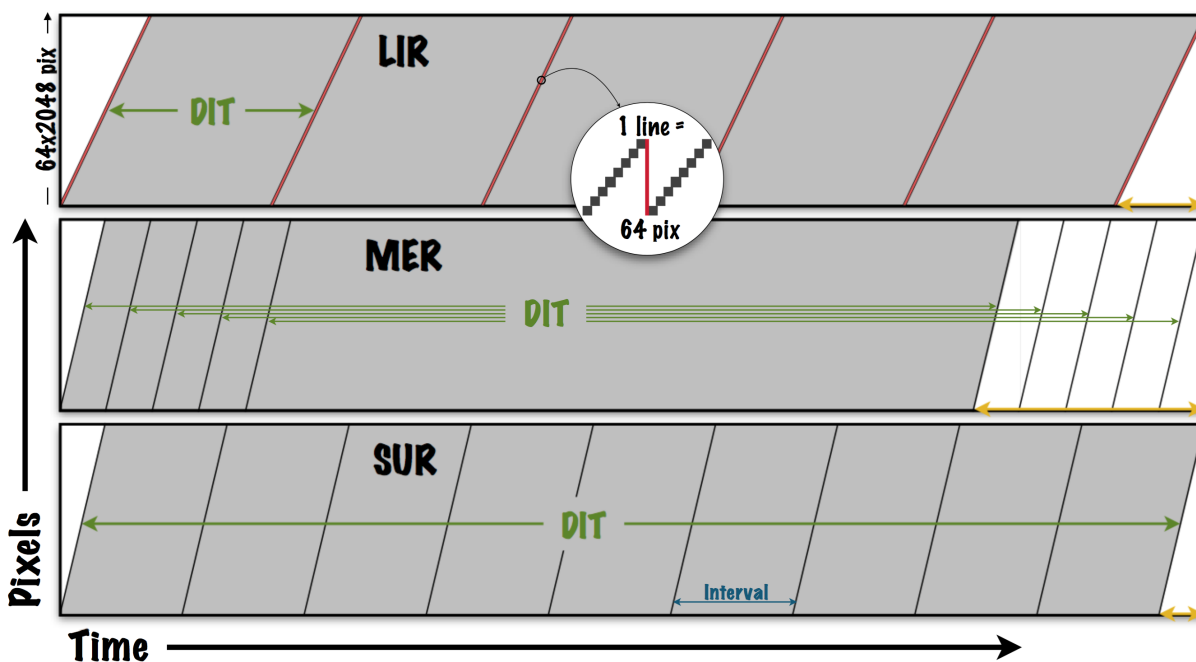


Figure 3: Timing details of the three readout modes. In each subpanel, the vertical axis represents the 64×2048 pixels in one amplifier channel and the horizontal axis represents one “exposure”. Green arrows show a DIT, while the yellow arrows at bottom right show the overheads. The inset shows how for LIR mode each 64-pixel line is read out for the second read of the previous DIT, reset (red), then read again as the first read of the next DIT.

LIR mode is most useful when your observations reach a background-limited state quickly. Use this mode if the shot noise from the sky and/or source is much higher than any contribution from the intrinsic read noise of the detector. This is most commonly encountered when imaging through the N3.75 camera or in any mode (imaging or spectroscopy) if your target is bright enough that you would saturate with longer exposures, such as telluric star spectroscopic calibrations. The top panel in Figure 3 shows an LIR exposure

consisting of NDIT=5 readouts of short exposure (DIT).

In LIR mode, as you clock through the 64 pixels in each *line* of an amplifier channel, the pixels are read out for the second read of the previous exposure, reset, then read again for the first read of the next exposure. This is represented in Fig. 3 as the slanted black-red-black lines, with black being a read and red being a reset. So the previous and next exposures are *interlaced*, and there is very little dead time between exposures...only about 700 microseconds. The trade-off is that the minimum exposure time is double what it might otherwise be, but the overall gain in efficiency over a standard double-correlated readout (DCR) is quite significant.

MER mode, also known as *Fowler sampling*, is most useful when it might otherwise be difficult to reach background-limited conditions in a reasonable exposure time. Use this mode when the background from the sky between the OH emission lines is low ($<1.65\ \mu\text{m}$), you are working at higher spectroscopic resolutions (spreading the background light over more pixels), or using narrower slits (not letting as much background light into the instrument). The middle panel in Figure 3 shows a single (NDIT=1) MER exposure of longer exposure time (DIT), with the five initial and five final readouts.

In MER mode, the detector is reset then read out non-destructively five times as fast as possible at the start of the exposure, and again five times at the end of the exposure. We use five samples for LUCI as there is a trade-off between larger overheads and increasing amplifier glow and other effects that limit the effective reduction of the read noise. The file saved to disk is the average of the five equivalent DCR exposures (shown in Figure 3) constructed from the data, so an MER mode readout has the read noise reduced by $\sim\sqrt{5}$ compared to a single LIR mode readout. You may see this written as MER10 elsewhere in LUCI documentation as that is how it was originally called (5+5 readouts for MER10). DITs shorter than 60 seconds are not likely to need MER mode readouts.

SUR mode, or sample up-the-ramp, is being implemented as part of a means to actively control the internal flexure in LUCI, which can affect any longer exposure observations. This can occur with low background spectroscopy or narrowband imaging, especially when using the N30 camera for AO observations. Use this mode only when active flexure correction (AFC) is needed. As of this writing (July 2016), this mode and its use in active flexure compensation is still being developed and is not yet released for general use. The bottom panel in Figure 3 shows a single (NDIT=1) SUR exposure of longer exposure time (DIT), with ten equally spaced readouts. You may also see SUR mode referred to as SRR mode.

In SUR mode, the image saved to disk is derived from a fit through the measurements up the ramp for each pixel. Because N readouts are involved, the effective read noise is also reduced by a factor of $\sqrt{N/2}$ with respect to LIR readouts. If N=10, the read noise for SUR mode should be about the same as that of MER mode readouts. Normally N will be automatically set by the needs of the AFC algorithm, as the spot images formed from the fiducial holes in the masks must be detectable in each interval.

2.6 Calibration Units

Both LUCIs have *Calibration Units* (CUs) available, equipped with three arc lamps (Neon, Argon and Xenon) for wavelength calibrations and three continuum halogen lamps (Halo1, Halo2, and Halo3) for flat fields. These CUs are mounted on top of the rotator gallery, above each instrument (see Figure 1). They are articulated, so they first pivot out over the primary mirrors and then bend down to position their exit port in front of the LUCI entrance window.

Recommended exposure times for the various combinations of camera, filter, and grating are discussed in more detail in Section 6. Other options are also discussed there, like using twilight flats or doing wavelength

calibrations using OH emission lines from the night sky, as well as their relative merits.

When the CUs are deployed in front of LUCI, they occupy the same space as the ARGOS laser dichroic. Thus there is an interlock preventing the CUs from moving in the beam when the ARGOS dichroic is deployed, and vice versa.

The CUs do not provide perfectly even illumination to the instrument, although they are not bad. For the arc lamps this does not matter, but for flatfields you should be aware of this, how it can affect your data, and take the necessary additional steps to correct it if it matter to your science.

3 The LUCI User Interface

The LUCI user interface has four major components which allow you to fully operate both of the LUCI instruments and carry out observations: the observation execution panel, the real-time display and the instrument control and readout control GUIs. Observations can be carried out just with the first two of these (scripting control and image display). There are additional GUIs that can also be opened for special purpose tasks, like the GEIRS (GENeric InfraRed detector Software) GUI or the telescope service GUI. In this section each of the components is more completely described. Much of this information is also covered on the [LUCI observers cookbook](#) webpage. That link also contains lots of tips and hints for failure recovery.

3.1 Observation Execution Panel

The most important GUI is the observation execution panel. It is here where you load and execute scripts, monitor the status of both instruments, and do the majority of problem recovery. In Figure 4 we show what the observation execution panel looks like. It has six main components, including: the *queue execution panel* at top center, the instrument *status panels* on the left and right of this, and a *log message panel* across the bottom. In the middle, between the *queue execution* and *log message* panels are the last two components, the row of seven green (or red) buttons in the *modification section* that allow one to mask out portions of a script, and a *queue action section* where the basic queue control is located. Each of these is discussed in more detail below.

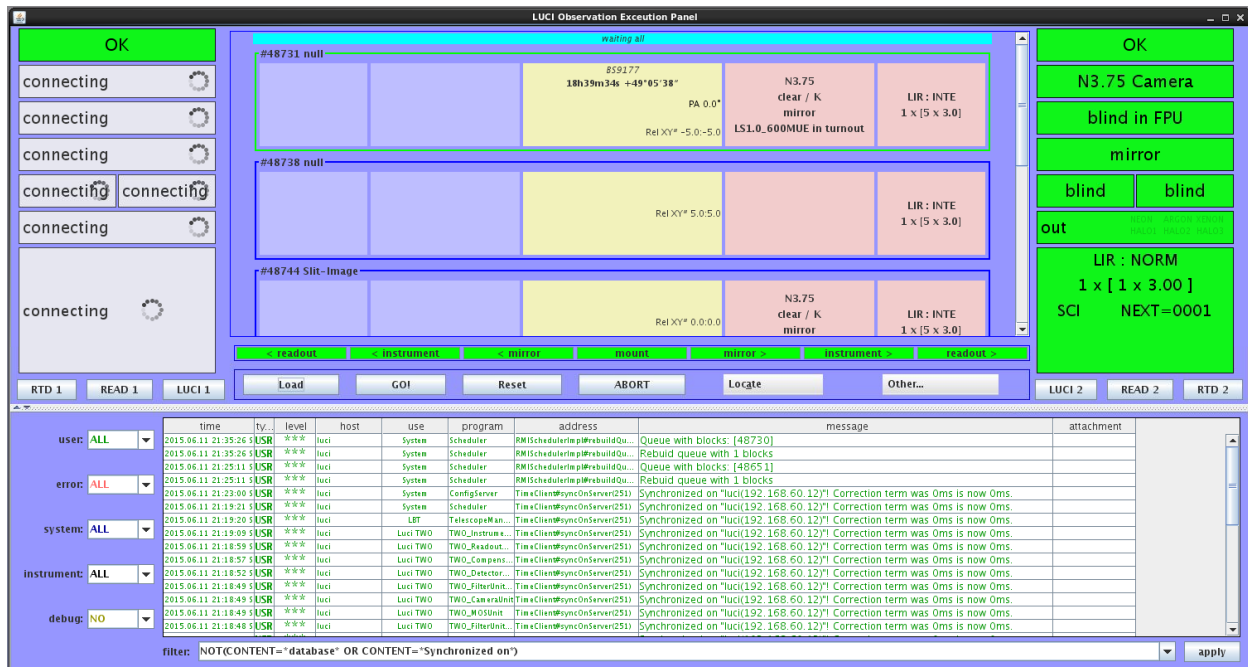


Figure 4: The LUCI observation execution panel

The queue execution panel This section is where the observation items (obsItems) in a given program show up when a new script is loaded. Each obsItem is divided into five sections, from left to right these are: LUCI1 readout and LUCI1 instrument (blue backgrounds), the telescope mount and optics (yellow background), and LUCI2 instrument and LUCI2 readout (pink backgrounds). Other placeholders will also

show up in the queue execution panel, like the cyan bar across the top with the “waiting all” label that represents the synchronization of the two sides prior to a telescope preset. Pauses, which can either be put into the scripts or added interactively, will also show up here. If one of the two LUCIs is not used in a particular script, the corresponding sections of the obsItems will be blank, as in Figure 4 for LUCI1. The instrument sections will also be blank if there is no instrument reconfiguration needed in that obsItem.

Each of these five sections of an obsItem will indicate its state, with the segments that are currently executing given a green outline and a “running” label. Items that are ready to be executed are labeled “ready” with a blue outline, and items that have completed and are waiting for something (either a pause, or at script completion) are labeled “done” with a white outline. Fully completed items are greyed out as a script progresses. In order to fully support binocular observations, each section is processed separately, in seven different threads (corresponding to the seven buttons in the *modification section*, three are associated with the central telescope panel: the mount, mirror1, and mirror2), and synchronized where necessary for proper control. For example, instrument re-configuration and telescope motions (presets or offsets) must complete before the exposure is taken in each obsItem.

Starting from the outside obsItem fields, the detector sections display the basic exposure parameters: read-mode (LIR, MER, or SUR), savemode (NORMal, INTEgrated, or CUBE) and the detailed exposure request: NEXP x [NDIT x DIT]. DIT is the *Detector Integration Time* in seconds, NDIT is the *Number of DITs*, and NEXP is the *Number of EXPosures*. NEXP is almost always kept at 1 because it is usually better to dither on sky rather than repeat an exposure in the same location.

The instrument sections give the new configuration that the instruments will be set to when that obsItem is processed. This includes the camera, filters, mirror or grating, and the mask selection and position.

In the center column of the obsItems the telescope section gives the object name, coordinates, and position angle at top, corresponding to motions of the mount. The bottom left and right report the mirror commands, normally just small offsets that can be implemented only by moving the optics of that side. The offsets include the offset type (RELative or ABSolute), the offset coordinate system (RD=RADEC or XY=DETXY) and the two offset values in arcseconds requested for that side.

Some manipulation of the queue is possible whether a script is running or not. The three main actions are: insert or remove pauses, continue a script after a pause or problem recovery, or jump to a specific obsItem in a script. These can be done when you bring up the *context menu* by right-clicking on the appropriate obsItem. Note the context menu contents will change depending on what functionality might be needed.

To insert a pause in a script after an obsItem, right click the item to bring up the context menu and select pause after this item. You can now insert a pause after an item that is currently executing, and for binocular operations it is also possible to insert a sided pause that only affects one side. To continue a paused script, right click the paused obsItem and select *continue*.

If you encounter recoverable errors, for example a camera wheel error that just needs an init to recover, first fix the problem and then right click the obsItem subsection with the red error box to bring up the context menu and select continue. Problems that are recoverable by the observer, and other basic troubleshooting notes, are detailed on the LUCI cookbook page. Anything beyond that and the OSA should be notified. They will call the ISA on duty as needed.

It is possible to skip forward or backward in a paused script or one that has not been started yet with the “Go!” button, though it is not advisable to do this when there is an error (instrument or telescope). To do this, locate the obsItem you want to skip to and right-click to bring up the context menu, then select “skip to this item”. Clicking “Go!” will then start or resume processing the script at that point. Skipping can also get you into trouble. You do not want to skip over obsItems that change the instrument configuration as those changes will not be implemented correctly. When skipping over or into a series of offsets, be sure you know where you are in the dither pattern.

3.1.1 The status panels

The instrument status panels show you the current configuration of the instruments. These are from top to bottom: an overall status indicator, the camera, the mask ID and position, whether the mirror or a grating is in place as well as the wavelength the gratings are set to, which filters are in use, whether the Calibration Unit is *in* or *out* of the beam with the name of any lamps that are on, and the detector configuration. The detector configuration sub-panel includes the readout configuration as well as image type (SCI, FLAT, etc), the next image sequence number, and the last (full) filename saved to disk. There will also be a countdown timer visible in this sub-panel when the detector is actively integrating an exposure.

For the MOS status, note that there are three valid positions for a mask to be in: *no mask in use* when all masks are in storage, *mask <MaskName> in FPU* when the named mask is locked in the FPU, and *mask <MaskName> ID in turnout* when the named mask is held in a “staging position” near the FPU during MOS or longslit acquisitions. This staging position is used to reduce the amount of time waiting for the mask to be moved into the FPU at the appropriate time. The MOS status sub-panel will be yellow when the mask is in turnout as it is not supposed to be left there for more than the few minutes needed for a spectroscopic acquisition. An alarm will sound if the mask is left in turnout more than 10 minutes. If your mask is in the focal plane unit, it is ready to be used. If a MOS error is encountered, the sub-panel will turn red. **ALL** work must immediately stop if this happens and the OSA notified.

Below the status panels there are three buttons. These allow you to open the *Real Time Display* (RTD1/2; see Section 3.2), the *LUCI instrument manager GUI* (LUCI1/2; see Section 3.3) and the *Readout Manager GUI* (READ1/2; see Section 3.4), specific to that instrument (LUCI1 or LUCI2). Normally you only need to open the RTDs, the others are for manual control of the instrument configuration or detector readout. They can be opened if needed, and then closed when done.

3.1.2 The messaging panel

In the messaging panel all mechanical and software actions carried out by the instrument are reported in a running log. Errors will be highlighted in various shades of pink and the ones connected to mechanical bits of the instruments will also show up on the status panels. The log messages can be difficult to interpret, but this is the first place you should look for answers when something goes wrong. The scroll bar on the right edge can be used to look back at earlier messages.

The queue modification section As noted above, the queue modification section includes seven buttons that control whether commands implied in the obsItems get executed or not for the seven threads controlling the instrument and telescope (two instruments, two readouts, one mount and two mirrors). Normally all seven of these buttons should be green, meaning everything in a given script will be processed. They should all be left on (green) even when running a monocular script on just one side. The LUCI software knows what to do when only one instrument is authorized to use the telescope.

These controls will primarily be useful when trying to recover from problems encountered on the instrument or telescope while running a binocular script. Their operation is simple enough: to turn off one of the threads, click the corresponding green button and answer the popup. To turn it back on, just click the now red button and answer the popup.

Binocular operations are just starting to be used and we will need to gain some more experience with error recovery before adding more detail here. Details of exactly how the instrument and telescope behaves when parts are masked out in the queue modification section will be left to a future update.

The queue action section The queue action section is the one you will use the mostly while observing, other than monitoring the instrument status. The actions that occur when clicking any of these buttons are summarized here:

LOAD Navigate to your script in the pop-up and double-click it. This will load the script and display the individual obsItems in the queue panel.

GO! Starts the execution of the script.

Reset When a script is not executing, for example it is paused or stopped because of an error, the reset button will reset the pointer to the top of the script and clear out any displayed ready, error or done messages.

Refresh A refresh will update the current status of both instruments and the display of the progress on your script. Normally these stay in sync, but start with a refresh if you notice any problems.

Locate While the script is being processed, the queue execution panel does not auto-scroll to keep the active segments visible on the screen. You can use the *Locate menu* to jump to the position in the queue that is currently executing or done and waiting for other sections to catch up.

Other Here you can enter names for the support personnel (metadata). The edit queue button currently does not work. See below for details on the Abort option.

ABORT Yes, there is an abort button, but we have hidden it in the *Other* button's dropdown menu. This is because abort tends to be overused and probably does not do exactly what you think it does. When you abort a running script, LUCI will, as appropriate, stop waiting for a reply from the telescope and will interrupt any in-progress readout of the detector. Instrument reconfiguration, in particular MOS mask motions, will not be interrupted as it is not safe to do so. Since this is usually the part that takes the longest to complete, you are better off waiting until the instrument configuration completed before considering an abort.

3.2 Real-Time Display

The real-time display (RTD) is the other primary UI element used regularly in normal observing. It is the GUI where the images are displayed and all interaction with the images takes place. It consists of two parts: the *RTD control GUI* and the *RTD* display server itself. The display server is based on *Aladin* (<http://aladin.u-strasbg.fr/>) and was modified by the developers in collaboration with the LUCI Team to better fit with LUCI's needs.

Aladin is a powerful tool, with some more extended data analysis routines (measuring fluxes, FWHM, etc.) built in. A full description is beyond the scope of this manual. For additional information, refer to the Aladin manual on the developer's website (see link in Section 1.2).

3.2.1 The Real-Time Display Control GUI

To start the RTD control GUI for either instrument, you just click the *RTD1/2* button below the corresponding status panel on the LUCI observation execution panel and the RTD control GUI will pop up (see Figure 5, left side).

The control buttons on top are used to start/stop the Aladin display server, reset everything and load a BadPixelMap into the buffer. Below this are the five function tabs: *LiveView*, *MOS*, *Long slit*, *Sub windows* and *AFC* (active flexure compensation). The *LiveView* tab is where you should work if you are examining data as it is generated by a script. The most recently saved image will automatically be displayed. You can then subtract off a background/sky or dark frame as needed. The *MOS* and *Long slit* tabs are used during spectroscopic acquisitions. When everything is working correctly, the filenames will be auto-populated in the appropriate fields.

The *AFC* tab is used to make a correction to the field stop position on the detector when AFC is to be used. Masks that are usable for AFC observations must have fiducial references (holes) cut in them, to provide point-like reference sources for the AFC algorithm. During alignment, **specific** spots are adjusted to known positions. This is also currently under development. Further details will be added when the commissioning is completed.

Sub windows (use of this feature has not released yet) may be used when integration times well below the standard 2.503 sec in LIR-mode are required. Because of the detector architecture, you can estimate the minimum DIT for a given number of pixels in the X direction on the sub window as: $(X_{subwin}/2048) \times DIT_{min}$ for the full frame. For example, for a sub-window width of 128×128 pixels the minimum exposure time is about $(128/2048) \times 2.503$ sec or ~ 0.16 sec. With 32 parallel readouts, the Y dimension can be anything up to the full detector height.

3.2.2 Image display and image analysis

In Figure 5 we see the RTD GUI with the LiveView tab selected, on the left. The Aladin display panel itself, on the right, allows you to perform some simple checks like photometry or image quality using eg. the *phot* button on the right hand side. For a full description of the options, please refer to the Aladin User's Manual (see link in Section 1.2). We do strongly recommend you take a little time to familiarize yourself with Aladin as it is not completely intuitive.

3.2.3 Long Slit alignment

For long-slit alignment you need to identify the source you want on the slit, either the science target itself or a nearby reference from which you plan to make a blind offset, and then the place on the slit where you want the source to be moved to. The details are given on the cookbook page and won't be repeated here. When you prepare your script in Scriptor, be sure to include an offset sky frame for subtraction if your source is faint enough. If you are not sure, as in anything other than a telluric star, it is best to take a sky frame.

During long slit alignment you only correct the source position with XY offsets. The position angle of the slit is assumed to be correct, and is within a small enough uncertainty ($< 0.1^\circ$) that it does not matter for single targets.

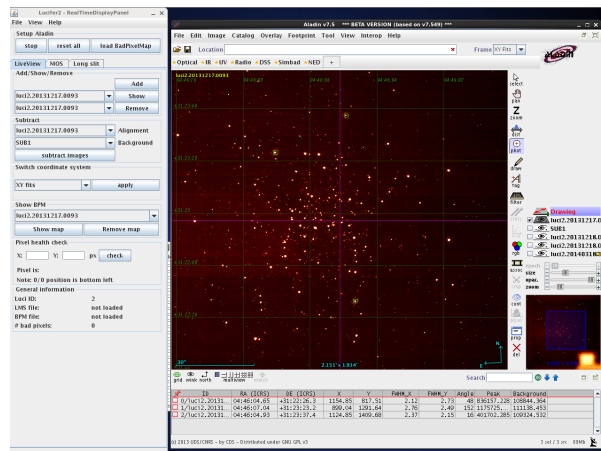


Figure 5: The LUCI Real-Time Display with the Real-Time Display Control GUI on the left and Aladin on the right.

3.2.4 MOS alignment

For alignment of a MOS mask the process is similar, but you need to correct the translation *and* rotation of the mask and sky on the detector so that the multiple science targets will all be well-aligned in their slitlets. For this, you need multiple reference stars that were identified when the mask was generated using the LMS software. You will still need sky, source, and through-slit images. The details of the acquisition process are given on the cookbook page and won't be repeated here. When everything is working smoothly, the sky, source, and through-slit images will be correctly populated on the MOS tab on the RTD GUI.

As of this writing (August 2016) note that alignment boxes are *required* on at least three stars visible in the acquisition images in order to successfully align a mask on sky. It is better to have more stars because often one needs to be deleted from the fit. The main reasons a star might need to be deleted include that it is too faint for acquisition, although anything even faintly visible on 2MASS data should work, or it was not corrected for a higher than average proper-motion. We are working on restoring the ability to use more stars without alignment boxes to improve the acquisition accuracy, though it will always be a good idea to include at least a few on boxes as a sanity check.

3.3 Instrument Control Manager GUI

The *Instrument Manager* GUI allows you to manually configure all of the relevant mechanisms inside LUCI, including the camera and filter wheels, grating turret, and MOS masks. You can start or stop flexure compensation, move the calibration unit in or out, and turn calibration lamps on or off. It is generally only used for quick tests on sky, or sometimes to take calibration data, so it can be left closed during observing. To open the IMGUI, click the “LUCI1” or “LUCI2” buttons at the bottom of the status panels on the observation execution GUI.

Figure 6 gives you an overview of the IMGUI. The background color for this (and all other engineering) GUI is blue for LUCI1 and pink for LUCI2. The right hand side shows the state of the instrument the last time it was changed via that GUI. It does not automatically keep in sync with the current configuration of the instrument, so we recommend you always click on the *refresh* button at bottom before making any manual reconfigurations. This will re-read all of the mechanism positions and update the GUI entries on the right side, and set the left side to be the same.

At the top of the IMGUI there is an “initialize” dropdown menu where you can initialize individual mechanisms separately, all mechanisms, or all but the MOS unit. Start any given night by initializing all units. If you have any mechanisms encounter an error *except for the MOS unit* and the log does not seem to indicate more than a random error, then initializing that unit should clear the error. For MOS errors, all observing must stop immediately and the OSA must be notified.

When you select a grating you must also supply an appropriate wavelength (Table 4) in microns. Hovering the cursor over the input field will show a tool-tip with the allowed ranges. Make sure to select the appropriate filter(s) for your grating and order.

If you are happy with your selection, simply click on the green *submit* button. The button will turn yellow indicating something in the instrument is *moving*, and the LUCI configuration will be changed accordingly. Mechanism motions will also be indicated on the status panels of the observation execution GUI.

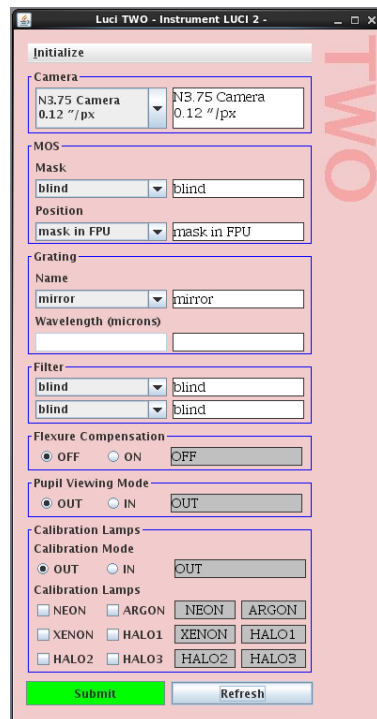


Figure 6: The *Instrument Manager* GUI.

3.4 Readout Manager GUI

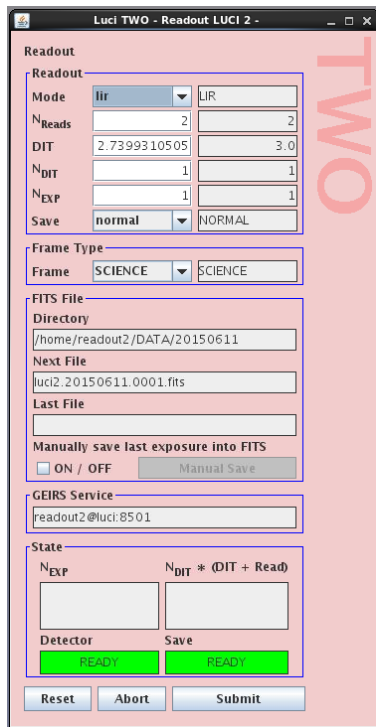


Figure 7: The Readout Manager GUI.

As with the IMGUI, the *Readout Manager GUI* allows you to manually set all of the relevant parameters for reading out the detector (DIT, NDIT, NEXP, readmode, savemode, frame type). The last and next filenames are also shown, as is an exposure countdown timer. The RMGUI is not normally needed for routine observing and can be kept closed unless needed. To open the RMGUI, click the “READ1” or “READ2” buttons at the bottom of the status panels on the observation execution GUI.

The RMGUI is shown in Figure 7. The right hand side shows the parameters for the last readout of the detector and this will update every time a new exposure is taken, scripted or manually. On the left side you can change all of the standard parameters. At the bottom of the GUI are “Reset”, “Abort” and “Submit” buttons. Reset is like a software initialize for the detector controller, loading in defaults for the parameters. The “Abort” button will immediately interrupt any ongoing exposure and that data will be lost. “Submit” is used to trigger an exposure that will use the parameters you have entered on the left.

You can also turn off auto-save, though this only affects manually triggered exposures as all scripted exposures are saved. Checking the ON/OFF button means you are required to click the *Manual Save* button to save an exposure. When there is an exposure to be saved, this button will turn red. Uncheck this box to return to automatic saves.

The frame type can be set to CALIB, FOCUS, FLAT, DARK or SCIENCE. It is useful to set the frame type properly, as it helps with archive queries, however, the scripts do not currently allow for this to be set. For other parameter:

- MODE The readout mode - LIR, MER and SRR (SUR) modes. Others may be listed, but they are intended just for engineering tests.
- N_{Reads} The number of reads. This should be fixed at 2 for LIR mode and 10 for MER mode, and auto-set for SUR mode from scripts. Please don’t change this manually.
- DIT The detector integration time in seconds. Enter zero here to get the minimum exposure time possible.
- N_{DIT} The number of DITs.
- N_{EXP} The number of exposures (normally left at 1). One exposure is $[N_{DIT} \times DIT]$ of data.
- Save The save mode: normal (NDITs saved separately), integrated (NDITs summed, saved as one image) and cube (NDITs saved in a 3D FITS file).

For normal seeing-limited or AO imaging observations, you would set DIT by the sky background or bright source peak count rates to avoid saturation and/or reach the background limit as needed for your science. N_{DIT} is set so that the product $[N_{DIT} \times DIT]$ is at least 60s so that the AGW can keep the telescope well collimated. N_{EXP} is almost always 1 as it is better to dither in order to get good sky subtraction.

For normal spectroscopic observations you follow a similar plan, though the exposure times are usually long so both N_{DIT} and N_{EXP} are almost always 1.

3.5 Telescope Service GUI

Another optional GUI only occasionally needed during normal observing is the *Telescope Service GUI* (see Figure 8). This GUI allows you to perform telescope presets or offsets manually, interrupt waiting for collimation, and some other telescope-related functions. The *Telescope Service GUI* is not automatically opened during the LUCI startup procedure (see 3.7). Instead, you need to open an XTerm on your console and type `open_observer luci2 telsvc` to open it.

The two main functions of the telescope service GUI are to (1) execute manual offsets to tweak spectroscopic mask alignment and (2) abort waiting for the telescope collimation.

(1) To execute offsets manually, enter the offsets you want, set the coordinate systems (normally this would be DETXY, but check), click “Right Offset” or “Left Offset” to enable them (the buttons will turn green) and then click Commit Offset to send the offset request to the telescope.

(2) LUCI will automatically wait for the telescope to reach a set wavefront error (≤ 600 nm) to be reached before the telescope is considered to be collimated after each new preset. If your collimation is good enough, for example you had to re-send the preset to the same target where you were already collimated, you can save a little time by bypassing this wait for collimation. Click the Abort wait for coll. button. LUCI will automatically reset to wait for collimation on the next target.

The remainder of the fields on the telescope service GUI are needed for manually sending telescope presets, binocular operations, or recovering from problems, and will not be described further here.

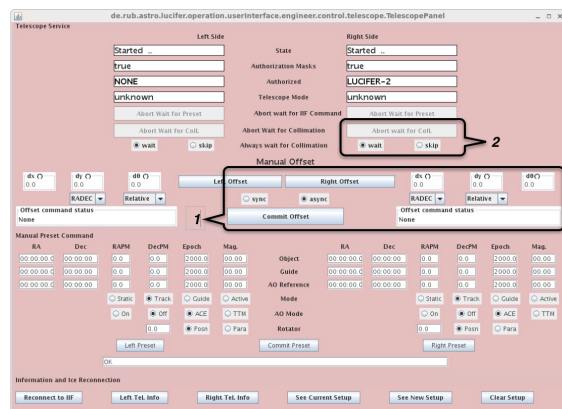


Figure 8: The *Telescope Service GUI*.

3.6 GEIRS

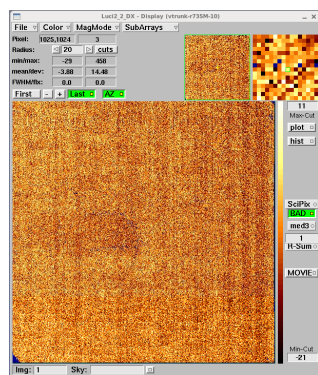


Figure 9: The GEIRS Display GUI.

The LUCI HAWAII2-RG detectors themselves are controlled by a lower level engineering service known as GEIRS (GENeric InfraRed detector Software), developed at MPIA. As part of the normal LUCI UI startup we currently have GEIRS open. First a gray initialization panel pops up (not shown), where you should enter your Observers Name and click OK. Then a small GEIRS control GUI (not shown) and the GEIRS display (Figure 9) will show up. Since these will not be used by regular observers it will not further be described. They are also not normally needed during regular observing, so their automatic startup will probably be stopped.

3.7 LUCI Software Start-Up

LUCI can be run from the mountain obsN ($N = 1..6$) computers or from the Tucson remote operations room rm525-N ($N = 1..5$) computers. The LUCI User Interface is still in active development, so keep in mind that some labels may change or move. The startup is now completely scripted, so you can open everything you need with one command. The full startup procedure is detailed on the observing cookbook page.

4 Observation Preparation Tools

There are a number of steps to take to prepare an observation of a given source, including standard stars and all other calibrations like flat-fields and spectra of arc line sources. Many tools, programs, or web pages are available to help set up your observations. We will cover each step in more detail below, but list here a basic summary:

1. **TELMODE:** Understand the *telescope mode* you want to use for your observation.
2. **ETC:** Visit the ETC to determine if you can reach a sufficient SNR on your target(s) of interest.
3. **LMS:** Design a MOS mask if you have multiple targets in the same field of view (optional).
4. **Scripts:** Create the observing script(s) needed to take the data.
5. **FCs:** Create finding charts so the fields can be easily and quickly identified.
6. **README:** Write up a README file to summarize your program, give special instructions, provide contact information, etc.

Please keep in mind that in most cases you are assembling this information so that *any* observer (i.e. not you) can successfully take the data you need. The more thought and care you put into the preparation, the smoother and quicker your program can be executed. Avoiding unnecessary overheads, last minute corrections to scripts, or problems identifying the science target(s) from the finding charts all save telescope time, leaving more time available for other programs.

4.1 Telescope Mode

To date, almost all science observations with LUCI have been done in seeing-limited mode with an off-axis guide star used to close the guiding and collimation loops, known as the *ACTIVE* telescope mode. With the adaptive optics modes and ARGOS coming available in the near future, it makes sense to start by considering which telescope mode will let you best accomplish your science goals, so we briefly describe them here.

ACTIVE In *ACTIVE* mode the off-axis AGw uses your selected guide star to keep the telescope on source and collimated. This is the traditional seeing-limited mode familiar to previous LUCI users. The patrol field for the AGw probe is large (see Figure 18) and guide stars can be used with R-band magnitudes in the range of 12^m0 to 16^m5 under most conditions encountered at the telescope. The guide loop cycles every 4-8 seconds while the collimation loop cycles every ~ 45 seconds.

We do see some residual PSF variations in the delivered image quality across the LUCI 4 arcminute field of view in *ACTIVE* mode. Stars towards the top of the LUCI FoV, that are closer to the guide star, tend to be rounder and with a smaller FWHM than those towards the bottom of the FoV.

ADAPTIVE In *ADAPTIVE* mode the on-axis high-speed wavefront sensor uses your selected AO reference star to correct atmospheric turbulence, delivering a diffraction-limited image to LUCI in a 30 arcsecond field of view. The AO reference star, that can also be the science target, can be as faint as for the AGw with R-band magnitudes down to 16^m5 , but the system works better with brighter stars and you need stars brighter than $\sim 10^m0$ for the best performance. Anisoplanatism limits the useful distance of the reference star from the science target to a few tens of arcseconds or less, so the patrol field is smaller (see Figure 18) than for the AGw.

You do still need to provide an off-axis guide star as well as the AO reference star for ADAPTIVE mode observations. This is because the telescope may not be collimated enough at a new position to directly close the loops, so the off-axis star is used to collimate the telescope first. Scriptor or the OT will guide you through selection of both stars.

ESM In Enhanced Seeing Mode (ESM) the AO system is used to correct tip-tilt and also the low order Zernike modes. It runs at 100 Hz independent of the brightness of the reference star, and only corrects 10 modes ($Z_2 - Z_{11}$: tip-tilt, focus, coma, astigmatism, trefoil and spherical aberration). ESM will work with reference stars down to $R < 16^m.5$.

In comparison tests, ESM mode consistently delivered rounder PSFs and a better FWHM (about $0.75\times$) than standard ACTIVE mode data taken on the same test fields. The improvement was fairly consistent across the full 4 arcmin LUCI FoV, reflecting the large ground-layer contribution to seeing at the LBT. In addition to the rounder PSF, you could use somewhat narrower slits ($0''.75$ vs $1''.00$) to improve the spectral resolution and reduce the background.

The improvement is not as good as with ARGOS (see below), but it is significant enough over ACTIVE mode that we suggest ESM mode be used instead of ACTIVE mode if a suitable reference star is available in the AO patrol field. You do still need to provide an off-axis guide star as well as the AO reference star for ESM mode observations, for the same reasons as mentioned above.

ARGOS With ARGOS, three lasers are used as Rayleigh beacons on each telescope to directly sense the mean ground layer turbulence across the LUCI 4 arcminute field of view. It corrects more Zernike modes than the 10 done with ESM mode, and the system runs at 1 kHz. ARGOS still needs a guide star for the AGw to do the initial collimation of the telescope at new positions, but with a restricted patrol field because of the laser dichroic (see Figure 18). You must also select an AO reference star, as with AO or ESM modes, to be used for the tip-tilt signal. The same star can be used for both guiding and as the tip-tilt reference as the AGw probe is parked when the ARGOS setup begins. The magnitude limits on these stars are the same as for ACTIVE, and ESM modes.

With ARGOS you get a better correction...about a factor of 2 improvement over ACTIVE (seeing-limited) mode. This allows you to use narrower slits ($0''.50$ vs $1''.00$), that give you higher resolution and lower backgrounds (higher SNR). The tradeoff is that ARGOS will always be block scheduled because of additional staff to run the system, targets will need advanced clearance from Space Command as with all US-based laser AO systems, there is air traffic interference, and overheads are higher.

GUIDE, TRACK and STATIC There are also GUIDE, TRACK and STATIC modes. Because of the way the LBT is constructed, with very fast optics, cantilevered primary mirror supports and one-armed secondary mirror swing-arms, the telescopes are very sensitive to changes in temperature and really need to be constantly collimated, but none of these modes do that. With STATIC mode the telescope is not moving. This is typically only used for twilight flats when the sun is still above the horizon. For TRACK mode, the telescope is just tracking source coordinates with no feedback, used for dithered twilight flats with the sun below the horizon, or sometimes to take standard stars during morning twilight once the sky is too bright for the wavefront sensor. In GUIDE mode the telescope is guided but the wavefront sensor is not correcting the collimation.

4.2 Exposure Time Calculator

The LUCI exposure time calculator (ETC) is a web-based tool to help you to estimate the total exposure time needed on your science targets to reach your desired SNR. The ETC knows the zero points and sensitivity of both LUCIs in the different available bands and modes. A link to the ETC can be found in Section 1.2. It is fairly straightforward to use. If you run into problems, contact the [LBTO Science Operations group](#).

The ETC does not currently directly support AO imaging or spectroscopic observations. For imaging you can, however, use it to estimate a source detectability in a straightforward manner. Use the seeing-limited mode on the ETC and enter a seeing of 0''.5, 0''.375, or 0''.25 for K, H, or J bands, corresponding to 4, 3, and 2 pixels on the N3.75 camera, respectively. This size in pixels corresponds to the approximate pixel size of the Airy disk on the N30 camera in those bands. Assume to first order the core of the Airy disk contains a fraction of the total flux corresponding to the Strehl ratio (*at your target!*), and for background-limited observations the sky noise is reduced by the square root of the ratio of the aperture areas. Since we have set this example up assuming equal FWHMs in *pixels*, this is equal to the ratio of the N3.75/N30 pixel sizes in arcseconds. So the magnitude limit for AO observations will be those from this seeing-limited estimate scaled by:

$$m_{AO} \simeq m_{SL} + 2.5 \log(\text{Strehl\%/100}) + 2.5 \log(0.12/0.015)$$

For 50% Strehl, this is about 1.5 magnitudes or a factor of 4 in flux over otherwise excellent seeing-limited conditions.

Is it really that simple? No, of course not! In reality, what you get is dependent upon the nature of the turbulence in the atmosphere at the time of observation, as well as the brightness of your AO reference star and the distance from the AO reference star to your science target. A full discussion of this is well beyond the scope of this *User's Manual*. If you plan to take AO observations, please discuss it in detail with colleagues familiar with adaptive optics observations, or contact the [LBTO Science Operations group](#).

4.3 LUCI Mask Simulator

To design a mask for multi-object spectroscopy (MOS) you need as input an astrometric catalog or image with accurate *relative* positions. The absolute astrometry is less critical as it is empirically corrected at the time of acquisition. To generate the mask design files you use the LUCI mask simulator (LMS) software (see link in Section 1.2). A full description of how to use the LMS software to design MOS masks is included in the LMS User Manual, so we do not repeat it here.

LMS produces as output a *Gerber file* (.gbr) as well as .lms and .eps files, all with the same root name. The Gerber file is uploaded to our laser milling machine to cut the masks. The masks are cut out of 150 μm thick rolled stainless steel sheet that has been painted flat black on the side facing into LUCI to reduce reflections. The .lms file is used by the LUCI observing software to know where the slits and alignment stars should be for mask alignment on sky. The .eps file can be printed. All files generated by LMS should be included when submitting masks to your Partner Coordinator.

4.4 Scriptor — Observing Tool

The new LUCI instrument control software (or *User Interface*) has been in use since September 2015 for monocular observations with LUCI2, but it was built with binocular observing in mind. Scriptor is a web-based tool for generating the XML-based scripts executed under this new software. Although the scripting format has changed, keep in mind that the basic approach to near infrared observing is the same as for LUCI1 or any other near-infrared instrument. As there is a complete webpage set up for PIs to refer to when running Scriptor, we defer all detailed discussion to that page:

http://scienceops.lbto.org/sciops_cookbook/writing-luci2-scripts/

While Scriptor currently works well for the majority of standard observations (seeing-limited imaging, longslit and MOS spectroscopy), some less common modes or those currently in commissioning (AO, ARGOS, ESM) are not as well tested. There are a couple of known problems, as well: editing existing spectroscopic scripts sometimes results in duplicated obsItems for acquisition, and currently the automatic creation of calibration scripts for spectroscopy fails. As we release new capabilities of the instruments to the partnership, those parts of Scriptor will be improved until the OT (see below) is ready. If you run into any issues generating LUCI2 scripts, the first step would be to reset the program and try again from scratch. If you still run into problems, want to do something really non-standard or cannot figure out how to do it with Scriptor, please contact the [LBTO Science Operations group](#).

Scriptor cannot directly create binocular LUCI1+LUCI2 observing scripts, although the UI can run properly prepared binocular scripts. As of this writing (August 2016) the only tool available to prepare a binocular observation is a Python script to “twin” a monocular script. In this mode, both sides must be doing exactly the same observations.

We are currently developing a more comprehensive *Observing Tool* (OT) for preparing observations for all of the LBT facility instruments. It is nearing initial release as of this writing (August 2016). It will become the default way to prepare LUCI scripts in the future, and Scriptor will eventually be deprecated. Your Partner Coordinator will pass along the announcements as they happen.

4.5 Finding Charts

The goal of a finding chart is to allow the observer to immediately identify the field and the science target, blind offset reference source, or MOS mask alignment stars rapidly. If it takes longer than 5-10 seconds to identify the field, usually the finding chart is to blame. In Figure 10 we show an example of a finding chart we consider to be good enough for a random observer to rapidly identify the target during spectroscopic acquisition.

Aside from your own (or published) imaging on your target field or pre-imaging with LUCI, the main sources for imaging data usable for finding charts are 2MASS, DSS, and SDSS (links below).

For 2MASS note that the point source catalog has 10-sigma source magnitude limits at 15.8, 15.1, 14.3 mag for J, H, Ks respectively for $|b| > 10^\circ$. 4σ would be a magnitude deeper than this. As the LBT is considerably larger than the 2MASS telescope, any source even *barely* visible in 2MASS will be quite well detected in LUCI on a 60 second exposure. Point sources down to $K \sim 17^m0$ are usable for alignment, and compact galaxies even a magnitude fainter than this should be visible in good conditions.

For DSS or SDSS, note that the relative brightness of sources can change considerably when comparing optical and NIR data, and these optical surveys are much deeper than 2MASS. If you must use either of these sources for your finding charts, consider using the reddest survey band and acquiring your field in the J band with LUCI in order to minimize the differences (your intended science and the properties of your target can modify this, of course). Also, don't stretch the images so hard you can see every little faint source...90 percent of these will not be visible on the LUCI images.

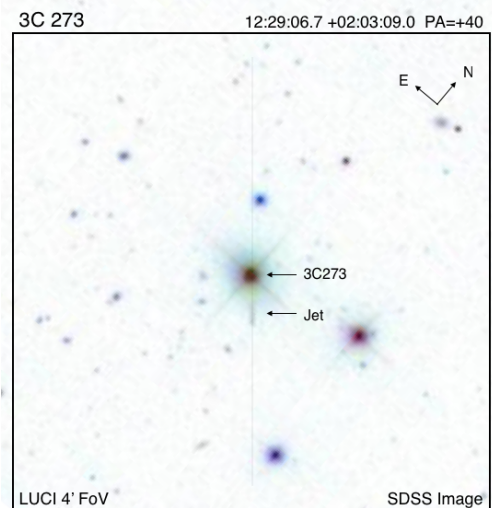


Figure 10: An example finding chart for a LUCI target made with a background image from SDSS.

Additional information, and example finding charts, can be found on our [writing scripts reference webpage](#). In particular, a good finding chart will have these properties:

- Similar depth and preferably wavelength band as the acquisition image on LUCI
- Background image rotated to the requested position angle
- Scale and orientation clearly marked; if larger than the acquisition FoV mark that as well
- Science target, blind offset reference source, or MOS mask acquisition stars clearly marked

In Section 1.2 you will find a link to the RSA finder chart tool, which is particularly useful for retrieving 2MASS and SDSS data for making finding charts.

4.6 The README File

A good README file should convey the most important information needed by someone *other than you* to correctly execute your program. It should include the following (in about this order, for consistency):

- A short summary, including the main goals and criteria for success of your program.
- Preferred conditions as well as minimum acceptable conditions
- Prioritized list of submitted observing scripts, including calibrations
- Note any time critical items, particular order of observations, or any other special requests
- Contact information for the PI or anyone who knows the science goals

4.7 Working with a Binocular Telescope

At present time (September 2016) it is possible to take a monocular LUCI1 or LUCI2 script and *twin* it, so that the exact same observation is run on both instruments simultaneously. We would like to keep this something that is done at run-time by the observers so that we can continue to develop the twinning capability. PIs, please continue to build *monocular* scripts for LUCI2. If both instruments are available the intention is to automatically run the observations on both sides, almost halving the needed clock time to gather your data. In the discussion that follows we seek to convey a basic general understanding of how binocular observations are constrained on the LBT. This will help you as we generalize the operations to include mixed modes (e.g. imaging and spectroscopy) and mixed instruments (e.g. MODS1 and LUCI2).

Functionally the two telescopes of the LBT, SX and DX, are independent of each other. The optics are articulated and can move in 3 axes by quite a bit, one of the things that makes the LBT unique among large telescopes. The primary mirrors can move ± 2.6 mm and the secondary mirrors can move ± 10 mm. Some of this range is used to keep the optics collimated with changes in elevation, but it also gives the two telescopes their independence from each other. The TCS treats them as independent telescopes and you should approach your binocular observation planning from this point of view as well. Of course, there is only one azimuth axis and one altitude axis carrying both telescopes, so there is one primary constraint enforced on all binocular observations: both sides must remain *co-pointed* to within $\sim 40''$ of where the mount is pointed, with some subtle nuances described below.

While technically there is no direct concept of a “mount” in the TCS, it is useful to consider a “mount point” projected on the sky in the discussion here. Assume that on completion of any preset to a new target, the mount point is at the midpoint between the target RADEC coordinates requested for the SX and

DX telescopes, often these will be the same coordinates, so everything would be co-pointed. Interferometers like LBTI by default must operate co-pointed, but for binocular observations with the facility instruments (LUCI, MODS and LBC) as long as both sides remain within $40''$ of this mount point you are free to work completely independently on the two sides. This includes any dithering within this co-pointing radius. A good example of this would be MOS spectroscopy, where the alignment offsets are usually only a couple of arcseconds and the dithering is kept small because of the slitlet lengths. Offsets are applied by moving the optics of that telescope, *not the mount*, so the *other* side never knows anything happened. This is known as an *asynchronous* motion. Asynchronous motions have only one constraint, modifying slightly the original statement above: that *all* points, starting and ending, for both sides must lie within the $40''$ co-pointing radius from the mount point. The mount point does not move.

It is also possible to do motions that exceed this co-pointing limit. This is done every time you move (preset) to a new science target, but you would also do this to take off-source sky frames when observing large extended sources or need to do a blind offset that exceeds the co-pointing limit. In order to do so *both* instruments must agree to the motion for it to be executed. If the request from one side comes in early, the TCS will wait until it receives the second request. This is so a request from one instrument *cannot* affect any ongoing exposure on the other side. Because the mount is involved, a new mount point is defined at

the destination, and the co-pointing constraint is applied to the new telescope positions. This is known as a *synchronous* motion. Synchronous motions have only one slightly different constraint: that *only the end points* for both sides must lie within the co-pointing radius of the newly defined mount point.

Although this is a LUCI User's Manual, this discussion of binocular observations is generic. It applies to LUCI-LUCI as much as LUCI-MODS or any other combination of non-interferometric instruments on the LBT. We illustrate these two types of motions in Figure 11. On the left we show the mount point (plus) at the initial midpoint of the SX and DX positions (circles). Offsets done asynchronously can only be to points within this initial co-pointing radius as the mount point does not move, and the offsets do not have to happen at the same time. On the right we show an offset that will exceed the co-pointing radius. Here a new mount point is defined at the midpoint of the new SX and DX positions, and because the mount is involved the offsets on both sides must happen at the same time.

The key to planning efficient binocular observations is to ensure that both sides get to any synchronous operations (presets or offsets) at about the same time. To do this, the planning tool must include a fairly detailed knowledge of all instrumental overheads incurred during the planned observations, and guide the user to adjust the observations to make better use of the available time. This is beyond Scriptor's current capabilities, however the two LUCIs are sufficiently identical that most LUCI observations can be "twinned" - doing exactly the same thing on both sides (the same is true for binocular MODS observations). The OT being built as part of **Q** will include more complete and general method to build binocular scripts.

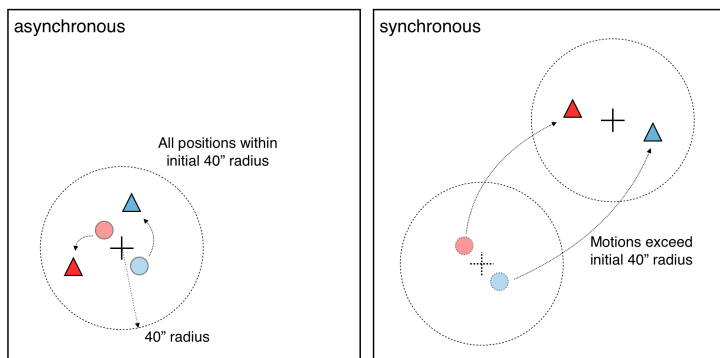


Figure 11: How to apply the co-pointing constraints to binocular motions.

5 Sensitivity

The imaging throughput of the LUCI instruments was determined from observations of standard stars from Persson et al. (AJ 116, 2475, (1998)) through the N3.75 camera (standard imaging mode). It is about 30% in J and H-bands and almost 40% in K-band. This is consistent with the expectations from the individual component’s efficiencies or transmissions, including the instruments, telescopes and atmosphere.

Similarly, the spectroscopic throughput was determined from observations of stars with known spectral type (A0V-stars) and magnitudes using a wide slit and the N1.8 camera (standard spectroscopic mode). It is about 14%, 20% and 20% for the G210 grating through the J, H and K filters, respectively, and about 21% for the G200 grating in the H+K bands. As for imaging, this is consistent with expectations considering the measurements of the individual components, including the instruments, telescopes and atmosphere.

When changing cameras, filters or gratings from these standard configurations, the total system throughput should only change by the relative throughput of the changed parts.

5.1 Photometric Zero Points and Sky Backgrounds

The photometric (imaging) zero points and sky background count rates for both LUCIs are listed in Table 9. All of these measurements were determined through the N3.75 camera in standard imaging mode. The zero points are effectively the magnitude of a source that would generate 1 ADU/second of flux integrated over an arbitrary aperture, i.e. independent of the seeing. To convert these values to electrons, you must include the gain factor of $2e^-/\text{ADU}$.

Table 9: Imaging ZPs and sky background count rates.

Filter Name	LUCI1		LUCI2	
	ZP [mag]	Sky [ADU/s/pix]	ZP [mag]	Sky [ADU/s/pix]
z			25.49±0.01	35
J			26.34±0.15	220
H			26.02±0.01	950
K			25.74±0.08	1310
K _s			25.40±0.01	710
Y1			24.74±0.02	10
Y2			24.96±0.01	20
OH_1060			22.83±0.03	1
OH_1190			22.94±0.02	1
HeI			21.65±0.02	5
P_gam			22.79±0.01	5
P_beta			23.02±0.03	10
J_low			25.57±0.01	45
J_high			25.34±0.02	65
FeII			21.57±0.01	35
H2			21.17±0.02	25
Br_gam			22.74±0.02	25

The sky background count rates are average values measured on photometric commissioning nights. The

longer wavelength filters, especially K band, can vary with ambient temperature while the shorter wavelength filters can vary with the phase of the moon as well as the angular separation of your target from the moon. Keep in mind that the NIR sky background is strongly variable, with $\sim 10\%$ changes over a few minutes timescale, as discussed in Section 8.1.2.

5.2 Limiting Magnitudes

These ZPs, background count rates, estimates of extinction (see Section 8.1.1), as well as assumptions on the seeing and transparency allow one to calculate the expected signal-to-noise ratios for a source of a given magnitude. This is all built into the LUCI ETC (see link in Section 1.2). The limiting magnitudes presented below for both imaging and spectroscopic observations are meant just as a rough guide. Investigators are strongly encouraged to use the ETC for their specific science goals.

Table 10 includes the expected 3-sigma limiting magnitudes for imaging through the main broadband filters (JHK). We assumed a seeing of $0''.8$, an airmass of 1.5 and 1.6 mm of water vapor. We used a DIT of 10 sec (fully background limited) and NDIT=360 to obtain one hour on source integration. For real observations this would typically consist of 60 dithered exposures of 6×10 sec each, but the ETC only works with total exposure times and does not care how the data are taken. The typical sky background is also given, expressed as magnitudes per square arcsecond. For background noise contributions, we assume an extraction aperture of twice the seeing.

Table 10: Limiting magnitudes for imaging at SNR=3 in one hour integration

Filter	Sky mag.	Limiting mag.
J	15.9	24.1
H	14.0	23.0
Ks	13.7	22.5

Table 11: Limiting magnitudes for spectroscopy at SNR=5 in one hour integration

Grating	Band	λ_{cen}	Limiting mag
G210	z	0.96	19.2
G210	J	1.25	18.8
G210	H	1.65	17.8
G210	K	2.20	17.5
G200	zJ	1.17	19.2 (J)
G200	HK	1.93	18.0 (K)

For spectroscopic observations, Table 11 includes the expected 5-sigma limiting magnitudes for the main seeing-limited spectroscopic configurations. We assumed a $1''.0$ slit, a seeing of $0''.8$, an airmass of 1.5 and 1.6 mm of water vapor. We use a DIT of 300 sec and NDIT=12 to obtain one hour on source integration. For real observations this would typically consist of 12 dithered exposures of 300 sec each. For the grating/orders their standard central wavelength was used. The SNR is extracted over a single pixel width in the dispersion direction (per pixel, not per resolution element), while in the spatial direction we include pixels covering twice the assumed seeing.

For AO observations there is one other parameter and some side effects to consider. In seeing-limited imaging mode, one assumes all of the source flux is within the usual near-Gaussian point-spread function (PSF). For AO imaging observations, only a fraction of the total flux is within the central peak of the Airy disk, with the remaining flux in the diffraction rings or uncorrected wings of the PSF. To first order you can assume that fraction is the Strehl ratio, so there is a correction factor of $2.5 \log(\text{Strehl})$ in the limiting magnitudes for AO observations. The main sensitivity gain with AO observations, though, still comes from decreasing the contribution from background noise. The same is true for AO spectroscopy, but also note that the standard AO longslit width of $0''.13$ is quite a bit larger than the central core of the Airy disk. This is to minimize diffraction effects at the slit. Spectroscopic resolution will thus be driven by the size of the Airy disk and not the width of the slit.

6 Calibration

Calibration data needs to include all of the necessary information so that the signatures of instrument (LUCI: e.g. saturation, linearity, QE variations, grating curves), the telescope (LBT: e.g. pointing, collimation, throughput), and the site (Mt.Graham: e.g. extinction, seeing, transparency, telluric absorption) can be understood, measured and removed from the data, leaving just the science result. You always want to take *enough* data, but not overdo it as that often can take up a lot of telescope time.

6.1 Darks

The purpose of darks is to measure the detector response when it has no instrumental signature of anything other than the dark current signal (where hot pixels are understood as pixels with unusually high dark current, for whatever reason). Given the fairly strong persistence with the current detectors in LUCI, and the long timescale for it to truly decay down to un-measurable levels (hours), the BEST time to take darks is in the afternoon, before you open LUCI up for that night's work and after it has had a chance to sit un-illuminated for the whole day. That said, if you *need* darks for your project then you are far better off with darks taken in the morning rather than no darks at all.

However, one should (always) ask what the darks are to be used for. Standard IR observing practice is to dither the telescope between exposures. Twilight flats or data taken with the calibration unit are normally obtained as high/low or on/off pairs of data. This provides a built-in "dark" that you subtract along with the sky. You DO need darks for:

- Making a bad pixel mask
- Dark-subtracting night-sky imaging data for a "superflat"
- Dark-subtracting twilight flats if you don't take two sets at different flux levels
- Removing hot pixels from through-slit MOS or longslit acquisition data

As for stability, you will see some changes from night-to-night but this is mostly in the "unstable" hot pixels that really are not usable and should simply be masked out. The dark current for vast majority of the pixels is quite stable over many-day timescales. Thus it is NOT necessary to take a full set of darks on a nightly cadence. This is especially true for imaging where you are completely background-limited in the typical exposure times.

How many dark exposures does it take to properly calibrate data? The actual dark current signal in a dark exposure for IR detectors is normally low ($<0.1e-/s/pixel$ in LUCI, see Table 8) and an individual dark exposure is dominated by the read noise. You want to average a sufficient number of frames to get the read noise down to a level that is negligible with respect to what you are trying to correct. For strongly background-limited data, five darks are usually more than enough. When you are read-noise limited, ten dark frames increases the noise by $\sim 5\%$, while 50 darks keep the noise increase below 1%.

For dark frames, it is critical that the DITs and readout modes match the science data as these affect the actual exposure each pixel sees. The other parameters (NDIT, NEXP, savemode) can be compensated for during the data reduction.

6.2 Flatfields

A proper flat field is an accurate map of the pixel-to-pixel variations in quantum efficiency (QE), with all other instrumental effects (dark signal, linearity, accuracy of the flat field, illumination gradients, slit functions, internal scattered light, etc.) removed. In addition to the pixel-to-pixel (spatial) changes, each individual pixel can have a different response to light of different wavelengths (spectral), thus a flat field taken at one wavelength or band will not necessarily be an appropriate flat field at another wavelength or a different band. Flats are photon shot noise limited, so the read noise of the detector is generally not a concern. An example imaging flatfield, showing some of the cosmetic features of the detector in LUCI2, is shown in Figure 12.

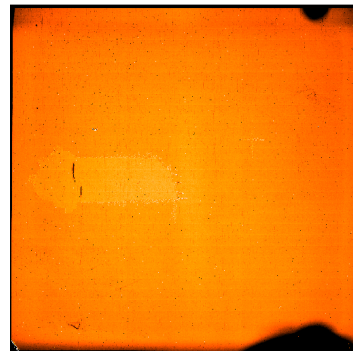


Figure 12: A LUCI2 H-band flat showing the “Keyhole” feature left of center. The dark regions are shadows at top and bottom right from things outside the LUCI dewars.

There are three ways typically used to construct imaging flatfields: twilight sky, nighttime sky, and the CU. Twilight flats are the most common option, but need to be taken in photometric conditions because clouds can introduce non-uniform variability in illumination during readout. Flats taken with the CU are often the highest SNR, but the CU does not illuminate the field of view perfectly uniformly. Nighttime sky flats normally require a large number of dithered frames to reach a reasonable SNR.

Table 12: Intensities of the flatfields per second for the filters and the N3.75 camera.

Filter Name	Lamp	LUCI1	LUCI2
		Counts [ADU/s]	Counts [ADU/s]
z	Halo 3	1000	1000
J	Halo 3	6000	6000
H	Halo 3	9800	9800
K	Halo 3	15700	15700
K _s	Halo 3	9800	9800
Y1	Halo 3	500	500
Y2	Halo 3	750	750
OH_1060	Halo 3	900	900
OH_1190	Halo 3	170	170
HeI	Halo 3	370	370
P_gam	Halo 2	3750	3750
P_beta	Halo 3	500	500
J_low	Halo 3	900	900
J_high	Halo 3	4800	4800
FeII	Halo 3	170	170
H2	Halo 3	1500	1500
Br_gam	Halo 2	900	900

slit widths scale inversely by the ratio of the slit widths (1'' slits should need half the time of 0''.5 slits) and also inversely as the square of the ratio of pixel scales (Table 1, so flats with the N3.75 camera should take ~4 times as long as the equivalent flats through the N1.8 camera). Halo2 is about ten times brighter than Halo3, and Halo1 is about 10 times brighter than Halo2. These values are applicable for either LUCI1 or

How many flat fields do you need to take to calibrate your data? This is a straightforward SNR calculation. From Poisson statistics we know that 10^4 e⁻ will give you a flat with 1% accuracy. This is ~5000ADU with either LUCI. Five such exposures give you 5×10^4 photons and 0.45% accuracy. This is well below the level of uncertainty that can arise from uncorrected linearity of the detector, illumination gradients, slit functions, or internal scattered light. In Table 12 the intensities of the flatfields per second for the filters and the N3.75 camera using the Calibration Unit are given.

When is the best time to take CU flat field data? Since the flat fields WILL illuminate the detector they need to be done after any darks. Since uniformity of the signal is a goal, they should be done before anything else that might leave a structured persistence signal on the detector (arcs, normal nighttime observations). So the best time to take flats is in the afternoon, after darks have been taken and before the night’s observations begin.

For spectroscopy, only the CU is a viable option as the sky has emission lines and the solar spectrum has absorption lines. Recommended *flatfield* exposure times for the standard spectroscopic configurations (N1.8 camera, 0''.5 slit width) are given in Table 13. Exposure times for other

LUCI2. The scripted LAMP exposures (arcs or flats) will automatically take “lamp off” and then “lamp on” exposures for dark subtraction.

6.2.1 Twilight (Imaging) Flats

You break two fundamental requirements for proper flatfields when you use the twilight sky: that you have a stable and uniform light source. So you must take the data with eventually correcting for this in mind. The twilight sky is not a stable light source, especially right around sunset or sunrise. Nor is it uniformly illuminated. While the scattered sunlight is reasonably uniform over the $4' \times 4'$ field of view in LUCI, the sources we so diligently study at night are still there as well. To mitigate these issues, work when the sky is brighter to keep exposure times to the minimum possible, and either dither (when the Sun is below the horizon) or stare at zenith (while the Sun is still up) and take enough exposures so that any artifacts from real sources can be masked out. Where possible, select relatively blank fields well off the Galactic plane and free of bright stars. You may refer to the GTC (Gran Telescopio CANARIAS) collection of blank fields as a starter (see Section 1.2). We recommend you stay below 25k ADU.

For twilight flats you either need a single set of well-exposed images and matching dark frames, or two sets of flats with one set taken at least a few thousand counts higher than the other. The latter is slightly better as the second set will subtract off any contributions from the telescope, but in practice they differ only slightly and the choice is driven by how many sets of data need to be taken. A generic flatfield script is available, which does 10 dithered flats at near the minimum exposure time. All you need to do is to tell the telescope operator where to point the telescope in *TRACK mode*, manually configure the instrument and then execute the script.

Table 13: Recommended spectroscopic flat integration times for the N1.8 camera and $0''.5$ longslit.

Grating	Filter Name	Lamp	Exp.Time [sec]	Counts [ADU/s]
G210	K	Halo2	10	7500
	H	Halo2	15	7500
	J	Halo2	40	8500
	z	Halo1	20	6000
G200	zJspec	Halo3	3	5500
	HKspec	Halo2	3	8000

6.3 Photometric (Imaging) Standards

For seeing-limited imaging, the FoV with LUCI is large enough that there are often multiple 2MASS stars in the images and this should yield a photometric accuracy of $\pm 0^m.1$ or so. With in-field calibrators, you are not sensitive to variations in transparency while observing. All 2MASS point sources are easily visible in a typical 60s broadband exposure with LUCI.

On truly photometric nights, it is possible to improve somewhat on this uncertainty, though it requires multiple observations of photometric standards, spanning the night to show photometric stability as well as airmass to derive an extinction correction. On the Calar Alto Observatory website (see link in Section 1.2) you can find a nice compilation of NIR photometric standard stars including finder charts.

6.4 Spectroscopic Standards

In the near infrared, the atmosphere is not perfectly transparent across all wavelengths. Various molecules in the atmosphere, primarily water, also have strong rotational and vibrational transitions that create significant absorption at certain wavelengths (Fig. 15). Correcting for this absorption is what a telluric (meaning “of or relating to the earth”) standard is used for.

There is a nice discussion on how to select an appropriate telluric standard on the Gemini website (see Section 1.2 for a link), so there is no need to go into detail here. Their pages include a large compilation of stars from the Hipparcos catalog usable for this purpose. These are the stars selectable in Scriptor when planning your observations.

To the best of our knowledge, no good sample of true NIR spectrophotometric standards exists in the literature. What can be done is to use the observations of the Telluric itself for a rough flux calibration, or simply make an adjustment to the flux to match the known broadband flux of your target. This allows you to achieve an accuracy of about 20%.

6.5 Wavelength Calibration

Emission line spectra are used to obtain a high-quality dispersion solution (wavelength vs. pixel). Arc lamps are commonly used at visual wavelengths, and the LUCI CUs are equipped with three arc lamps (Argon, Neon and Xenon), but most of the near-IR night sky spectrum is densely populated with intrinsically narrow OH emission lines. These will often be sufficient for wavelength calibrating seeing-limited data. At lower resolution the OH lines can blend together. At high resolution or in the red half of the K band you may have too few OH lines to get a good dispersion solution. Arc- and OH-line identification plots are shown in Appendix B.

It should normally be enough to take a single arc lamp exposure for each lamp (Ar, Ne, Xe) needed, but 2-3 are OK. Recommended *arc* exposures times for the standard spectroscopic configurations (N1.8 camera, 0''5 slit width) are given in Table 14. The exposure times for other slit widths with a given grating or camera are about the same. The arc lines don't get brighter, they just get further apart at higher spectroscopic resolution or spatial sampling. These values are applicable for either LUCI1 or LUCI2. The scripted LAMP exposures (arcs or flats) will automatically take "lamp off" and then "lamp on" exposures for dark subtraction.

Table 14: Recommended integration times for spectroscopic arcs with the N1.8 camera and 0''5 longslit.

Grating	Filter	Argon	Neon	Xenon
G210	K	60	60	60
	H	20	x	60
	J	30	60	60
	z	10	x	5
G200	zJspec	5	60	X
	HKspec	20	20	20

The arc lamp exposures have both structure and high contrast, so they WILL leave persistence on the detector! Thus the best time to take arcs would be after the night's observations have been completed, or in the afternoon after the darks and then the flatfield data have been taken. Multiple spectroscopic configurations can make these best practices difficult to follow.

6.6 Correcting for

6.6.1 Non-linearity

There is no such thing as a "linear" regime for infrared detectors! While with older near-infrared HgCdTe detectors you could expect to be ~4-5% non-linear at 80% full well, the H2RG detectors in LUCI are well over 10%. Thus, all data taken with LUCI should be linearized before further processing.

IR detectors are commonly read out using double-correlated sampling, where you save the difference between an initial and final non-destructive readout of the detector. Without a shutter understand that you are also collecting photons between the reset and the first read! Even though they do not show up in the final data saved to disk, they DO affect where your data are on the linearity curve. Ideally a correction for this needs

to be included in the linearization prescription. For data taken in LIR mode, this overhead is only $\sim 700 \mu\text{s}$ and thus negligible. For MER mode data, normally used for long spectroscopic exposures, the flux rates are usually much lower and thus any correction smaller, but this is still under investigation.

A correction prescription of the general form shown in Table 15 can be used to linearize LUCI data, with S representing the flux in any given pixel. Linearization should be the *first* step in the reduction process. Using a global second-order constant like this should reduce the photometric uncertainty to $\leq 1.2\%$ if one stays below 80% of the full well capacity. However, there is some structure in the linearization fits across the detector, with an outer “frame” and the keyhole showing slightly different corrections from the remainder of the detector. Thus for particularly demanding observations, where data spans the full dynamic range of the detector or there are particularly tight requirements on the overall photometric accuracy, linearization using a full 2D pixel map will be necessary.

Table 15: LUCI H2RG Linearization

Correction	$S_{lin} = S_{raw} + k \times S_{raw}^2$
LUCI1	$k = 4.xxx \times 10^{-6}$
LUCI2	$k = 4.xxx \times 10^{-6}$

6.6.2 Persistence

The H2RG detectors are strongly affected by persistence. Persistence is due to “trapped” charge (electrons or holes) in the detector that is not cleared out completely when the detector is reset. It manifests itself as an enhanced dark current wherever the persistence exists. The persistence in the LUCI detectors originates from two different sources: non-uniform response across the detectors, and non-uniform illumination of the focal plane. The latter can be from sources significantly brighter than the sky background, from the pattern of slits on the MOS mask or long slit that is imaged as part of the alignment procedure, or even from bright sources or OH emission lines in dispersed spectra.

Note that you **DO NOT** need to saturate the LUCI detector to leave a persistence signal! The persistence will start to decay as soon as the source flux is removed, and fades proportional to $\sim 1/t$. While it fades fairly rapidly, it can often be seen in the first few spectra taken on any given source.

Persistence shows up most frequently when performing spectroscopic acquisitions, where high illumination but short exposure imaging is followed by a high-contrast through-slit image, followed by long low background spectroscopic exposures. In Figure 13 we show how this looks in LUCI2 data. In the left panel the non-uniform persistence response of the LUCI2 detector from a (mostly) uniform illumination is seen in the through-slit image taken after the on-sky source acquisition imaging. The enhanced persistence is seen in the bright spot and the much larger but fainter quarter circle area at lower right. In the right panel of Figure 13 we show the response from the non-uniformly illuminated through-slit image on the subsequent spectroscopic exposure (faint trace of the slit image from alignment). You can also still see the spot and quarter circle features from earlier in the alignment process.

During data reduction you should have a record of almost everything that might contribute to persistence signals in the data itself. When combining dithered imaging or spectroscopic data, the usual procedure would be to reduce all data, even ancillary data like acquisition images when running a MOS or longslit alignment, and then create masks covering all potential sources of persistence. These persistence masks can then be

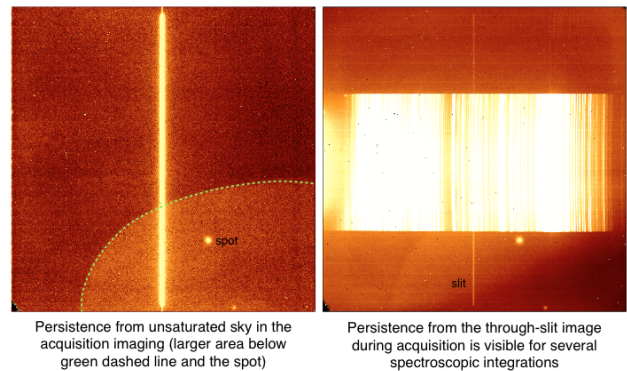


Figure 13: Left) Through slit image taken after an on-sky source image. Right) First spectrum after a successful alignment. Both show strong persistence.

added to any other bad pixel mask used at the point where dithered data are combined. For dealing with persistence effects on spectroscopic data, as in the right panel in Figure 13, you might try creating a noise-free model of the input signal and empirically scaling and subtracting it off the affected data.

6.6.3 Crosstalk

The HAWAII2-RG detector in LUCI2 shows two types of crosstalk: channel crosstalk and pixel crosstalk. Recall (Section 2.5) that the detector is read out by 32 amplifiers in parallel, with each channel 2048 pixels wide and 64 pixels tall. When the detector is read out, a strong signal in one amplifier channel can induce a small signal in some or all of the other 31 channels. This is known as amplifier or channel crosstalk.

Because of the detector architecture, the crosstalk images are always offset by $\pm(N \times 64)$ pixels in the Y-direction from whatever source is causing them. The crosstalk images range from $\leq 0.05\%$ of the source signal for the fainter ones, up to $\sim 0.2\%$ for the brighter ones. An example is shown in the left panel of Figure 14, where the bright source was a 9th magnitude double star corrected by the adaptive optics system.

Channel crosstalk is difficult to correct, and we have not yet developed a suitable and proven correction algorithm. Unfortunately, you cannot simply mask out the visible crosstalk signals in imaging data without taking data dithered in position angle (not a normal way to observe). In principle, the strength of the crosstalk needs to be measured for each amplifier pair (32×31 values). It is a fixed property of the detector and only changes if the pixel read-out rate (currently 100 kpix/sec) or the detector is changed.

If you want to develop a channel crosstalk correction algorithm, please contact [LBTO Science Operations](#).

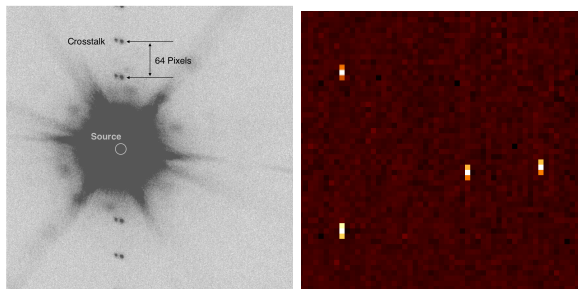


Figure 14: Left: Channel crosstalk appears $\pm(N \times 64)$ pixels from the saturated source image, in this case a double star. Right: Pixel crosstalk appears above and below hot pixels. In both panels, only a fraction of the full detector is shown for detail.

The second form of crosstalk in H2RG detectors is known as pixel crosstalk. For the LUCIs, this is most easily seen on dark frames, where the pixels immediately above and below a hot pixel show excess counts of about 1% of the signal in the hot pixels. This is easily seen in the right panel of Figure 14.

As with channel crosstalk, this pixel crosstalk is a fixed property of the detector, and we have not yet developed a suitable and proven correction algorithm. Note that the pixel crosstalk is there for every pixel on the detector, not just near hot pixels, so it is not sufficient to simply include them in bad pixel masks! However, since the hot pixels are a small fraction of the detector, it would not hurt to mask them.

The impact of pixel crosstalk on science data is significantly less obvious than with channel crosstalk. In normal observations the pixel crosstalk signal is completely overwhelmed by other effects. In practice, it very slightly smears out features in the Y direction on the detector. The largest impact may be on AO observations where the core of the Airy disk is small and at very high contrast with the immediately surrounding pixels.

6.6.4 Photometric Gradients

A photometric gradient here means that in flatfielded imaging data an astronomical source might have a different magnitude depending on where on the detector it lands. These can be induced in data if flatfields

are created with a non-uniformly illuminating light source, or if there is scattered light within the instrument that remaps the input focal plane non-uniformly on the detector. An analog from CCD observations at visual wavelengths is fringing. If creating a super skyflat then the fringing must be correctly removed.

In LUCI2 commissioning data with the N3.75 camera we see no obvious photometric gradients across the detector. In LUCI1 it does appear that there are gradients at up to $\sim 5\%$ in broadband data and as much as $\sim 25\%$ in narrowband data. We do not currently know the source of these gradients, but if high precision photometry is your goal, consider including sufficient observations to map and remove this *feature*. The usual way is to take well-dithered data of a field with a large number of stars with known (2MASS) magnitudes, and use them to derive a fit to the zero point offsets as a function of position on the detector. This fit is used to correct the flatfield that is then used to re-reduce your data.

6.6.5 Image quality and distortions

The aberrations in the LUCI optics are overall quite low. We regularly measure this using an internal precision sieve mask whenever the internal focus of the instruments is checked. The N30 cameras, of course, can produce diffraction limited images. This means that the other optics involved, fold mirrors, collimators, and dichroic windows that are always in use are all high quality. The N3.75 cameras deliver images dominated by atmospheric seeing almost down to the Nyquist limit (2 pixels = $0''.25$). The N1.8 cameras trade off some increased chromatic aberration for a wider field, allowing a larger free-spectral range to be covered in spectroscopic data. Thus the three cameras have primary uses as described in Section 2.1.

There are some other low-level contributions to the delivered image quality, from slightly tilted detectors with respect to the focal plane image, or radial effects with distance from the off-axis guide star. If your program requires accurate knowledge of the IQ across the full field of view, we suggest you plan to take the necessary data to derive what you need.

Table 16: Radial Distortion Coefficients

Camera	LUCI1	LUCI2
N1.8	$x.xx \times 10^{-6}$	4.30×10^{-6}
N3.75	$x.xx \times 10^{-6}$	2.97×10^{-6}
N30	$x.xx \times 10^{-6}$	$x.xx \times 10^{-6}$

The distortions in the LUCI cameras are dominated by a radial change in scale coming from the instruments' optics, with a much smaller contribution from the Gregorian telescopes. This follows a simple functional form: $D(r) = c \cdot r^2$. In Table 16 we list these coefficients, derived from the optical designs. For the N3.75 cameras it amounts to ~ 3.1 pixels at the edge of the field of view, and ~ 4.4 pixels at the corners.

We do not yet have distortion correction prescriptions in a format directly usable by stacking software such as *Drizzle* or *Swarp*. Imaging is not an often-used mode, and for single source observations correcting the distortions are not really necessary. If you have widely dithered data, or need to stitch together multiple pointings, then distortion correction becomes important. If you need something like this, please contact [LBTO Science Operations](#) and we will work with you.

6.7 Ghost Images

Particularly bright stars ($\ll 7$ mag) can show ghosts above the background in your data. These are due to reflections off various optical surfaces, perhaps including back reflections off the detector, within LUCI. Usually they look like pupil images: a uniformly illuminated disk with a central obstruction, sometimes distorted. For brighter ones, you can also see the secondary swing-arm shadow. Their total intensity is of the order of 10^{-4} of the incident flux, and spread out over many pixels. They are difficult to avoid completely. The best way is to not let the light from the parent star into the instrument in the first place. Depending on the science goals of the observation, you could consider taking data with the N30 camera to

block the light from the bright star(s), or design a special mask that will do this for the full field of view. If you choose to attempt the latter, please contact the [LBTO Science Operations group](#) for further advice.

We have seen some additional ghosts, likely from scattered light within the instrument, with the N3.75 camera in LUCI1. In imaging this appears as a “porthole” or ring around the image, while spectroscopy with this camera can show some additional features. The origin of these features is not completely clear yet, and may complicate your data analysis. We do not see similar features in the LUCI2 N3.75 camera.

6.8 Internal Flexure

The LUCI instruments show internal flexure which is a strong function of the rotator angle, somewhat less on telescope elevation and for changes between the gratings and mirror. This is regularly measured, normally at four telescope elevations and over the full 540° range of the rotator at 15° intervals in order to build up a model of the flexure. Flexure manifests itself in the data in two ways: a given exposure can be smeared out by flexure while the detector is integrating, and the image on the detector can drift from one frame to the next. The former affects the delivered image quality on each exposure while the latter affects how well the night sky emission subtracts out when differencing two spectroscopic frames. Flexure has the greatest impact on long exposures and when the parallactic angle changes the fastest at high elevation meridian crossings.

This flexure can be corrected by moving one of the fold mirrors inside LUCI. We are currently exploring two ways to correct this flexure while data are being taken: a *passive* correction regularly applied from the flexure model, and an *active* correction using SUR mode readouts (Section 2.5) to measure one or more fiducial holes in the mask. The latter is still under development, but will be needed for the longer exposure times expected for AO spectroscopy.

The passive flexure correction algorithm was recently re-worked in the LUCI software to improve the positional stability of the image on the detector. We don't yet have a good measurement of how well it works, but the expectation is that it should be an improvement over the previous applications.

7 Overheads

Everything we do has an overhead associated with it. Breakfast requires preparation, work requires getting to your office, travel requires getting to the airport a couple hours early. Overheads become a critical consideration when the resource, in this case the telescope time, is expensive. The colloquial unit for the LBT: *one espresso per second!*

Obtaining astronomical observations at any telescope will typically face four different sources of overhead: from the telescope, instrument, detector and any operation that requires human interaction. These are each discussed in more detail below.

Overheads are particularly important to consider when planning binocular observations for the LBT. While many observations can treat the two sides as independent telescopes (as does the TCS), some operations require moving far enough that *both* sides are involved as the mount needs to move. This includes the obvious presetting to a new target field, but also dithering to an off-source sky position when observing large targets or executing blind offsets that exceed the telescopes' co-pointing limit. Such operations must happen synchronously, or one side would impact observations taking place on the other side.

To maximize efficiency in taking binocular data, the observations preceding synchronous moves should complete at about the same time, including all exposures, dithers, and other overheads. This was discussed in more detail in Section 4.7. It is the role of a good binocular planning tool to simplify this process.

7.1 Telescope overheads

Presetting the telescope to a new target is an obviously unavoidable overhead at the beginning of each program. A preset triggers a complex series of actions in the telescope control system (TCS) depending on the specific request(s) sent from the instrument(s). Near-IR observations also typically involve regular dithering (offsets) to allow for better measurement and removal of the variable sky background and instrumental signature. We won't cover this in much detail here because from the instrument's viewpoint any requests to the TCS either succeed or fail. However, we do include a table of the overheads associated with major parts of presets and offsets in Table 17 as well as some discussion about where observers might run into problems.

Operations on the left (SX) and right (DX) telescopes and both LUCIs take about the same time, so they are not tabulated separately.

Telescope slews depend on the distance that needs to be covered. We assume a quarter-sky move to be typical (75 s), though a full unwrap of the azimuth axis takes 300 s even for a small move. Occasionally you will also run into rotator unwraps (72 s). Once on target, the AGw will auto-find the supplied guide star and begin guiding and collimating. At the LBT, the speed of collimation often depends on the thermal state of the telescope and weather. Unstable nights or a telescope out of equilibrium can make the collimation loops struggle. For any collimation taking longer than 300 s, the OSA should be notified. Occasionally a preset will fail because no guide star was found. In these cases, the OSA may need to do a local (manual) correction to the pointing model.

Both ARGOS and Adaptive Optics (AO) observations require that the telescope first be collimated by the AGw. This is to ensure that when the higher speed loops are closed there is no large correction applied to

Table 17: Overheads from telescope motions.

Action type	Typical Time [sec]	Maximum Time [sec]
Preset	75	300
Pointing Correction	150	300
AGw Collimation	100	300
AO setup	180	240
ARGOS setup	240	1200
Dither (SL)	14	20
Dither (AO)	10	20
Dither (ARGOS)	20	60

the secondary mirror. Once collimated by the AGw, the AO system must acquire the reference star on the pyramid and optimize the gains. This normally takes 180s to get to where the loops are closed and the instrument can begin taking data. Similarly, ARGOS must acquire a reference star for the tip-tilt signal as well as its lasers on its ground-layer wavefront sensor. This normally takes about 4 min.

7.2 Instrument overheads

Overheads for moving mechanical parts in LUCI like the filter or camera wheels are short, just a few tens of seconds at most. Instrument and telescope configurations are also done in parallel so most instrument changes are done while the telescope is slewing to a new field. The two most time consuming steps are grating stabilization and mask exchanges, detailed below and collected in Table 18.

Table 18: Overheads associated with LUCI.

Action type	Typical Time [sec]	Maximum Time [sec]
Camera, filter changes	15	30
Grating tilt	20	60
Mask: Storage to FPU	180	200
Mask: Turnout to FPU	72	72

The gratings are stabilized with a voltage feedback loop. Normally they will be stable at the requested wavelength within 10-20 seconds, but will timeout and throw an error after 60s. A recovery procedure can be found in the Cookbook. As of this writing (August 2016) the G210 grating is having some trouble stabilizing at wavelengths longer than 2.2 μm .

of the FPU. Almost all observations require a mask in the FPU, only seeing-limited imaging with the N3.75 or N1.8 cameras runs with the FPU empty where the FPU itself then acts as the cold field stop. The time to move a mask from the FPU to the staging position called “turnout” is a very repeatable 72s. From FPU to storage normally takes about 3 min, but varies a little depending on the mask’s position within the storage cabinet. The reverse motions take the same time as the forward motions. So, when you must move one mask from FPU to storage and then a new mask from storage to FPU, the full cycle takes about 6 minutes.

The longest overheads for instrument reconfigurations in LUCI occur when moving a mask in or out

7.3 Detector overheads

Detector readouts tend to be a bit more deterministic than telescope or instrument motions. Each of the three readout modes offered for science (LIR, MER, SUR) were described in some detail in Section 2.5, here we just discuss the overheads involved with reading out the detector and saving the data, see Table 19.

As noted before, the interlacing in LIR mode makes it quite efficient. When many readouts (DITs) are necessary to build up an exposure because of high background, the full [NDIT \times DIT] exposure incurs only one 2.51s of readout overhead. However, MER mode readouts are not interlaced. Since every MER readout (DIT) incurs the full 6.26s of readout overhead they are best reserved for long exposures (>60s), typically for faint-object spectroscopy where it is only the sky’s OH emission that limits exposure times.

SUR mode is a special case, and is being implemented as a way to actively close a flexure compensation loop. Because the detector is read out non-destructively, each readout of the detector can act as half of a double-correlated exposure, allowing the image position on the detector to be monitored, and corrected,

Table 19: Overheads associated with detector readout and image saving.

Action type	Typical Time [sec]
LIR Readout	2.51
MER Readout	6.26
SUR Readout	1.26
Save LIR/MER FITS image	7
Save SUR FITS image	XX

regularly during a long exposure. These reads are not interlaced, so each takes half the time of the LIR readout and only the last read in SUR mode contributes to the overhead.

There are additional overheads needed to retrieve data for the image headers, sum the NDIT images if needed, create the FITS image and then save it to disk. This averages about 7 seconds for LIR and MER modes. For SUR mode data, the system needs to fit the exposure time ramp data for each pixel as well, thus SUR data takes longer to create and save an exposure to disk. For SUR mode this is about XX seconds.

7.4 The Human Element

If you have made it this far in reading this User Manual, kudos to you! The fourth and final source of observing overheads comes from the humans involved in the process...this is where *you* come in. The observatory, as well as the instrument teams, continue to work hard to reduce the three other sources of overheads, but this last one is up to you. The PIs that prepared the observations and those sitting at the telescope taking them have critical but very different roles to play in the overall success of an observation at any telescope, but especially so at the Large *Binocular* Telescope. When the PI and the observer are the same person we call it “classical” observing, though most observations at the LBT are carried out in some form of queue where the observers are not the PIs of all of the programs.

The role of the PI...the person who knows more about their science target than almost everybody else on this planet...is not to prepare observations such that they can take the data, but to prepare them so that *anyone* can take them and do so efficiently. The role of the observers present at the telescope is to be very familiar with the normal operation of the instruments being used, aware of the quirks and eccentricities, recognize when things are not operating as they should, and also know the main failure modes and how to recover from them for the instruments in use.

Table 20: Human Overheads during observing.

Action type	Typical Time [sec]	Maximum Time [sec]
Field/source ID	5	1800
MOS Alignment	60	1800
Other	10	1200

There are three main sources of overheads we see at the LBT that arise from the human element: difficulties identifying sources from the finding charts, problems aligning MOS masks on sky, and unfamiliarity with the instrument or documentation causing delays. In Table 20 we list under the “typical time” column how long it *should* take a knowledgeable observer to accomplish those tasks, assuming they are well-planned. In the “maximum time” column we list how much time we have seen these operations take (on multiple occasions).

Note that these only include the human interaction time. MOS mask acquisitions typically should take 11-12 minutes in total, but most of that time is spent acquiring the necessary images or reconfiguring the instrument.

Unfamiliarity with the instrument and telescope will naturally decline over time as observers build familiarity with LUCI and the LBT. The other two are correctable with better preparation. Preparation of a good finding chart is covered in Section 4.5.

For MOS spectroscopy it is a good idea to also provide the observers with a printout of the mask pattern with the science slits numbered as in the LMS file and the two (or more) slits identified in which the telluric will land. This will make the telluric acquisition go faster.

MOS acquisitions also suffer when too few alignment stars are used, they are too bright or not bright enough, they are not optimally distributed across the field of view, and/or the alignment stars are not corrected for proper motion before making the mask with LMS. Any of these can lead to having the observers doubt the quality of the mask alignment, leading to delays starting the spectroscopic observations. An absolute minimum of three stars on boxes are currently required for alignment, but we recommend five.

8 Observational Considerations

The fundamental goal of any astronomical observation is to derive some quantitative value related to the science target, as well as an uncertainty for that value. The measurements might include a source position or magnitude, wavelength or flux of a spectral feature, or a measure of variability. To make these measurements, one must correct the raw data for the contributions from the atmosphere, telescope, and instrument, as well as be aware of the sources of uncertainty associated with these corrections. Contributions from Zodiacal light, the interstellar/intergalactic medium, cosmology and other astronomical issues are not considered here but you should be aware of how they can affect your results.

In this section we briefly cover the different properties, effects or phenomena that one should keep in mind when designing a set of observations on a given target. We briefly cover the major issues in Section 6, though additional details on correcting for each effect are available in the literature as well as the collective experience of one's colleagues.

8.1 The Atmosphere

From our vantage point here on the surface of the earth, we must peer at our targets through the atmosphere. Unfortunately, Mother Nature throws up many road blocks, including:

- Absorption: Spatial and Spectral
- Background: Thermal and OH Emission
- Variability: Turbulence, Weather

8.1.1 Absorption: Spatial and Spectral

The atmosphere is not perfectly transparent. Aerosols, and even the gases that make up our atmosphere scatter the incoming photons from your astronomical target. Fortunately this *spatial* absorption (atmospheric extinction) is relatively low in the near infrared. While we do not yet have measurements from the LBT, a reasonable estimate is 0.1, 0.07 and 0.04 mag/airmass for J, H and K-bands, respectively (Manduca, A. & Bell, R.A., PASP 544, 848 (1979)) on clear photometric nights. Exposure time calculators (ETCs) normally have these default corrections built in and the airmass of the proposed observation is an input variable.

The various molecules in the atmosphere, primarily water, also have strong rotational and vibrational transitions across the near-infrared window, causing significant absorption at certain wavelengths as shown in Figure 15. This *spectral* absorption is one of the things that drove the design of the standard z/Y, J, H and K photometric bands, centering them on the spectral ranges where this absorption was minimal. The standard LUCI broadband filter curves are plotted in Figure 15 for reference so you can see their correspondence with the relatively absorption-free windows.

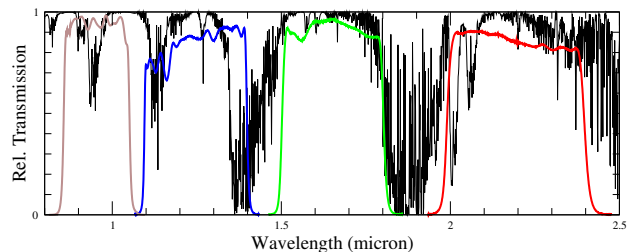


Figure 15: Relative atmospheric absorption in the near infrared, from 0.8 to 2.5 microns. The LUCI zJHK filter bandpasses are shown for reference. NSO/Kitt Peak FTS data produced by NSF/NOAO.

8.1.2 Background: Thermal and OH Emission, Moonlight

The atmosphere literally glows in the dark! The two major contributions to this background emission in the near infrared are thermal blackbody radiation and line emission from OH radicals. The line emission from OH radicals comes primarily from vibrational transitions and originates high up in the atmosphere. The emission lines are intrinsically quite narrow. Even in a perfectly baffled instrument (see below), the atmosphere itself also contributes some thermal background. The OH emission dominates the background in the zJH bands, while in K the background from OH and thermal emission are approximately equal (Fig. 16).

Moonlight also contributes to the background seen in near-infrared observations, by different amounts depending on the phase of the moon, and how close to the moon you are trying to observe. Moonlight, actually reflected sunlight, is relatively blue so shorter wavelengths are more strongly affected than longer wavelengths.

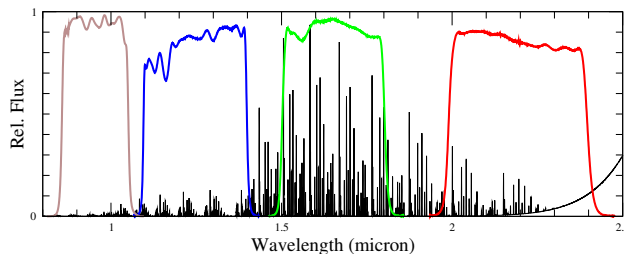


Figure 16: Background emission in the near infrared, over the same 0.8 to 2.5 microns shown in 15. The LUCI zJHK filter bandpasses are again shown for reference. The thermal background is seen as the rising baseline at the longest wavelengths, while the emission lines come primarily from OH radicals at high altitude.

8.1.3 Variability: Turbulence and Weather

The atmosphere is a dynamic place. The atmospheric effects discussed above are all time variable, and on different timescales. Other local and global events, such as forest fires, dust storms, volcanic eruptions (the eruption of Mount Pinatubo in 1991 affected atmospheric absorption for years) or even distant thunderstorms can have a significant effect on the absorption or emission characteristics of the atmosphere at the time your observations are taking place.

The absorption, background and variability issues discussed above are all well known and reasonably stable, that is they are always there and affect the data about the same from night to night. They all affect how you might design your observing program, from the spectroscopic resolution you select to the rate at which you dither. For example, you can count on the OH emission to vary by several tens of percent over a few minutes timescale. This is the basis for the well-known near-IR recommendation to dither your observations about once a minute for imaging, and as fast as is reasonable given other constraints for spectroscopy.

The last two atmospheric issues, weather and turbulence (seeing) are so important that they can affect whether you even take observations or not. They should be clearly stated as constraints on all programs. Clouds act like neutral density filters only on the source flux. Usually you still get all the background, if not more, as well as the *noise* that comes with it. Clear-sky seeing does not change the source flux, but does affect the number of pixels over which you extract your data and also affects the slit-losses in resolution-constrained (fixed slit width) spectroscopy. In either case, a factor of two change in the constraint (half the source flux blocked by clouds, or an increase of the seeing from 1 to 2 arcsec) requires a factor of four change in exposure time to reach a comparable SNR as originally planned. Thus it does not make any sense to observe programs when the weather or seeing constraints are not met, and it is always a good idea to have backup programs available to do in poorer conditions than needed for the primary science targets.

8.2 The Telescope

Once the light makes it through the atmosphere, it must traverse the telescope optics. The telescope must actively correct the pointing, maintain the position on source (guiding) and also the optical alignment (collimation). As with the atmosphere, the telescope glows in the dark above a wavelength of two microns, and unless freshly cleaned the telescope optics might be a little dusty. We include here some discussion about the additional constraints and preparations for adaptive optics, so you can see how they fit into this paradigm. Thus the telescope-related features to keep in mind include:

- Guiding
- Collimation
- Thermal Background
- Adaptive Optics Observations

The good news here is that the telescope control system (TCS) takes care of a lot of this for you. There is one key and unique aspect of the LBT that is important to keep in mind when designing observations: *the instrument is in control of the telescope*. It was done this way at the LBT in order to make the full binocular operation as efficient as possible. Thus, observation programs for the LBT must be fully-prepared in advance, including the selection of a suitable guide star. The guide star gets passed to the TCS when the script is executed. The TCS will then slew the telescope, acquire the guide star, correct the telescope pointing, verify stable guiding, and *begin* wavefront sensing before the preset request completes.

8.2.1 Guiding

Guiding is typically done through an r' filter with exposure times of 2 seconds. Guide stars brighter than $r \sim 12^m0$ can saturate on a clear night with excellent seeing, while stars fainter than $r \sim 16^m5$ may be a problem on nights with poor-seeing. One can push these limits by a magnitude in each direction for the inverse conditions.

The off-axis guider sits in front of LUCI and the probe can also vignette the LUCI field of view, so one should be cautious about using guide stars within about an arcmin of the side or top edges of the LUCI field of view (see Fig. 17). The probe appears fuzzy in Figure 17 because it is about 30 cm outside the telescope focal plane, and appears bright in this K band image because it is at ambient temperature.

The guide probe patrol field is a consequence of how the AGW unit was constructed (see Figure 18). The guide probe is on an $r - \Theta$ stage, and the probe always appears to come down from the top edge of the LUCI field of view. The bottom and angled sides of the patrol field are mechanical limits on the AGW stage motions, while the top edge is at the 5.5 arcmin radius of the *usable* Gregorian telescope focal plane.

In monocular observations guiding is done by moving the telescope mount, as is done for other telescopes. In binocular observing it is the telescope optics on each side that make the guiding corrections so that any

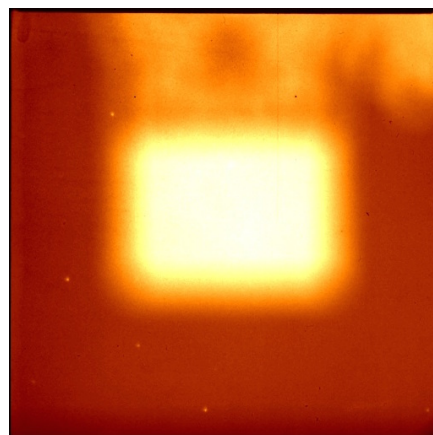


Figure 17: The guide probe is visible to LUCI when a guide star is used that is too close to the LUCI field of view, here shown when on axis.

usable Gregorian telescope focal plane.

ongoing observation on the other side is not disturbed. Moving the mount is faster than moving the optics, so with overheads the guider cycles every 4 (monocular) to 8 (binocular) seconds. In between guiding updates the telescope is effectively tracking open-loop, following the polynomials that govern the motion of the azimuth, elevation, and rotator drives. Our experience is that the LBTs pointing and tracking are stable over at least several tens of seconds, so this slow guiding rate is sufficient for seeing-limited observations.

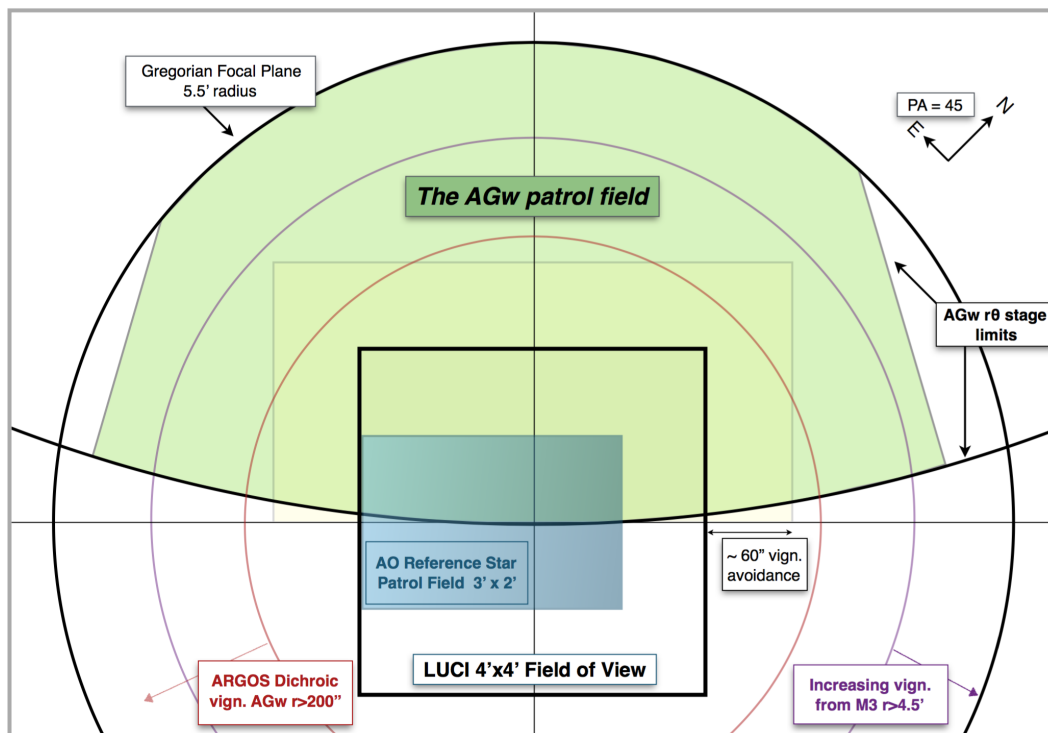


Figure 18: Patrol field for the LUCI AGw unit. The guide probe can reach anywhere within the green region, but caution should be used when selecting guide stars at high field angles (radius > 4.5), very close to any edge, or whenever the probe might vignette the LUCI field of view.

Guide stars beyond a radius of 4.5 arcmin start to vignette from the slightly undersized tertiary mirror and the delivered image quality could degrade.

When doing any observation where stability of the delivered PSF is a relevant consideration, such as alignment of a source on a longslit or a field to a MOS mask, it is a good idea to integrate over at least a few guider cycles to measure the average position of the source, not its instantaneous position. Thus, even on bright targets like telluric stars, we recommend taking the acquisition data with total exposures (DIT x NDIT) of 15-20 seconds even though that is overkill from a purely SNR point of view.

One of the most common problems encountered at the telescope with these pre-selected guide stars is that the *star* is actually a compact *galaxy* that is resolved enough that the AGw has problems either finding the source in the first place because of low surface brightness, or has difficulty in centroiding on the source for guiding or wavefront sensing. Thus you should be as sure as possible that your guide star is truly a star.

8.2.2 Collimation

The presets at the LBT *complete*, i.e. the instruments are notified the preset is done, before the telescope collimation is *verified* to be good. LUCI monitors an *isCollimated* flag in the TCS, generated by the guiding control software (GCS), and will wait until the measured wavefront error drops below 800 nm before starting any scripted observations.

Active correction of the telescope collimation uses the same guide star as for guiding. A beam-splitter separates the shorter wavelengths (r') for guiding and the longer wavelengths ($i+z$) for the Shack-Hartmann wavefront sensor. Any star you can guide on is also viable for wavefront sensing. The wfs exposes for 30 seconds to integrate over atmospheric and guiding effects to get a good measure of the collimation of the optics. The wfs cycles about every 45 seconds. Thus we recommend deep observations use a minimum dwell time on any on-sky position of about a minute to allow sufficient time for the telescope to stay well-collimated.

The AGw will automatically follow your selected guide star as you dither (Section 8.2.4) around to collect your data. Sometimes there will be a need to dither far enough that your guide star is outside of the patrol field, for example to collect some off-source sky exposures or you are working with a guide star right at the edge of the patrol field. In cases where the guide star is not reachable by the AGw probe, the telescope will automatically fall back to open-loop TRACK mode. As long as you do not run open loop for too long (<5 minutes), on any subsequent dither where the guide star is again reachable the telescope will resume guiding and collimating.

8.2.3 Thermal Background

Like the atmosphere, the telescope also glows in the dark. The parts of the telescope seen by LUCI when everything is well collimated and aligned, are limited to the swing-arms, mirrors and mounts for M2 and M3. These structures track the ambient temperature in the enclosure so they are warmer (about 273K) than the sky (about 200K), thus they appear bright in a pupil image taken in the K-band (Figure 19). This contributes to the thermal background seen by LUCI. Also visible in Figure 19 is a narrow bit of the primary mirror cell along the upper left edge. The bar at lower left is a crane in the enclosure that is not visible when observing.

This thermal background contribution from the telescope *will change* with changing ambient temperature, on roughly the same timescales. From summer to winter the background count rate in the K band can change by quite a bit. But diurnal changes, or even passage of a weather front can affect the background contribution from the telescope.

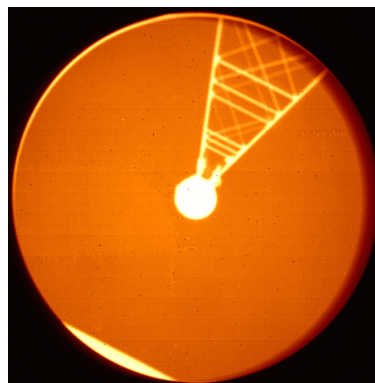


Figure 19: K band pupil and cold stop image.

8.2.4 Dither, Dither, Dither

The goal of a well-designed dither pattern is to allow for a robust removal of instrumental signatures and sky background from the RAW data. Bad pixels are a very small fraction of the total, so randomizing your dithering is usually sufficient. For a good sky measurement you must move completely off the largest structure you are trying to measure, and to keep the contribution to the noise from the background down, you need to do this over a number of exposures around each science image. For very extended sources, this often means moving completely off source to obtain a separate measurement of the sky. In spectroscopic observations you are further constrained in one dimension by the need to keep your science target somewhere along the spatial direction of the slit, but the same considerations apply.

Consider the typical 2-position ABAB dither pattern commonly used for spectroscopy, where only half of the data (the B positions) are available to sky-subtract the A data, and bad pixel clusters potentially remove half of your data at that point. Now consider a 4-position ACBD pattern where 75% of the data can be used as sky for each position in the pattern. The logical extreme of this is to never repeat positions in any dither pattern - potentially all but one exposure in a dataset can be used as sky for each science frame, and the impact from bad pixels is negligible. This reduces the noise added into the data by the sky-subtraction.

When the total observation on a source consists of just a few exposures, a standard pattern like a dice5 (for imaging) will suffice. For a 3×3 pattern it is far better to traverse it in a star pattern (center - corner - opposite edge - opposite corner...) than a spiral dither where many relative offsets are repeated as you step around the outside of the pattern. For longer total exposures it is better to randomize things even more. Repeating the same base pattern many times to build up a total exposure will bias the measurement of the sky wherever there is a real source in the sky frame. For a longer sequence, say you want to cover a 9×9 grid, consider approaching it like a Sudoku puzzle solution...do all the 1s' positions first, then the 2s', etc.

In Scriptor it is possible to upload dither patterns from an ASCII text file. Contact the [LBTO Science Operations group](#) if you need help setting something up. Some default patterns, including an optimized random offset generator, will be built into the OT.

8.2.5 Adaptive Optics Observations

In principle, adaptive optics does the same thing as with the AGw's guiding and collimation: it keeps the target in a stable position in the telescope focal plane and the telescope collimated. But AO does this hundreds or thousands of times faster than normal seeing-limited observations. The system also includes a correction for residual aberrations in the LUCI optics, known as non-common path aberration (NCPA) corrections. The result: atmospheric turbulence can be detected and corrected in real time, delivering a diffraction-limited image to LUCI.

To do this, the AO system needs an on-axis reference star, so the LUCI dewars were built with dichroic entrance windows tilted at 15° that pass IR light into LUCI and reflect the visual wavelengths ($<0.89 \mu\text{m}$ for LUCI1 and $<0.95 \mu\text{m}$ for LUCI2) out of the LUCIs field of view and into the high speed Wunits.

The patrol field for the Wunit is smaller than for the AGw. This is because anisoplanatism, an increasing de-correlation of the wavefront perturbations from atmospheric turbulence with radius from the AO reference star, limits the useful field of view around the AO reference star. The patrol field is 2×3 arcminutes, The field of view of the AO camera in LUCI is 30 arcseconds. As projected on the $4'$ N3.75 camera field of view, the Wunit patrol field is a centered $2 \times 2'$ square with a $1'$ extension to the left. Figure 18 includes this AO reference star patrol field as well as some updated vignetting constraints.

For science observations with LUCI in AO mode, rarely will the target of interest be the AO reference star itself. So there are a few things to keep in mind. The quality of the *on axis* (i.e. on the reference star itself) correction you get, often expressed as the *Strehl ratio*, is strongly dependent on the brightness of the AO reference star as well as the nature of the turbulence in the atmosphere at the time of observation. The off-axis correction will decrease with distance from the reference star because of anisoplanatism.

The AO system will automatically tune its performance based on the reference star flux and current seeing. Instability in the detected flux (e.g. from clouds) or fluctuations in seeing are detrimental to the AO system performance, to the point where the loops may open. Thus we recommend that LUCI AO observations only be attempted on clear nights with good ($<0''.8$ FWHM), stable seeing. Under these conditions, the AO system will work best on brighter ($R < 10^m$) stars, but can still give some correction with reference stars as faint as $R < 16^m.5$. At a radius of 10 arcsec from the reference star, the Strehl ratio may be down by a factor of two, but you should see some correction across the full 30 arcsec N30 camera field of view.

9 Archive

All of the data from the science instruments at the LBT are automatically copied into an archive at the observatory and then propagated to an equivalent server in Tucson. Appropriate partner-flagged data and all data marked as calibration are then sent to satellite archive servers in Germany, Italy, and simple storage at the Ohio State University. Thus it should not be necessary to copy the data while you are observing at the LBT.

At the telescope, all recently obtained data are available on cross-mounted disks on each workstation. If you are not at the observatory, access to the LBT archive web interface can be found at this URL:

<http://archive.lbto.org/>

at the University of Arizona. You will first land on the login page (Figure 20). The partner-specific or user-specific login information can be obtained from your local Partner Coordinator. All partners may access their data through the Tucson machine but are encouraged to use their local archive server if possible, especially for the European partners where the bandwidth from the US may be more limited. The *public* login allows you to search all data in the archive, but with no download rights except for those data that have been publicly released.

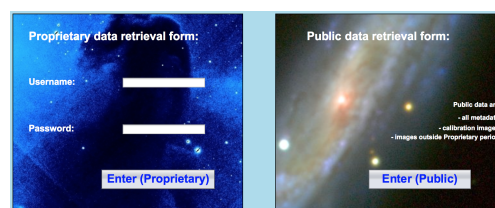


Figure 20: LBT Data Archive login page.

Figure 21: LBT Data Archive database search page.

on their names, or in batches by selecting the needed files in the checkboxes in the first column and clicking the *Get Files* button at top.

Once you have logged in, the database query form (Figure 21) allows you to query the information extracted from the headers and stored in the database. Wildcards are implied, so entering “20141209” without quotes in the *FileName* field, for example, will return a list of all files from all instruments with that UTDate in their filename. The advanced search option allows you to restrict the output to a single instrument as well as giving you some additional search fields specific to that instrument.

One known caveat, a carriage return anywhere while on the query page does not function as you might expect. Sometimes values entered into the text fields will revert to a previous entry. To initiate a search correctly, you must click the **SEARCH** button at bottom left.

You can then repeat the search with new or additional constraints to narrow down the matched files until you isolate the specific files you need. They

can either be downloaded individually by clicking

Appendices

A Filter and Grating Bandpasses

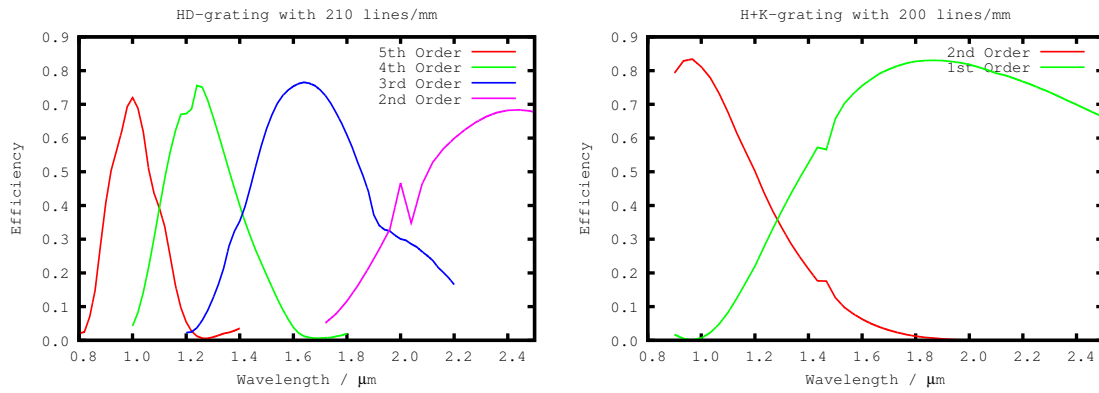


Figure 22: The efficiencies of the gratings versus the wavelength. Left) High-resolution grating 210zJHK. The different orders (5th - 2nd) are color coded. Right) Low-resolution grating 200H+K. The 1st and 2nd order are color coded. Bottom) G040 TBD

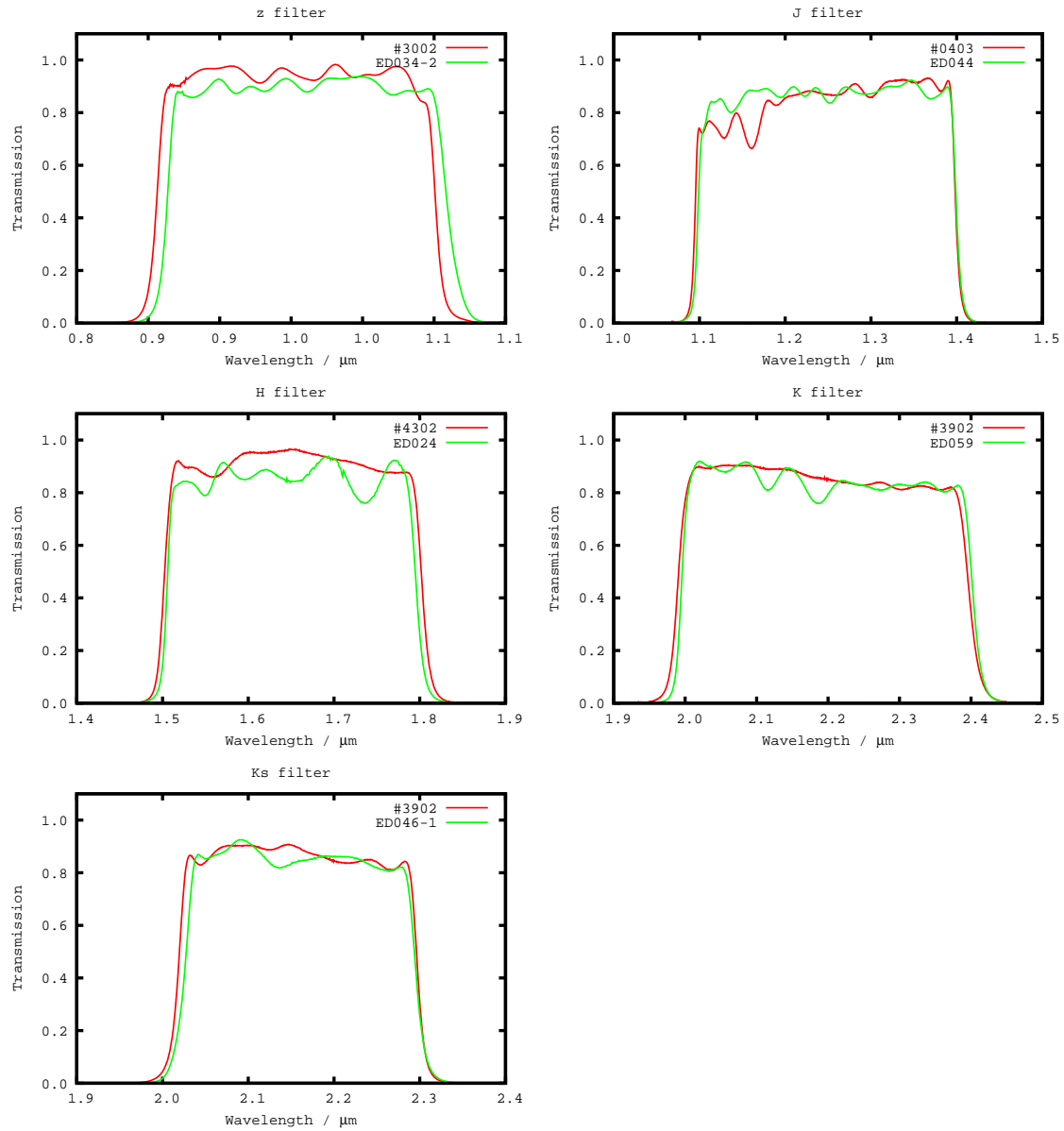


Figure 23: Transmission broad-band filters in LUCI1 (red) and LUCI2 (green).

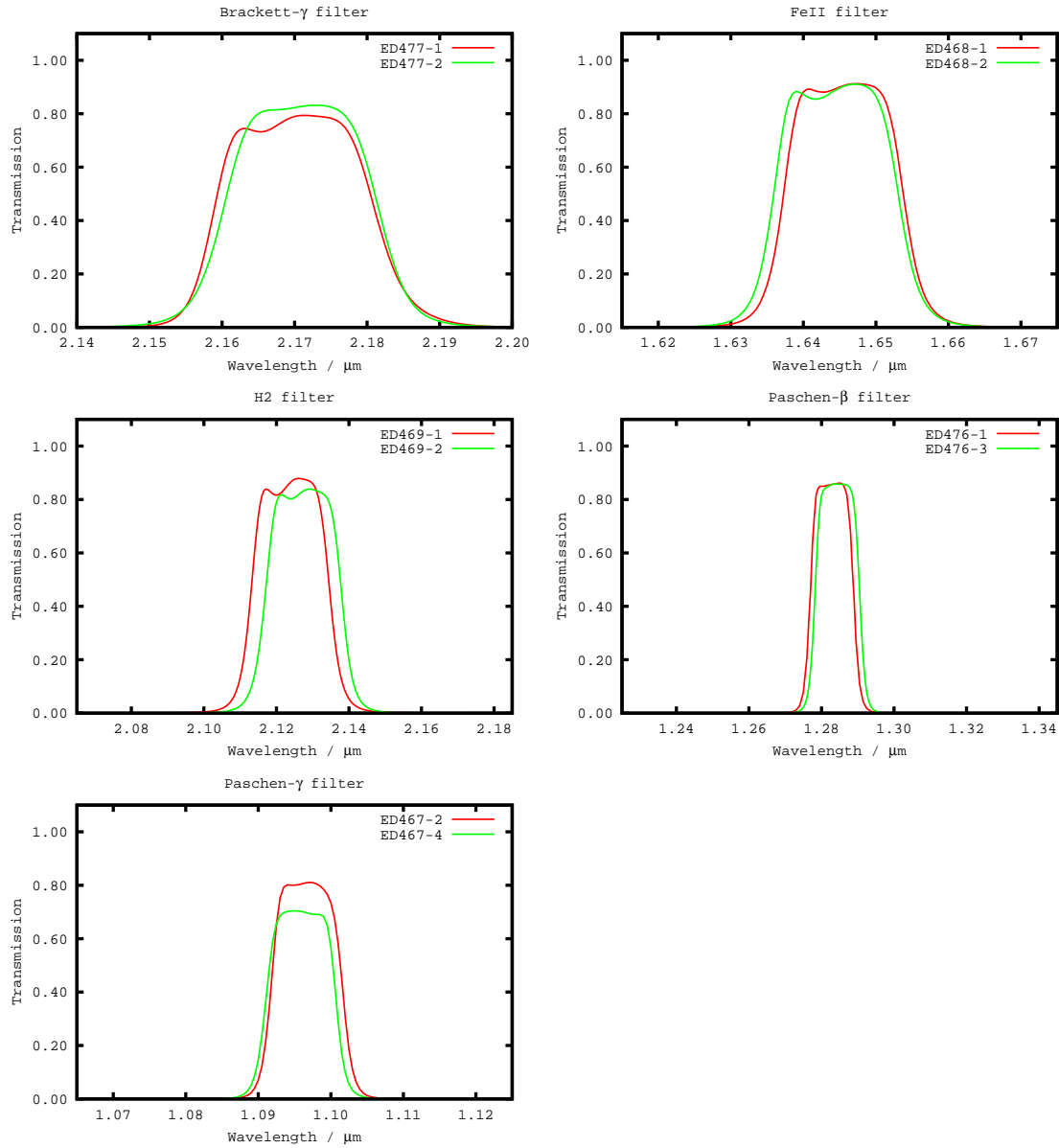


Figure 24: Transmission of the narrow-band filters in LUCI1 (red) and LUCI2 (green)

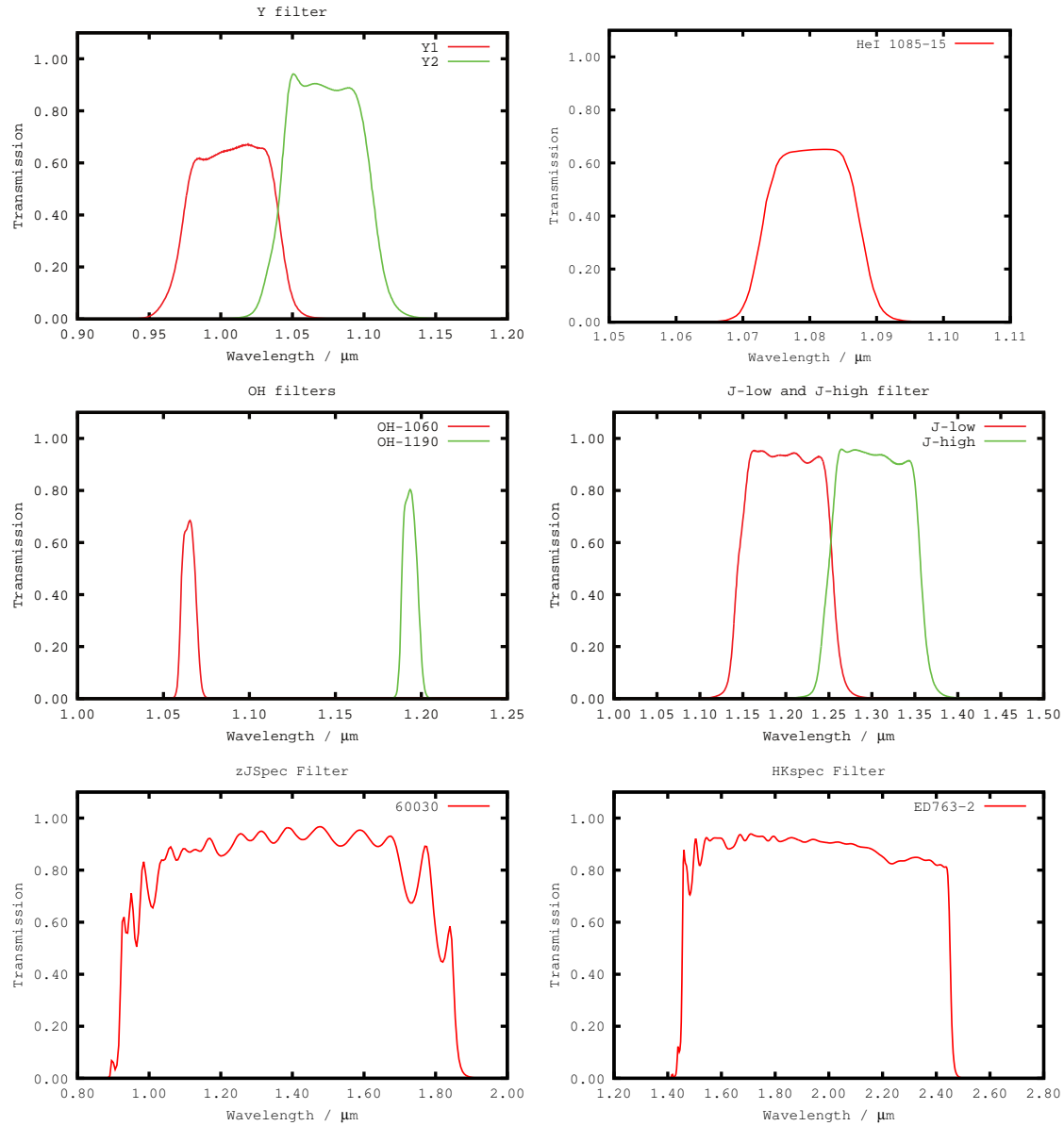


Figure 25: Transmission of the narrow-band (top, center) and order-sorting filter for the grating 200H+K (bottom). The filters for LUCI1 and LUCI2 are identical.

B Arc-line identification and night-sky emission line plots

G150 in K band for Ar

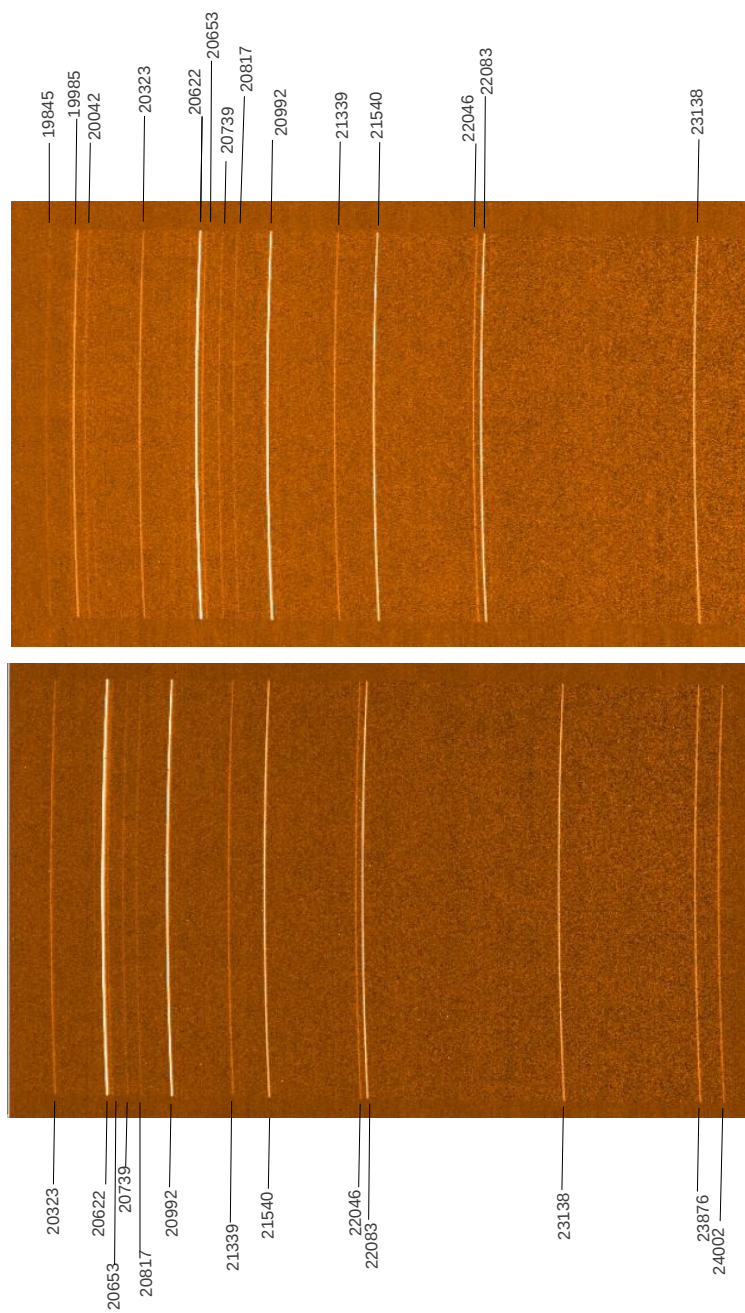


Figure 26: Argon arc-line identification plots for the G150 grating.

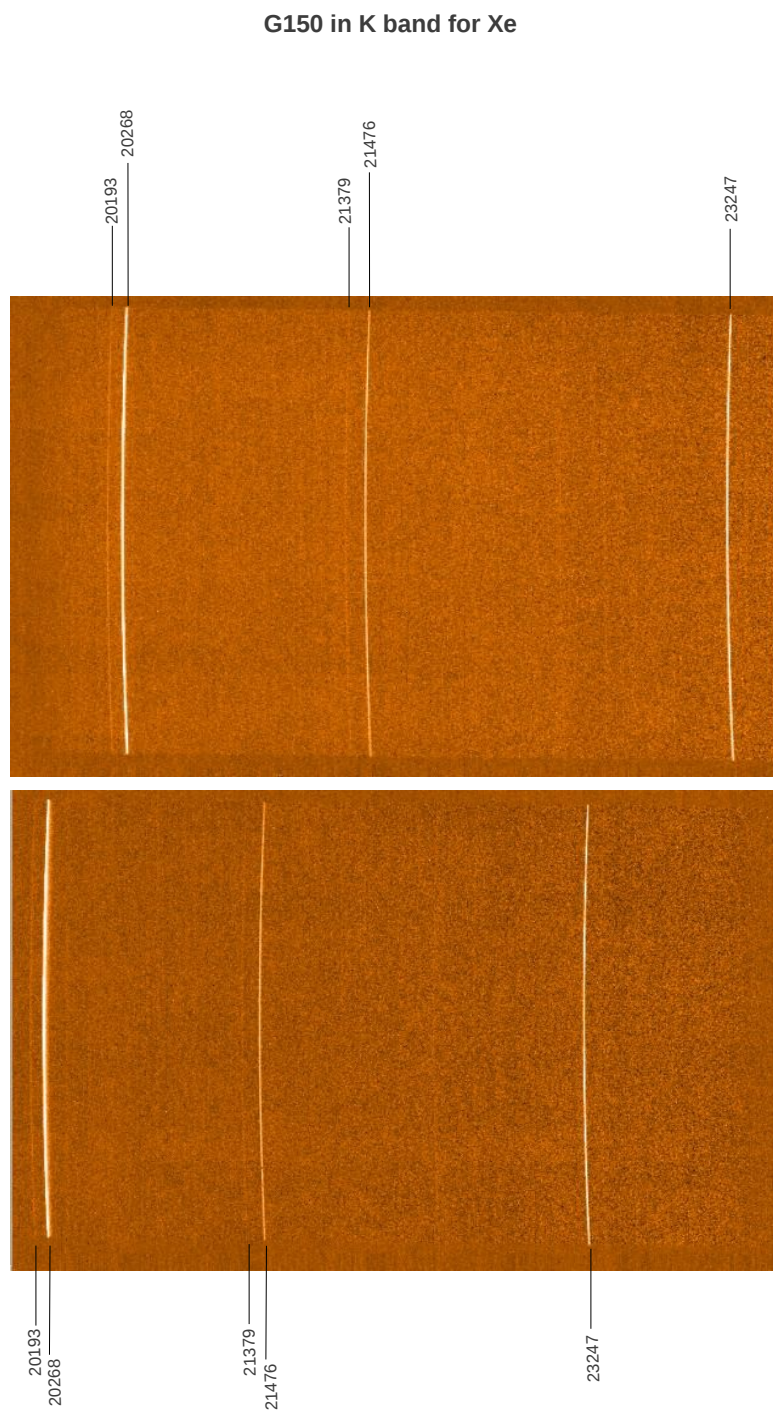


Figure 27: Xenon arc-line identification plots for the G150 grating.

G150 in K band for Ne

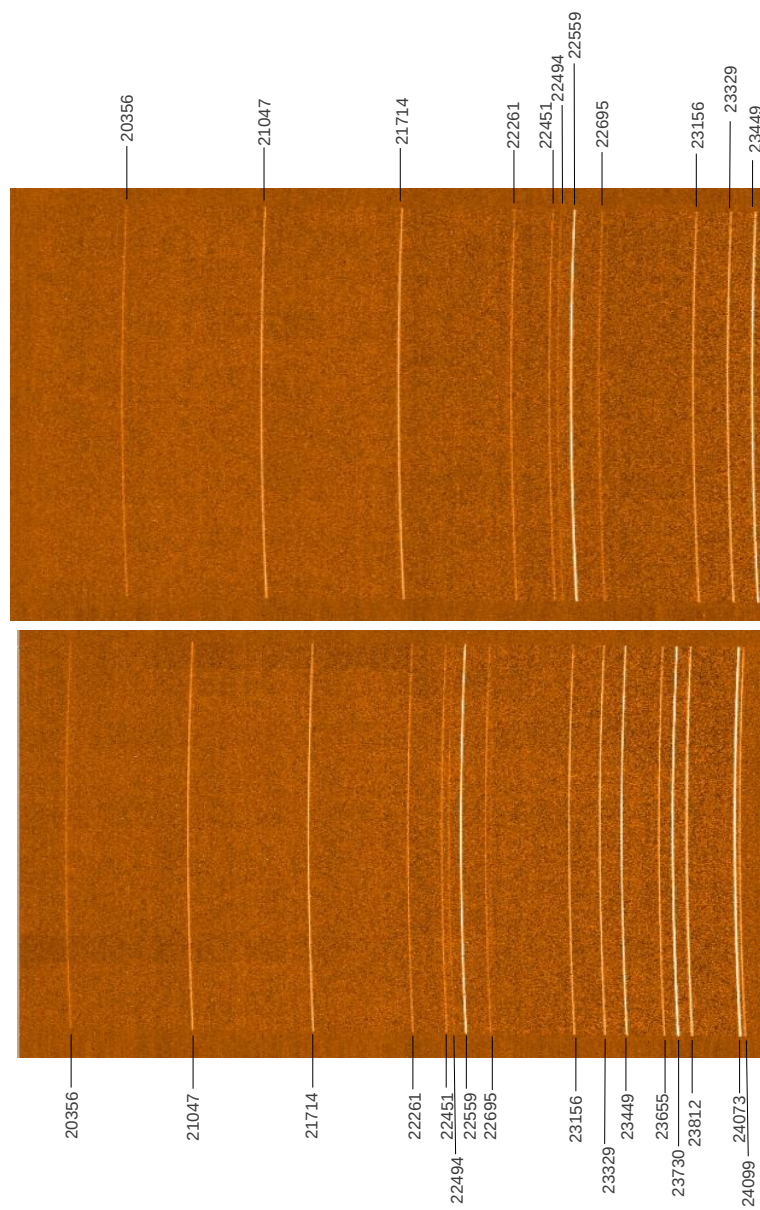


Figure 28: Neon arc-line identification plots for the G150 grating.

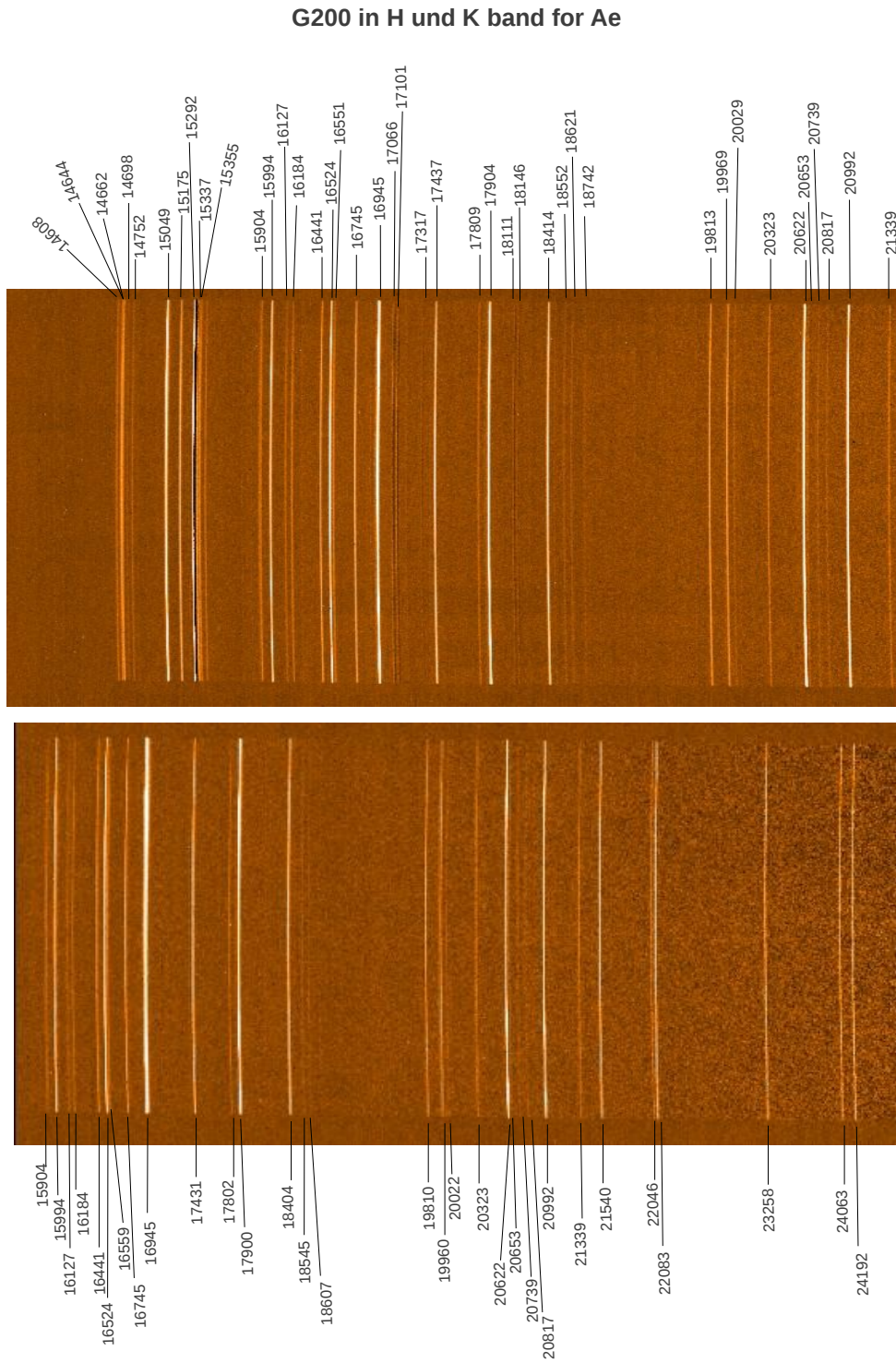


Figure 29: Argon arc-line identification plots for the G20 grating in H and K bands.

G200 in H und K band for Xe



Figure 30: Xenon arc-line identification plots for the G200 grating in H and K bands.

G200 in H und K band for Ne

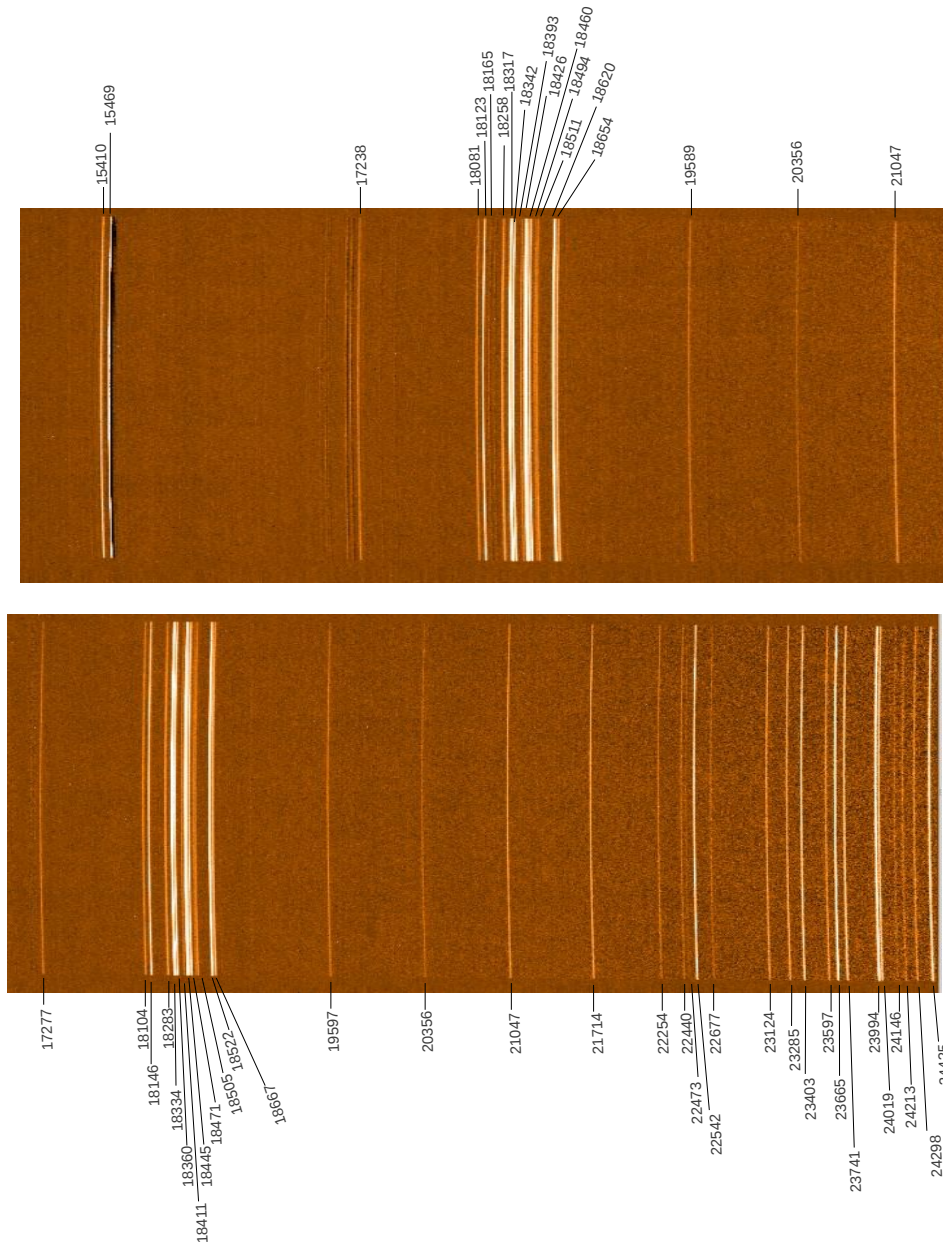


Figure 31: Neon arc-line identification plots for the G20 grating in H and K bands.

G210 in z band for Ar

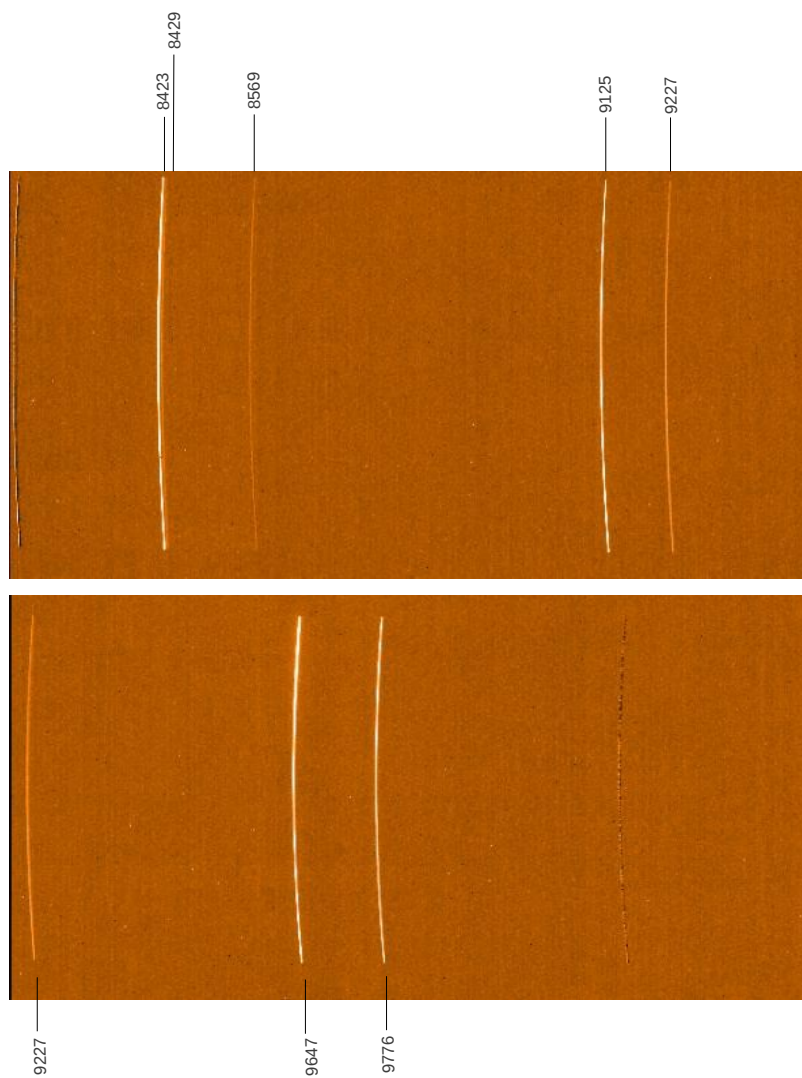


Figure 32: Argon arc-line identification plots for the G210 grating in z-band.

G210 in z band for Xe

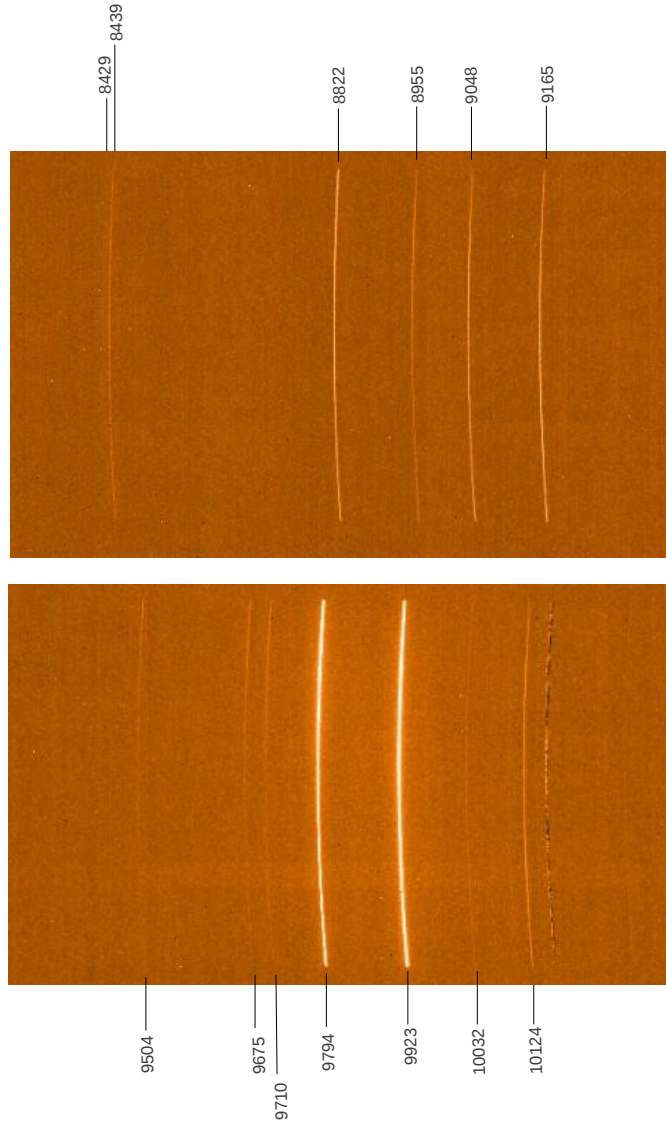


Figure 33: Xenon arc-line identification plots for the G210 grating in z-band.

G210 in z band for Ne

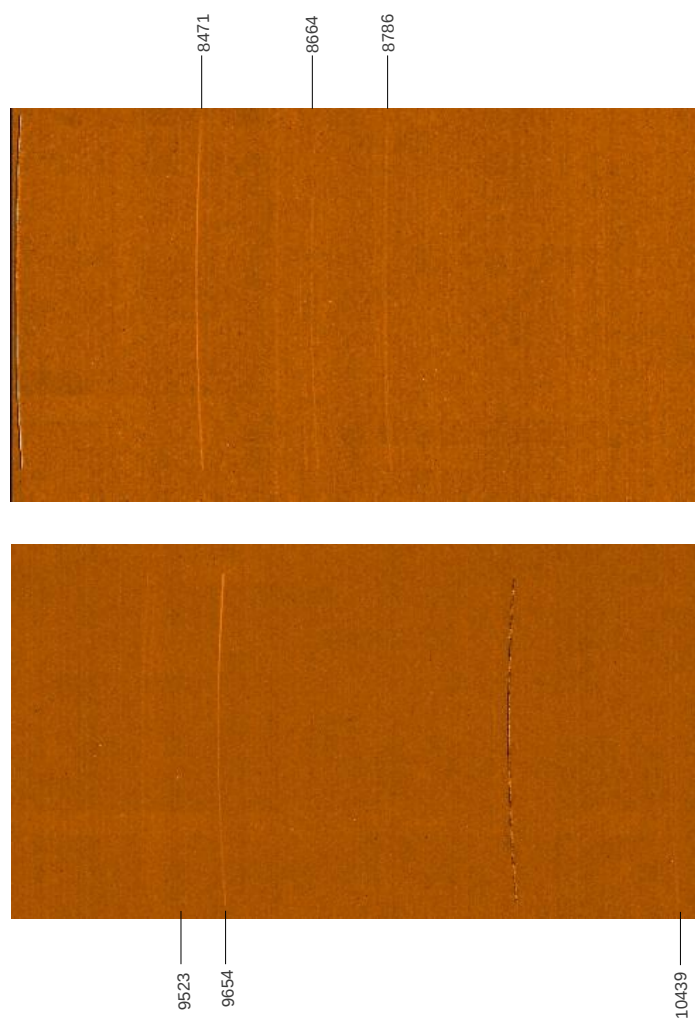


Figure 34: Neon arc-line identification plots for the G210 grating in z-band.

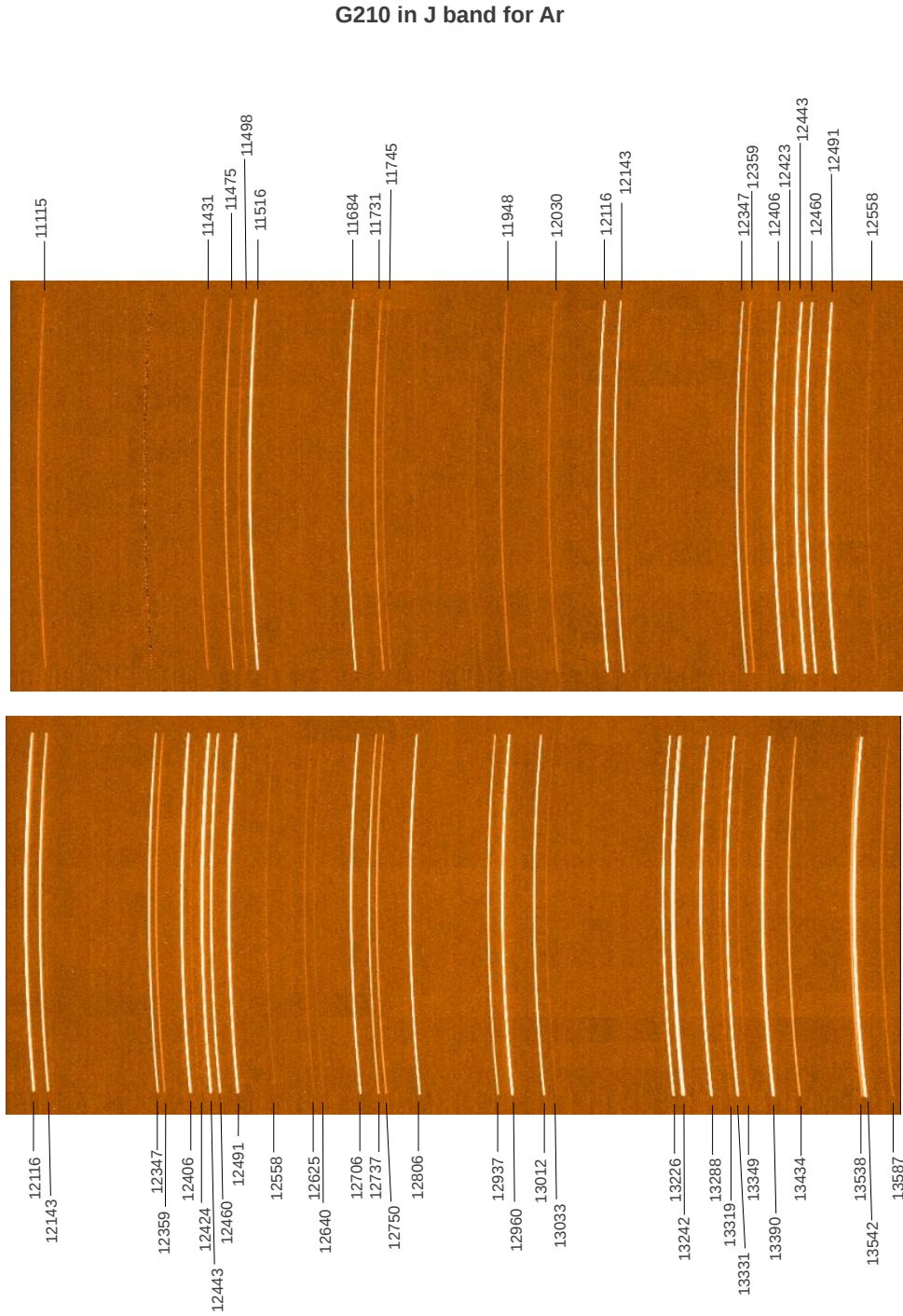


Figure 35: Argon arc-line identification plots for the G210 grating in J-band.

G210 in J band for Xe

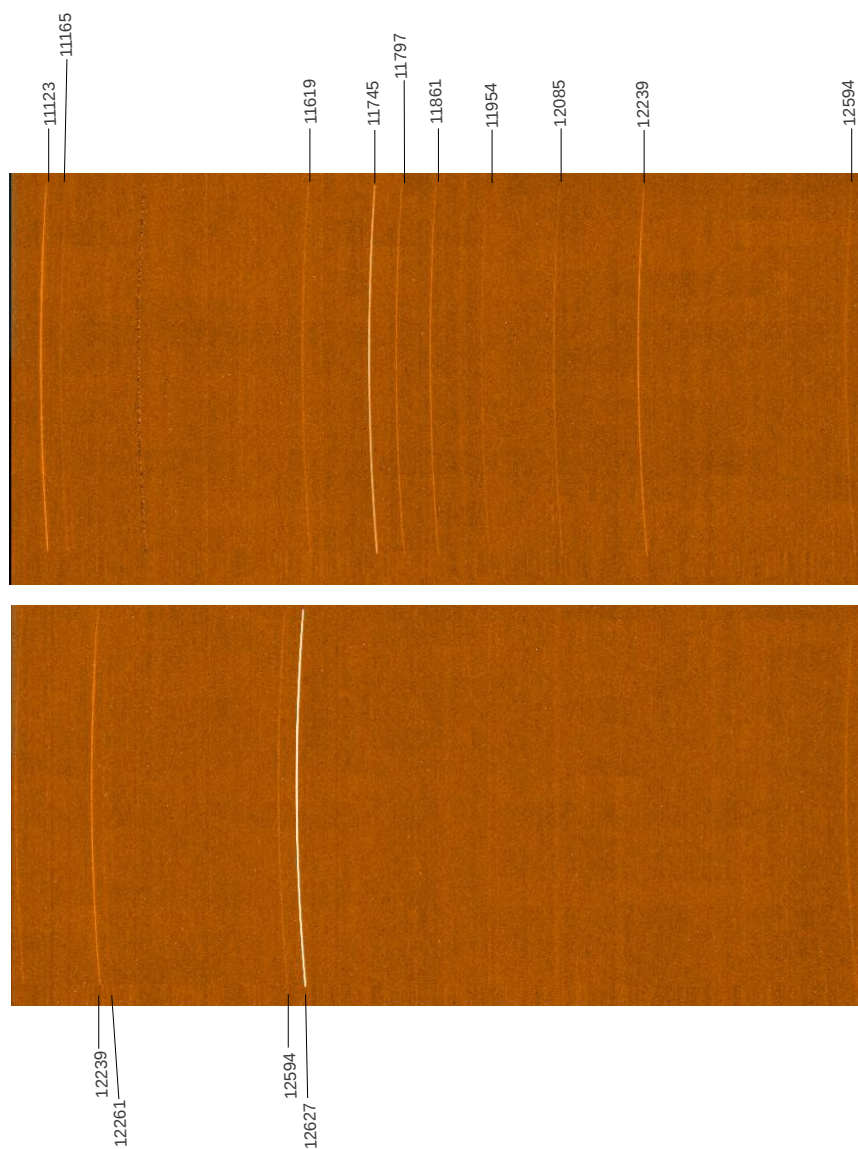


Figure 36: Xenon arc-line identification plots for the G210 grating in J-band.

G210 in J band for Ne

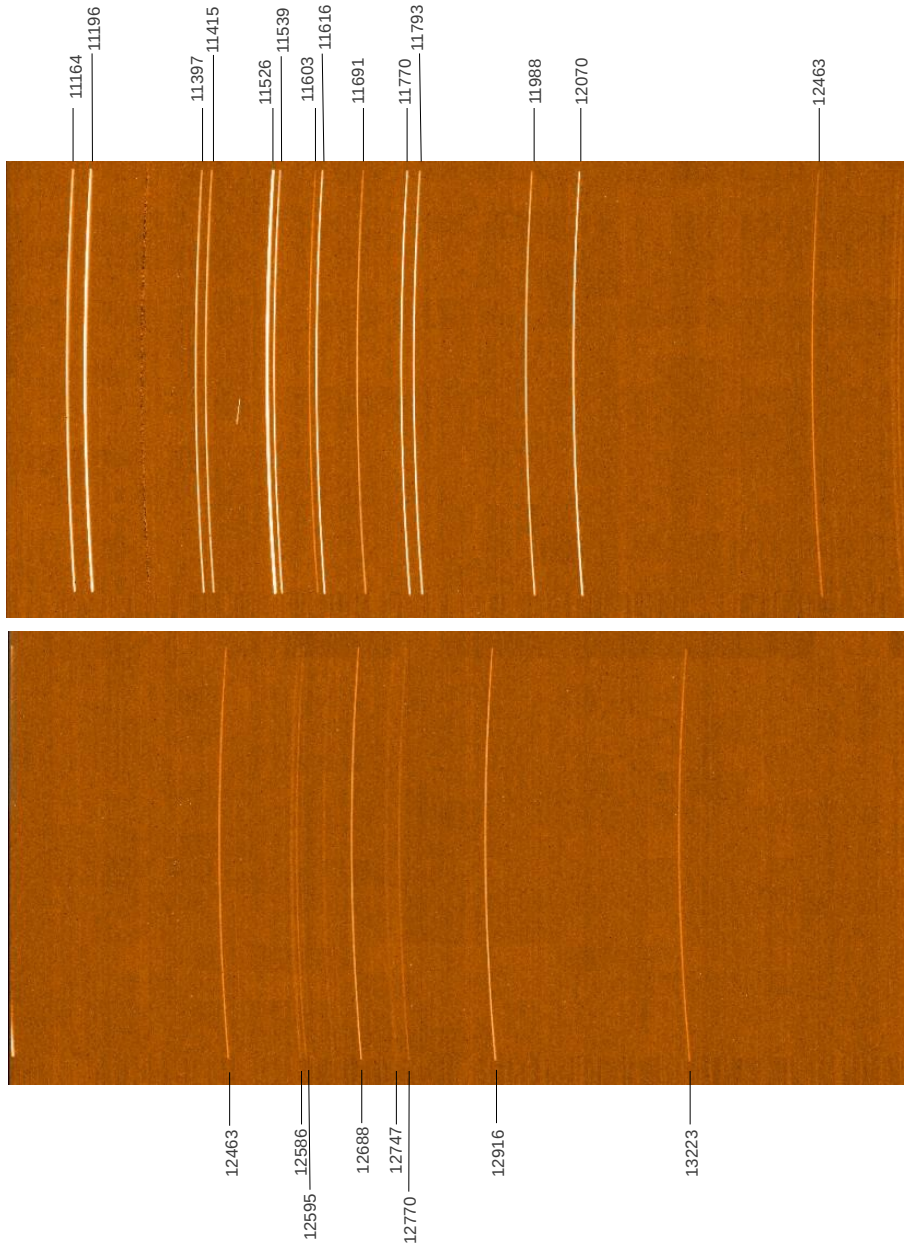


Figure 37: Neon arc-line identification plots for the G210 grating in J-band.

G210 in H band for Ar

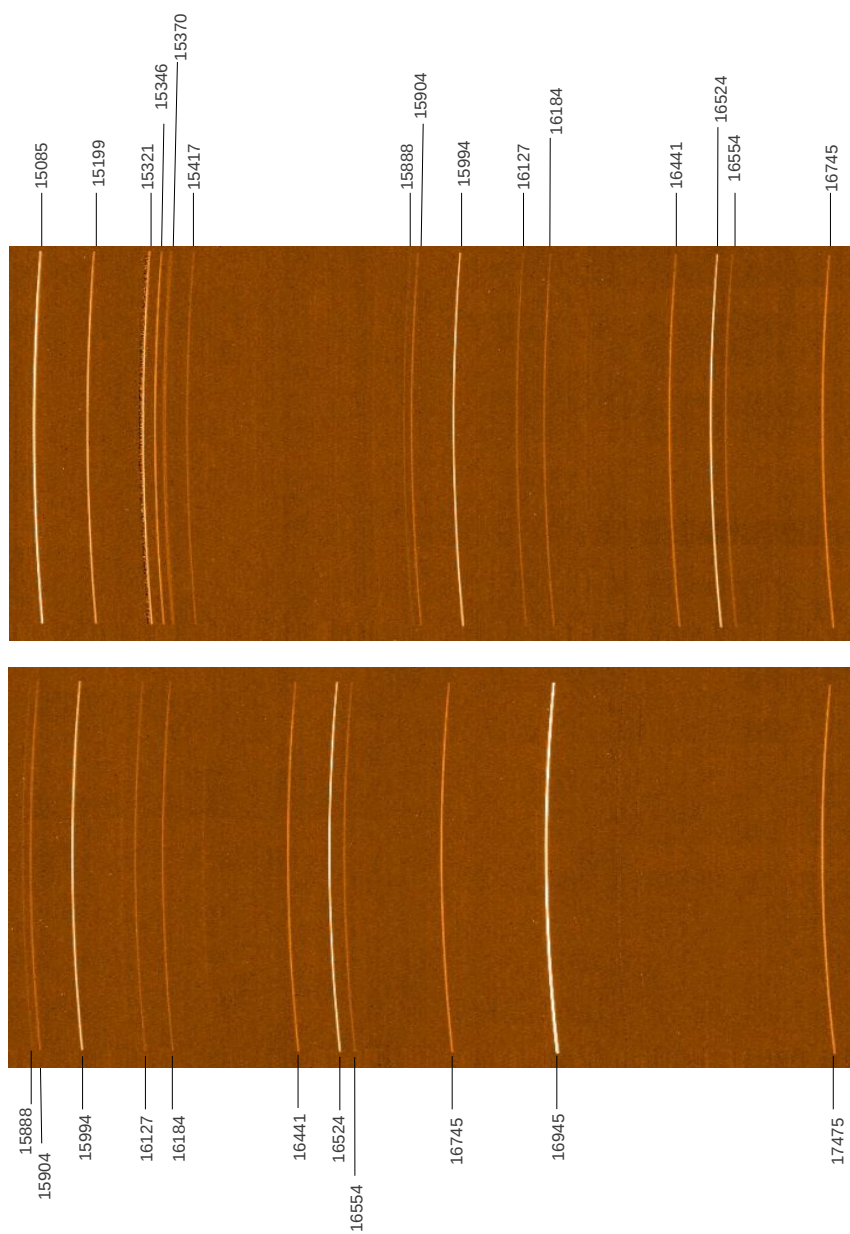


Figure 38: Argon, Xenon and Neon arc-line identification plots for the G210 grating in H-band.

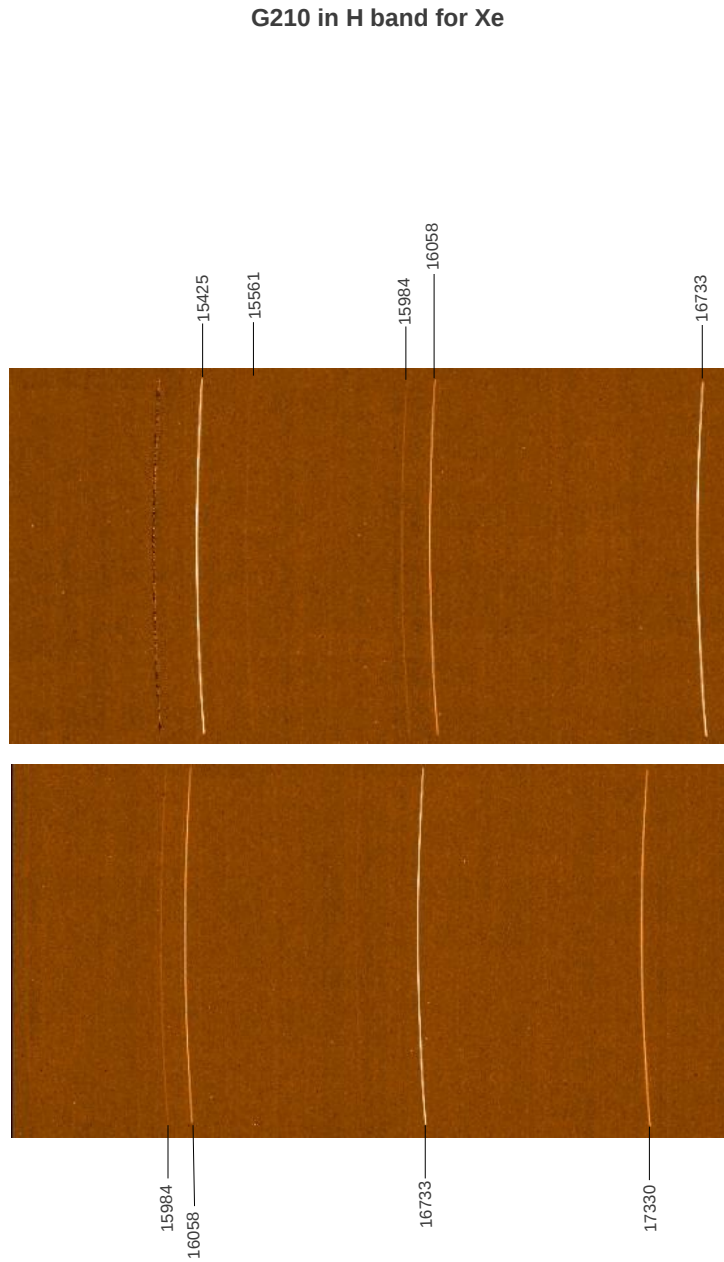


Figure 39: Xenon arc-line identification plots for the G210 grating in H-band.

G210 in H band for Ne

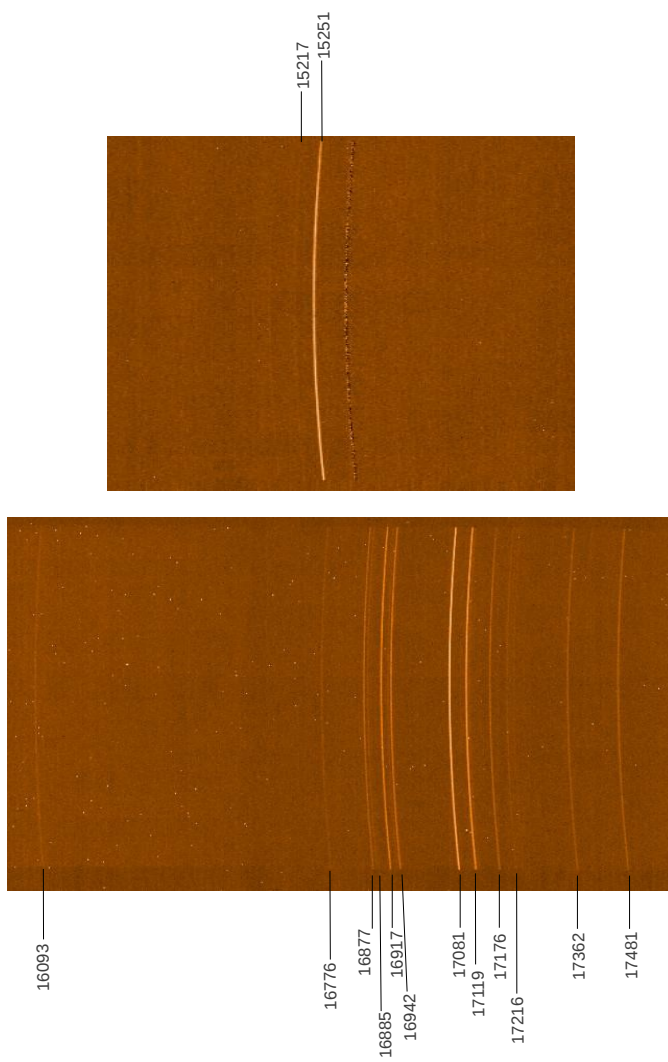


Figure 40: Neon arc-line identification plots for the G210 grating in H-band.

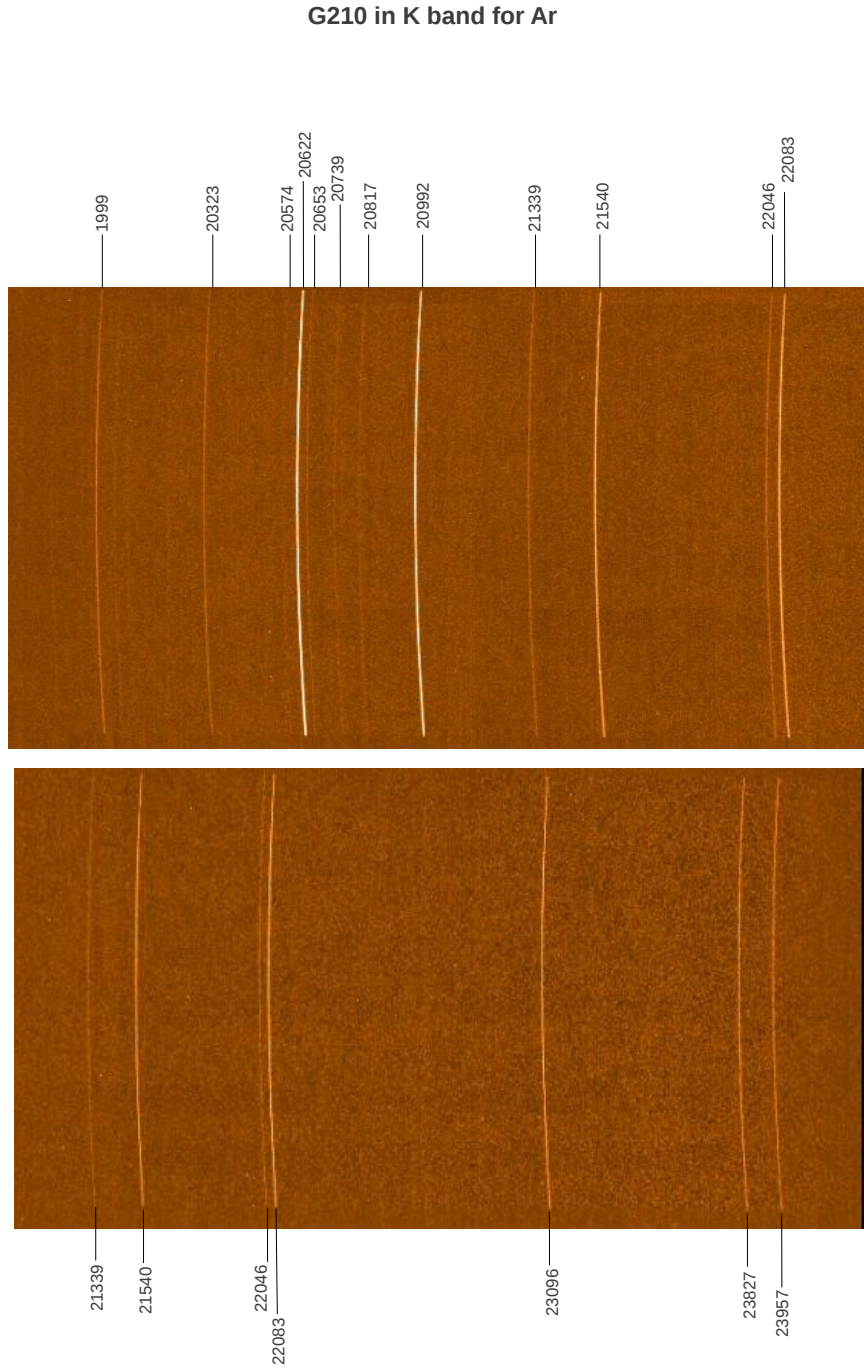


Figure 41: Argon arc-line identification plots for the G210 grating in K-band.

G210 in K band for Xe

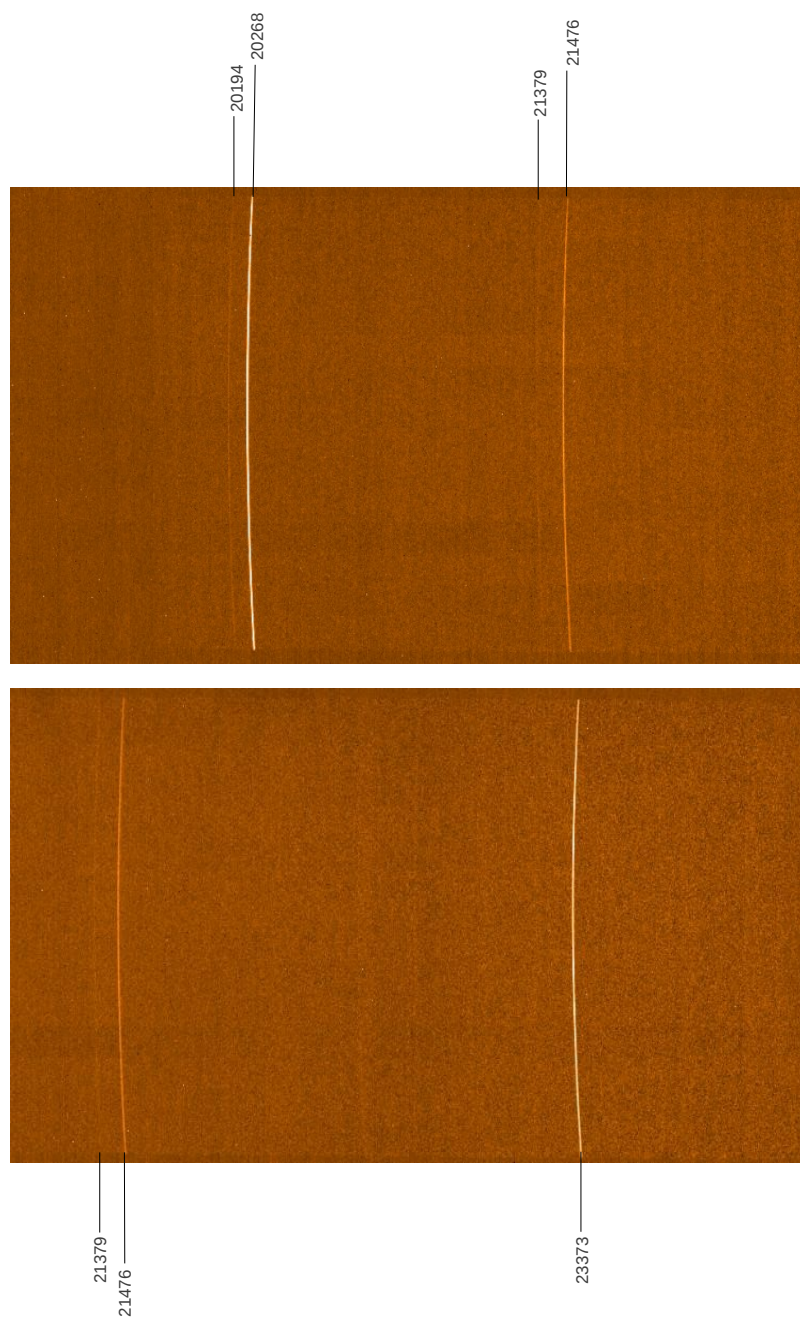


Figure 42: Argon, Xenon and Neon arc-line identification plots for the G210 grating in K-band.

G210 in K band for Ne

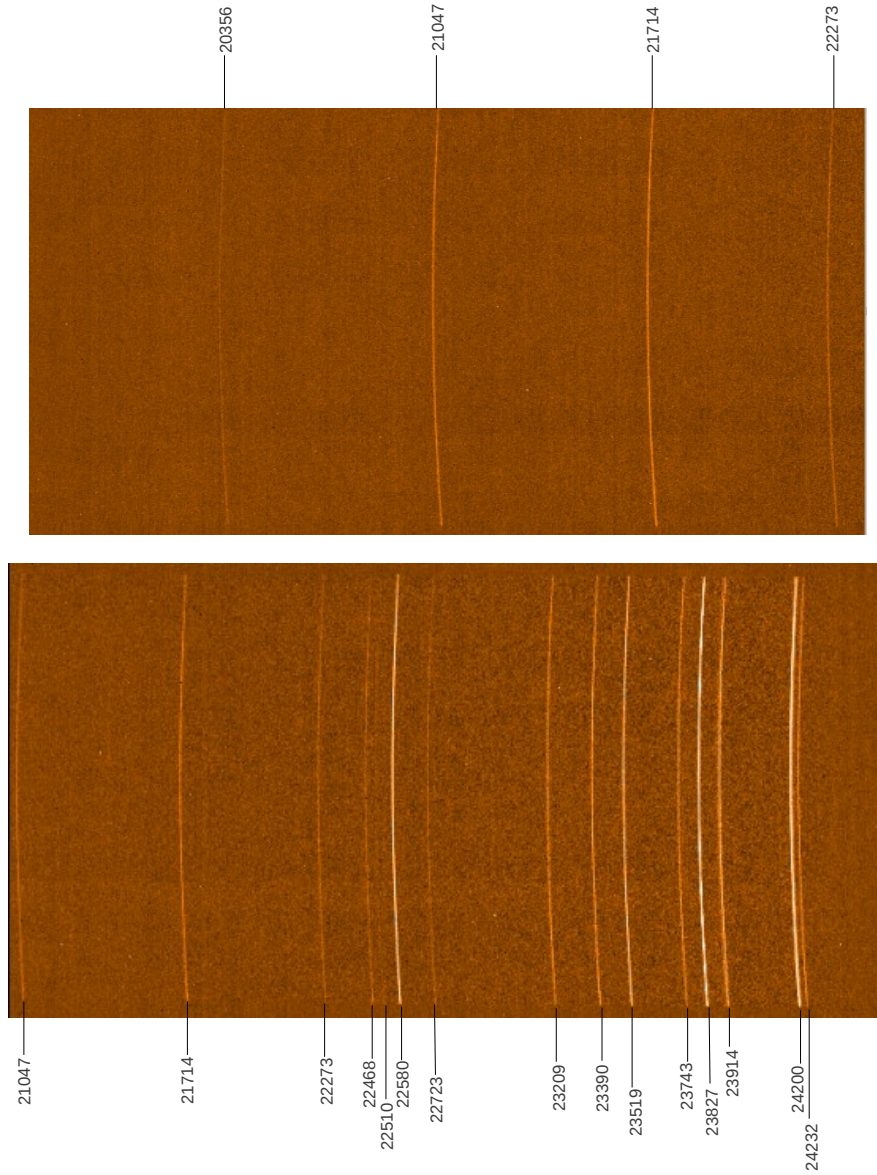


Figure 43: Neon arc-line identification plots for the G210 grating in K-band.

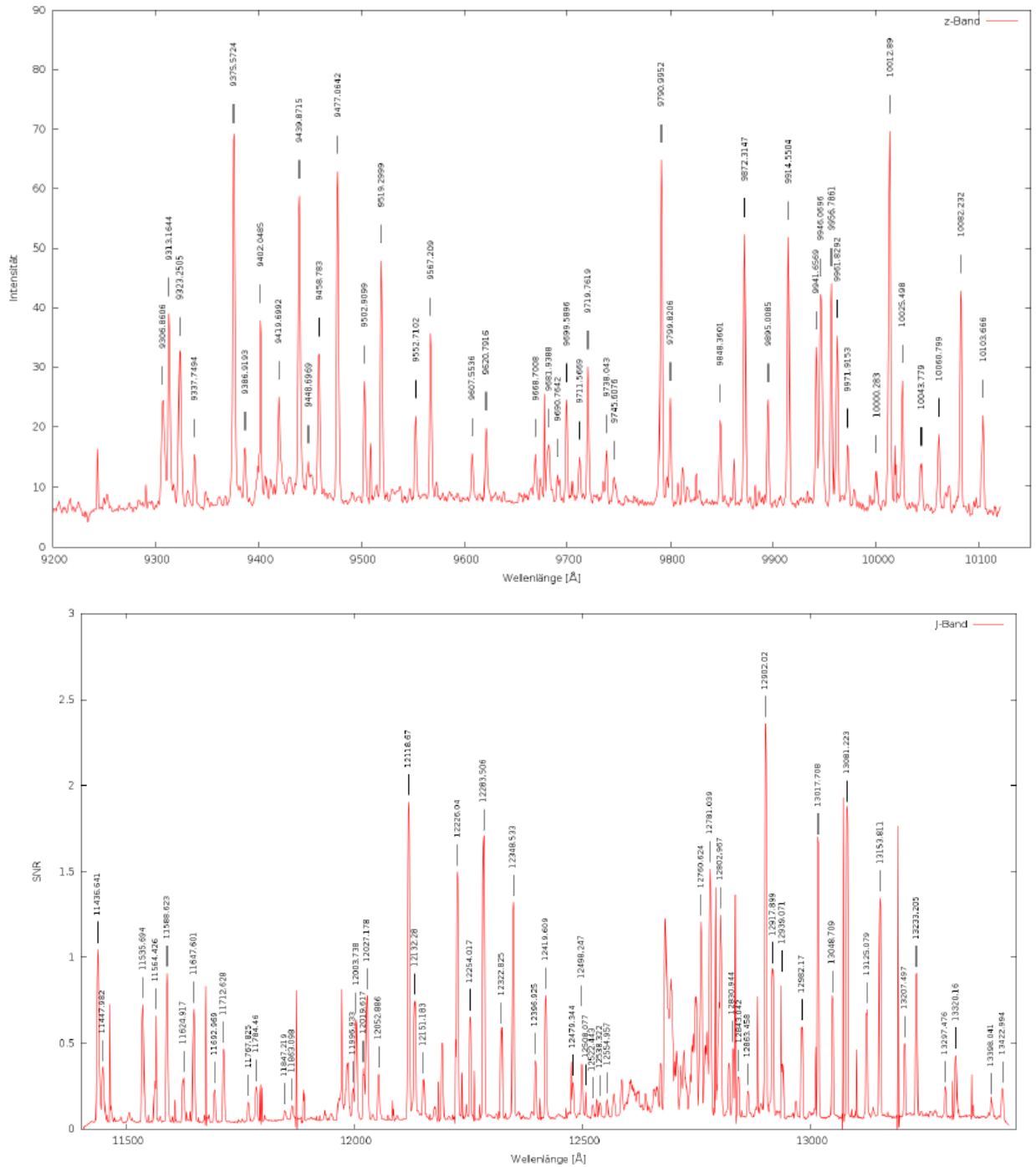


Figure 44: Nightsky emission line identification plots for the in the z- and J-bands from observations with the G210 grating.

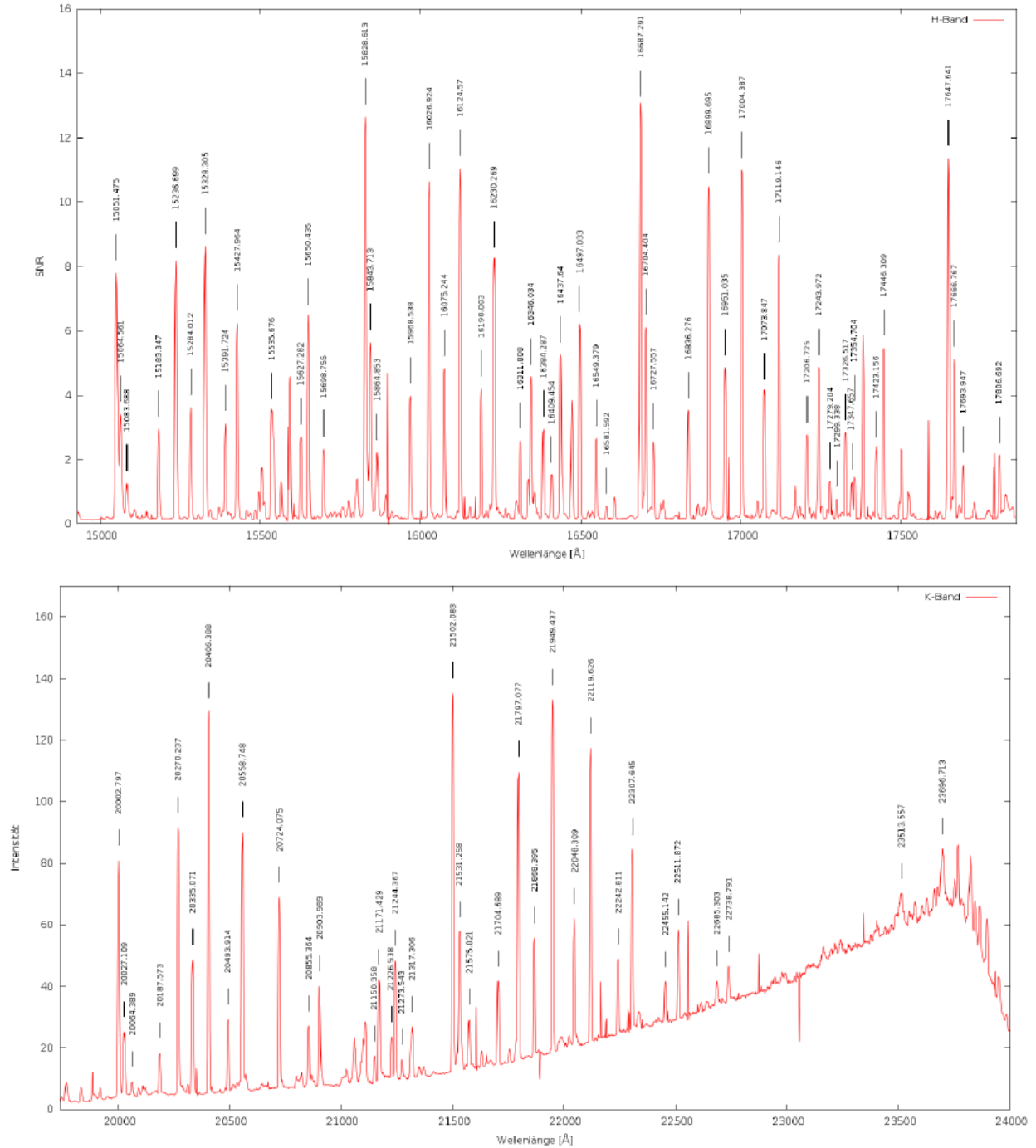


Figure 45: Nightsky emission line identification plots for the in the H- and K-bands from observations with the G210 grating.